VOLUME 39 / NUMBER 1 / 1997

Radiocarbon

An International Journal of Cosmogenic Isotope Research

…partment of Geosciences
…e University of Arizona
…7 East Ft. Lowell Road
…son, Arizona 85712-1201 USA

ISSN: 0033-8222

RADIOCARBON

An International Journal of Cosmogenic Isotope Research

Editor: AUSTIN LONG
Consulting Editor: A. J. T. JULL
Managing Editor: RENEE S. KRA
Acting Managing Editor: DAVID R. SEWELL
Assistant Editor: KIMBERLEY TANNER ELLIOTT
Published by
Department of Geosciences
The University of Arizona

Published three times a year at The University of Arizona, Tucson, AZ 85712-1201 USA.

Subscription rate (1997): $115.00 (for institutions), $55.00 (for individuals). Foreign postage is extra. A complete price list, including Proceedings of International Conferences, special publications and 1997 subscription categories, appears in the back of this issue. Back issues may be obtained by contacting *RADIOCARBON*.

All correspondence and manuscripts should be addressed to the Managing Editor, *RADIOCARBON*, Department of Geosciences, The University of Arizona, 4717 East Ft. Lowell Road, Tucson, AZ 85712-1201 USA. Tel: (520) 881-0857; Fax: (520) 881-0554; Internet: `c14@packrat.aml.arizona.edu`

Offprints. The minimum offprint order for each article will be 50 copies without covers. *No offprints will be furnished free of charge unless page charges are paid (see below).* Covers are also available.

Page charges. For 1997, each institution sponsoring research reported in a technical paper or a date list will be asked to pay a charge of $50.00 per printed page. Institutions or authors paying such charges will be entitled to 50 free offprints without covers. *No charges will be made if the author indicates that the author's institution is unable to pay, and payment of page charges for an article will, in no case, be a condition for its acceptance.*

Missing issues will be replaced without charge only if claim is made within three months (six months for India, New Zealand and Australia) after the publication date. Claims for missing issues will not be honored if non-delivery results from failure by the subscriber to notify the Journal of an address change.

Illustrations should include explanation of symbols used. Copy that cannot be reproduced cannot be accepted. Whenever possible, reduce figures for direct publication. Line drawings should be in black India ink on white drawing board, tracing cloth, or coordinate paper printed in blue and should be accompanied by clear ozalids or reduced photographs for use by the reviewers. Photographs should be positive prints. We can also print from many computer graphics file formats; please request our guide to graphics files for details. Figures (photographs and line drawings) should be numbered consecutively through each article, using Arabic numerals. Tables may be accepted as camera-ready copy.

Citations. A number of radiocarbon dates appear in publications without laboratory citation or reference to published date lists. We ask authors of research articles and date lists to include proper citation (laboratory number and date-list citation) in all publications in which radiocarbon dates appear.

List of laboratories. Our comprehensive list of laboratories is published in the third issue of each volume, and is also available on the WWW at `http://packrat.aml.arizona.edu/Info/lablist.txt`. We are expanding the list to include additional laboratories and scientific agencies with whom we have established contacts. The editors welcome information on these or other scientific organizations. We ask all laboratory directors to provide their laboratory code designation, as well as current telephone and fax numbers, and e-mail addresses. Changes in names or addresses, additions or deletions should be reported to the Managing Editor. Conventional and AMS laboratories are now arranged in alphabetical order by country and we include laboratories listed by code designation.

RADIOCARBON on the World Wide Web: `http://packrat.aml.arizona.edu/`

VOL. 39, NO. 1 **RADIOCARBON** 1997

CONTENTS

FROM THE EDITOR

ARTICLES

DATE LISTS

BOOK REVIEWS

[RADIOCARBON, VOL. 39, NO. 1, 1997, P. iii]

FROM THE EDITOR

The reader will notice that despite our previous announcement (Long 1995) of *RADIOCARBON*'s discontinuance of date-list publication, this issue contains four date lists, plus one article that is a compilation of dates with text related to a specific research topic. What is going on here? Do our actions belie our words? I prefer to call it institutional flexibility.

In view of the exploding volume of radiocarbon dates in recent years, mostly AMS-based, neither this nor any journal can be a repository of all dates. Individual laboratory databases and research publications are now the primary ^{14}C date archives. My back issues of *RADIOCARBON* have often been a valuable resource for dates that had been published only here. These date lists also revealed important details of laboratory techniques and pretreatment procedures that were often omitted in application-focused publications. In some cases, date lists served as formal announcements of the initiation of new ^{14}C dating facilities and personnel. When we received the date list submissions in this issue, we realized that nearly 50 years of tradition is hard to break. Moreover, we recognize the importance of providing a showcase for relatively new laboratories to demonstrate their capabilities and application interests.

Thus, we now find ourselves in a transition state. We cannot predict how the date-list situation will sort out. We do know that fewer date lists arrive in our mailbox. We also know that establishing a comprehensive, single-site ^{14}C database is not feasible. One possibility is that we could publish the web site address for each laboratory whose directors wish to make available details of their techniques and personnel. They could even advertise here the availability of online, searchable ^{14}C databases for dates they have produced. Meanwhile, recognizing that these are changing times, we will publish date lists at the discretion of the editors.[1]

Please contact us here with feedback about how we (the ^{14}C community) should deal with the future of ^{14}C data information.

Austin Long

REFERENCE

Long, A. 1995 From the Editor. *Radiocarbon* 37(3): iii.

[1]This reintegration of date lists also means that we are discontinuing our separate publication of *Radiocarbon Date Lists,* whose 1995 and 1996 issues were available as computer files only.

ERRATUM

Our annual laboratory list entry for the Gif beta-counting ^{14}C laboratory, published in *RADIOCARBON* Volume 38, Number 3 (1996), p. 620, had incorrect contact information for the lab director. The correct entry is:

Gif

Dr. Michel Fontugne
Centre des Faibles Radioactivités
Laboratoire mixte CNRS-CEA
F-91198 Gif sur Yvette Cedex, France
Tel: +33 1 69 82 35 25; Fax: +33 1 69 82 35 68
E-mail: Michel.Fontugne@cfr.cnrs-gif.fr
and
Laboratoire Souterrain de Modane
Laboratoire mixte IN2I 3-CNRS/DSM-CEA
90, Rue Polset
F-73500 Modane, France

Our apologies to Dr. Fontugne for inadvertently "retiring" him!

[RADIOCARBON, VOL. 39, NO. 1, 1997, P. 1–119]

Radiocarbon

1997

RADIOCARBON AGES OF MAMMOTHS IN NORTHERN EURASIA: IMPLICATIONS FOR POPULATION DEVELOPMENT AND LATE QUATERNARY ENVIRONMENT

YURIJ VASIL'CHUK,[1] JAAN-MATI PUNNING[2] and ALLA VASIL'CHUK[3]

ABSTRACT. Many mammoth remains have been radiocarbon-dated. We present here more than 360 ^{14}C dates on bones, tusks, molars and soft tissues of mammoths and discuss some issues connected with the evolution of mammoths and their environment: the problem of the last mammoth; mammoth taphonomy; the plant remains and stable isotope records accompanying mammoth fossils; paleoclimate during the time of the mammoths and dating of host sediments. The temporal distribution of the ^{14}C dates of fossils from the northern Eurasian territory is even for the entire period from 40 to 10 ka BP.

INTRODUCTION

Mammoth remains are very valuable objects for the study of Late Quaternary geochronology and paleoecology. The first finds of mammoth remains on northern islands in the Arctic and valleys of the great Siberian rivers drew the attention of scientists to the northern territories more than two centuries ago. The development of the mammoth population is one of the most interesting problems in reconstructing the dynamics of the environment during the Quaternary. The wide use of radiocarbon and paleoecological methods has provided valuable information on these dynamics. Today it is widely accepted that various fossil species of the genus *Mammmuthus* characterize Late Quaternary periglacial environments.

Since the ^{14}C method was first applied to the age determination of mammoth remains, the main problem has been reliability of the data. Geochemically, the most desirable materials for ^{14}C analysis are well-preserved organic residues, *i.e.,* bones rich in collagen, frozen carcasses, cud, dung or stomach contents from frozen ground or dry caves. In Russia, there are numerous sites from which whole carcasses of fossil mammoths have been dated by ^{14}C (Fig. 1, Appendix): Yuribey River (Gydan Peninsula), Gydan (Gyda River), Pyasina River (Taimyr Peninsula), Mochovaya River (Taimyr Peninsula), Mammoth Shrenk (Taimyr Peninsula), Chekurovka Settlement (Lower Lena River), Bukovskiy (Lena River), Beryosovka River, Shandrin River, Kirgilyakh River (baby mammoth "Dima"), Lyakhovskiy Bol'shoi Island, Tirekhtyakh River, Enmynveem (Chukotka Peninsula).

It has been established that woolly mammoths spread over a vast area in northern Eurasia in the Late Pleistocene and even into the Holocene. The first ^{14}C measurement of the fossil remains of mammoths was carried out by Heintz and Garutt (1965). Sulerzhitskij (1995) published more than 180 dates of Late Quaternary mammoths, most of which he had collected and dated himself. Stuart (1991) summarized the majority of ^{14}C dates of mammoths of various species from northern Eurasia and North America.

[1]Department of Theoretical Problems, Russian Academy of Science, Denezhnyj per. 12, 121002 Moscow, Russia
[2]Institute of Ecology, Kevade 2, EE0001 Tallinn, Estonia
[3]Institute of Cell Biophysics, Russian Academy of Science, 142292 Pushchino, Moscow Region, Russia

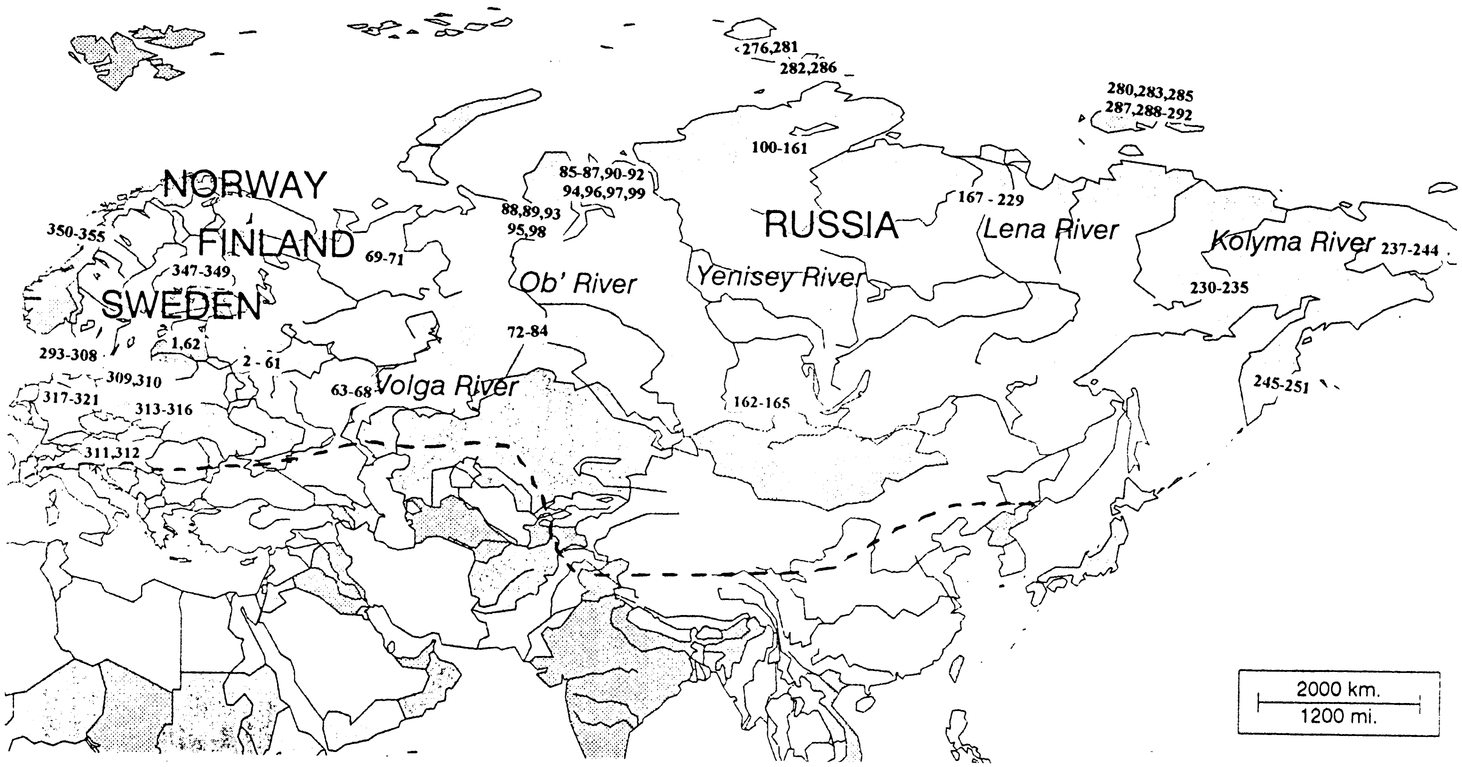

Fig. 1. Location of sites with dated mammoth remains. Site numbers refer to the number in the Appendix. --- = the southern limit of the ice wedge formation in the Late Pleistocene cryochron (40–10 ka BP) (in Asia after Vasil'chuk (1992), in Eastern Europe after Velichko (1984), in Western Europe after Maarleveld (1976).

METHODS

We sampled (Vasil'chuk 1992) mammoth bones from many reference sites in northern Yakutia: in the depression near Kular settlement (37.7 ka BP), near Zelyonyj Mys settlement (43.7 and >50 ka BP), Duvannyi Yar natural exposure (28.6, 33.8, 34.7 and >50 and 53 ka BP), and in Chukotka in the Mayn River valley and Ledovyi Obryv natural exposure (15.1 ka BP). We found redeposited bones (drifted fossils) in the Holocene alas sediments, in the Kolyma River valley near the Omolon River mouth (15 ka BP).

Earlier we summarized a number of ^{14}C dates on mammoth remains from northern Asia in order to reconstruct permafrost evolution during the last 40 ka (Vasil'chuk 1992). In addition to that list, we here summarize (Appendix) all the known ^{14}C dates (>360) of mammoth remnants from northern Eurasia, mainly from permafrost areas (Appendix and Fig. 1).

One serious concern in using data obtained by dating of mammoth remains is its reliability. The systematic checking of bone data is underway at the Radiocarbon Laboratory of the Geological Institute in Moscow (L. Sulerzhitskij, personal communication). It is possible to draw some conclusions using the data obtained by multiple analysis of material from the same layer. There are many samples in the Appendix dated by bone material with different degrees of weathering (samples 12, 127, 139, 156, 246). The differences in the data are <1000 yr, in most cases within the statistical uncertainty of the dates. In some cases, different materials from the same layers were dated (Appendix, samples 85, 86, 87; 170, 171; 210, 211; 265, 266; 268,269; 271, 272). The differences in data are modest and also within the limit of statistical uncertainty. This demonstrates that, in principle, fossils of mammoth fauna can be considered reliable as material for ^{14}C dating.

The dates in the interval from 10 to 40 ka BP are distributed rather evenly; furthermore, there is no remarkable spatial grouping of mammoth finds in northern Eurasia. If ^{14}C dates are an unbiased sample of mammoth populations, this indicates that mammoths lived constantly and continuously over northern Eurasia during the Middle/Late Würm. Eastern Europe is characterized by a series of dates from 9.7 to >47.7 ka BP. The finds consist predominantly of molars, bones and tusks. In the northwestern part of European Russia, mammoth remains have been dated from 18.3 to >36 ka BP. In southern parts of western Siberia the dates range from 12.8 to 41.9 ka BP.

Whole carcasses have been found in the Yuribey and Gyda River valleys in northwestern Siberia; mammoth remains from this region have been dated from 9.6 to 35 ka BP. On the Taimyr Peninsula, Sulerzhitskij (1995) obtained several dates ranging from 9.6 to >53 ka BP without any significant time gaps. In central Siberia, fewer dates cover the interval from 20.7 to 49.7 ka BP (Appendix); this reduction may be explained by the topography and, consequently, biogeographical conditions of this mountainous region. The abundant ^{14}C dates on mammoth remains in northern Yakutia range from 10.3 to >53 ka BP. From the Magadan region, data are available on the carcass of the Kirgilyakh baby mammoth and a few other finds, with ages from 21.6 to 41 ka BP. The Chukotka Peninsula is characterized by dates from 14.3 to 32 ka BP. In the Kamchatka Peninsula, ^{14}C dates were obtained in the interval 12.6 to 40 ka BP (Sulerzhitskij 1995) (Appendix). Interesting dates are available from Arctic islands, especially Wrangel Island. Dates obtained from a dwarf form of mammoth are the youngest for mammoth finds in the world, falling into the interval 3.9 to 7.7 ka BP. The dates from 12.7 to 20 ka BP from these islands belong to mammoths of normal form (Vartanyan, Garutt and Sher 1993; Vartanyan *et al.* 1995). The oldest date on mammoth remains from the Arctic islands is 32 ka BP.

Mammoth bones also occur rather often in western Europe (Kurten 1968). Berglund *et al.* (1976) and Hakansson (1976) refer to some ^{14}C dates on mammoth remains from South Sweden: 13, 19, 22 and >30 ka BP. In Norway, some ^{14}C dates on mammoth remains in the time interval from 19 to 32 ka BP have been obtained (Follestad and Olsson 1979). In Finland, Jungner and Sonninen (1983) and Donner, Jungner and Kurten (1979) obtained three ^{14}C dates on samples collected by Donner: 15.5, 25.2 and >43 ka BP. Mammoth remains from Denmark have ^{14}C ages from 13 to >39 ka BP (Aaris-Sorensen *et al.* 1990). In Germany, the dates vary from 15.8 to 30.3 ka BP; in Switzerland, from 12.2 to 34.6 ka BP; in Poland, from 20.2 to 23.0 ka BP; and in France, from 12 to 25.8 ka BP. Mammoth remains from Great Britain and Ireland have ages from 11.6 to >39.5 ka BP (Coope and Lister 1987; Stuart 1991).

The temporal distribution of mammoth remains (Fig. 2) displays no essential differences in the number of dated mammoths in the time interval from 15 to 45 ka BP. The spatial distribution of ^{14}C-dated mammoth remains shows that mammoth fauna were connected mainly with Late Quaternary permafrost conditions (Fig. 1).

Discussion

Several issues connected with mammoth evolution are of great scientific interest: the problem of the last mammoth; mammoth taphonomy; paleoclimate during the time of the mammoths and use of mammoth remains for the dating of host sediments.

The Problem of the Last Mammoth

The youngest ^{14}C data for quasi-mammoth remains from the Western Hemisphere are those from North America on the *Mammut americanum*: 4470 ± 160 (M-2436) from Kuhl, Michigan; 8910 ± 150 (GSC-614) from Ferguson Farm, Ontario, and 9568 ± 1000 BP (M-282) from Lenawee, Michi-

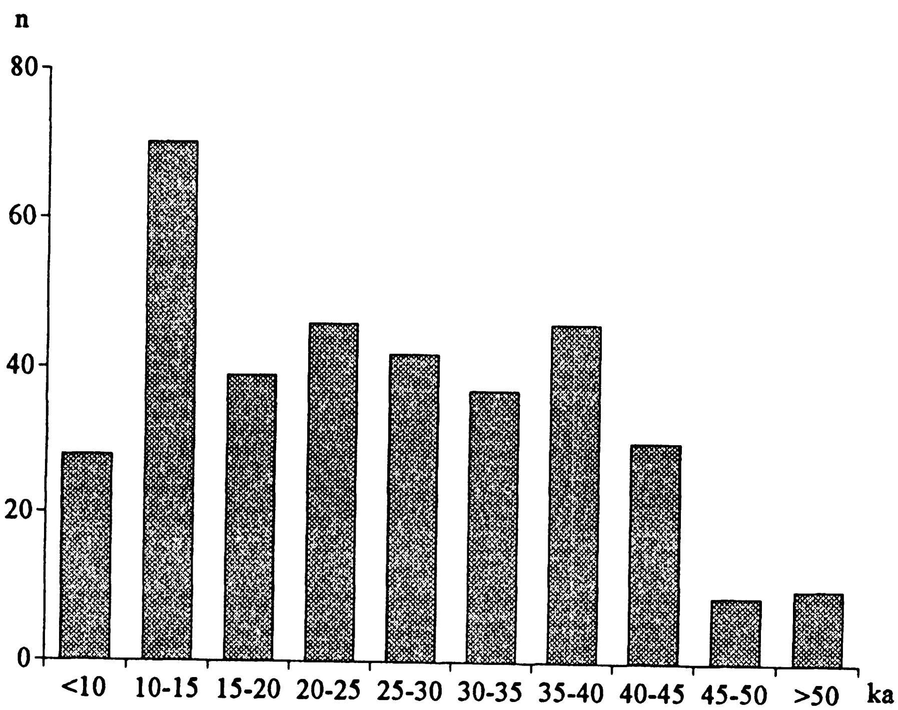

Fig. 2. The temporal distribution of ^{14}C-dated mammoth remains

gan (Meltzer and Mead 1985); and from the Southwest United States, remains of *Mammuthus columbi* from Sandy, Utah dated to 5985 ± 210 (SI-2341b), 7200 ± 190 (RL-464) and 8815 ± 100 BP (SI-2341a) (Semken 1983; Stafford *et al.* 1987; Agenbroad and Mead 1989). However, contamination of samples cannot be excluded, as has been shown by Stafford *et al.* (1987)—for different fractions from the Domebo mammoth sample, dates from 2050 to 11,490 BP were obtained. We also note that no archaeologically associated remains of mammoths younger than Clovis (*ca.* 11,000 BP) (Haynes 1993) have been replicated. It seems that the younger ^{14}C dates on mammoth remains in Northern America need replication.

More than 20 mammoth remnants from Wrangel Island collected by Vartanyan (Vartanyan, Garutt and Sher 1993; Vartanyan *et al.* 1995) were dated in the range 4–7 ka BP; the youngest dates are 3730 ± 40 BP (LU-2741) and 3920 ± 30 (GIN-6980). Two samples were replicated by the AMS dating facility at the University of Arizona (Long, Sher and Vartanyan 1994). Thus, the last mammoths now known lived on Wrangel Island *ca.* 4000 yr ago. The dated remains belong to a dwarf form of a mammoth that lived in isolation on the island under strictly limited food conditions (Grant 1985). One problem connected with these phenomena is that mammoths came to the island as a consummate form (Johnson 1978), but no data exist for the interval 12–8 ka BP. The mammoth refugium must have been disconnected from the continent, otherwise remains of Holocene dwarf mammoths should be found on the continent also. The dwarf form on Arctic islands is a common survival adaptation of large mammalians, such as deer, hippopotamus and elephantids. (Dwarf forms of elephantids lived on some islands of the Mediterranean Sea and on the Channel Islands of California during the Quaternary, with heights of ≤0.9 m.)

Mammoth Taphonomy

Two aspects of the taphonomy of mammoth remains deserve attention. First, bones occurring in an unarticulated condition, almost without exception, indicate the redeposition of remains, typical of deposits of fluvial origin (such as alluvial, lacustrine, fluvioglacial). Therefore, as a rule the ^{14}C dating of mammoth remains from these sediments gives the maximum age of sediment formation. Inclusion of younger bones in an older frozen deposit is not possible. As for syngenetic sediments of fluvial series, we can state with certainty that their ages are younger or equal to the ages of the enclosed bones. Second, the possible delivery of the bones by carnivores must be kept in mind.

The burial of whole mammoth carcasses is obviously an infrequent process, requiring the coincidence of several conditions. To remain intact, a carcass must be covered with sediments or be isolated from carnivores very quickly. Hence, the best conditions for preserving mammoth remains were offered by talus and alluvial sediments, high icy terraces and thermokarst depressions.

Plant remains in the stomach can be used to establish the season of a mammoth's burial. All the mammoth carcasses found belonged to mammoths that perished in the summertime. Remains of mammoths that perished in the winter may have been destroyed by carnivores. This suggests that an important factor for the preservation of mammoth carcasses is the existence of permafrost conditions, during both fossilization and preservation.

Plant Remains and Pollen Accompanying Mammoth Fossils

The majority of the finds of subfossil mammoths and other large animals in northern Eurasia are connected with polygonal ice wedge complexes. Possibly mammoths' pasturage depended directly on polygonal massifs. Palynological and plant macrofossil analyses have revealed an abundance of herbage in polygonal relief areas.

Pollen grains and plant remains in mammoths' guts (Table 1) indicate the feeding habits of the animals (Sukachev 1914; Solonevich, Tikhomriov and Ukraintseva 1977; Ukraintseva 1979; Sokolov 1982; Shilo *et al.* 1983; Guthrie 1990).

TABLE 1. Pollen and Spores in the Stomach Content of the Carcasses of Four Fossil Mammoths and a Selerican Horse (% of total content) (after Tikhomirov and Kupriyanova 1954; Kupriyanova 1957; Belorusova, Lovelius and Ukraintseva 1977; Belaya and Kisterova 1978; Ukraintseva 1979; Gorlova 1982)

Site (see Appendix)	^{14}C age (BP), number of samples	P_{tr}*	P_{sr}	P_{hr}	S
Yuribey River (Gydan Peninsula)	10 ka (4)	5–6	15–17	17–20	56–63
Shandrin River (northern Yakutia)	36 ka (1)	2	1	19	77
Kirgilyakh River (Magadan Region)	39 ka (6)	2–10	6–20	60–77	8–18
Beryosovka River (northern Yakutia)	44 ka (1)	1	1	97	1
Bolshoy Selerican (Indigirka River)	38 ka (1)	4	5	80	11

*P_{tr} = tree pollen, P_{sr} = shrub pollen, P_{hr} = herb pollen, S = spores.

The host sediments that enclosed the Kirgilyakh baby mammoth are characterized by the predominance of pollen of herbs and shrubs (60–77%). Pollen of grass and sedges occur in equal quantities (10–25%), and other grasses are represented by 28 families such as Ranunculaceae (2–4%), Cruciferae (4–10%) and Artemisia (up to 4%). There are also pollen of hydrophilous taxa such as Potamogeton, Myriophyllum and Alismataceae. The content of Ericaceae (<2%), which is usually dominant in subfossil pollen spectra, is very small. The presence of larch pollen is evidence of larch forest at that time (Belaya and Kisterova 1978).

Pollen analyses of mammoths' digestive tracts and host sediments show a predominance of herb pollen or spores, presence of larch pollen (1–5%) and pollen of species that now live in southern areas (*e.g.*, pollen of *Ribes, Betula* sect *Albae*), and the existence of typical tundra elements in the vegetation, *e.g., Dryas punctata.* The pollen and spores spectra showed some regional features, but these were evidence that mammoths lived in environments close to the modern larch forest and forest tundra.

Fossil flora found in the remains of the Yuribeyskiy mammoth (Gorlova 1982) consist of Cyperaceae (9 species), Poaceae (4 species), Salicaceae (3 species), Rosaceae (2 species), Betulaceae, Ericaceae and Pinaceae (1 species each). The present vegetation in the Arctic and the Subarctic is rather similar. However, the presence of macrofossils of *Larix sibirica* L. and *Ribes* spp. testifies to more favorable climatic conditions during the era of mammoths.

Naturally, to some extent, the content of the stomach reflects feeding preferences of mammoths. Plant remains belong to different life forms—shrubs, grasses, moss—and different habitats—dry meadows, steppe slopes, bottomland meadows, floodplain swamps, *etc.* This suggests the diversity of environmental conditions and biocoenoses in the areas where mammoths could live. Willow brushwood occurred in closed valleys, cereals and herbage occupied southern slopes of alluvial terraces, and sedges (particularly *Carex* strains) grew in meadows.

Analyses of both plant microfossils and pollen from dung and gut contents indicate a summer diet of grasses, sedges, mosses, and shoots of willow, draft birch and alder. A frozen forage mass from the stomach and gut of the Shandrin mammoth, found in Lower Indigirka, weighed *ca.* 250 kg. The greater part of it consisted of stems and leaves of sedges, grasses and cotton-grass and the smaller part of sprouts of willow, birch and alder (Solonevich, Tikhomirov and Ukraintseva 1977; Vereshchagin 1979). There were not any ripe seeds that might testify that the animal died in summer.

Well-preserved contents of mammoths' digestive tracts have been studied from the Shandrin mammoth carcass (Ukraintseva 1979). The remains of Cyperaceae, *Eriophorum* spp., Poaceae, *Larix Daurica* Turcz., Ericaceae, *Vaccinium vitis-idaea* L., some species of *Polytrychum, Aulacomnium* and *Sphagnum* have been identified. The main part of the pollen spectra from the enteron consists of spores of *Bryales* and *Sphagnum* (77%). Pollen of grasses makes up 19.4%, the majority of them pollen of grasses and sedges. Pollen of *Dryas punctata, Valeriana capitata, Artemisia* spp., *Ledum* spp. and *Saxifraga* spp. are also represented. All of these species presently grow in the same area. Pollen of larch, birch and alder bush were also found (*ca.* 4%). Nowadays analogous landscapes of larch light forests occur *ca.* 200 km to the south.

Sukachev (1914) identified grasses and sedges with ripe seeds in the stomach of Beryosovka mammoth, which evidently perished in late summer. Kupriyanova analyzed pollen and spores remains from the stomach of this mammoth: 8198 pollen grains and 7 spores were found (Tikhomirov and Kupriyanova 1954; Kupriyanova 1957). These are pollen of cereals (97%), forbs (2%), trees (1%) and spores. The pollen spectra are affected by the time of the mammoth's death (second half of summer), showing a small amount of tree pollen, with predominance of the cereal pollen blooming during that period. The species list of the pollen from the mammoth's stomach evidenced a varied flora corresponding to biocoenoses that exist at present *ca.* 1000 km to the south. Species of bunchgrass steppe with forbs and wormwood (*Artemisia*), upland meadow, inundation meadow, salt meadow and herb meadow have been determined.

Zaklinskaya studied the pollen content in the Taimyr Peninsula mammoth host sediments. All pollen spectra were characterized by the predominant herb pollen. The main part of the pollen consists of herbs of meadow plant communities of polygonal tundra, with cereals and sedges dominating (Zaklinskaya 1954). The paleobotanical and palynological data evidenced no sharp changes in the vegetation features, which therefore cannot be a cause of the mammoths' extinction.

One of the details of paleobotanical characteristics was obtained from Selerican horse remains (Belorusova, Lovelius and Ukraintseva 1977; Ukraintseva 1979). Plant remains are represented by fossils of poplar, birch and mosses. Pollen spectra show a presence of hazel, juniper, spruce and elm in plant societies and *Kobresia capilliformis* as a dominant of dry meadows.

Lister and Sher (1995) pointed out that one problem of the climatic model of extinction is explaining how woolly mammoths survived an earlier interglacial. They proposed that the vegetation of the interglacial differed from that of the Holocene. In Siberia several interglacials have been recorded, but during these intervals, the vegetation differed from the vegetation of the modern larch-dominated taiga. Unfortunately, even now the climate-driven models do not show uniquely the reasons for the extinction of the mammoth population. Undoubtedly, in many cases, human involvement was important (Stuart 1991).

The pollen and plant fossils in the sediments accompanying the mammoth remains and the content of their stomachs show that the favorable season for mammoths' fossilization in permafrost areas was late summer. More detailed paleoclimatic information about the time of mammoths' existence can be provided by stable isotope data both from syngenetic sediments with ice wedges and directly from mammoth remains.

Isotope Records

Variations of the oxygen isotope composition are not substantial in the Late Pleistocene permafrost syngenetic deposits where mammoth remains have been found. The interval of $\delta^{18}O$ in the syngenetic ice wedge that formed 40–10 ka ago (Table 2) varies in the north of western Siberia from –24 to –21‰, in northern Yakutia from –34 to –29‰ and in northern Chukotka from –32 to –29‰ (Vasil'chuk 1992). As snow meltwater was the main source of the moisture for ice wedges, the oxygen isotope records reflect mainly winter precipitation temperatures.

TABLE 2. Oxygen Isotope Composition in Syngenetic Ice Wedges ($\delta^{18}O$, ‰), Mean Winter (t_{mw}) and Mean January Temperatures (t_{mJ}) 40–10 ka BP in Different Regions of Siberian Mammoths' Habitats (after Vasil'chuk 1992, 1993)

Region of Siberia	$\delta^{18}O$ (‰)	$t_{mw_{D,J,F}}$ (°C)	t_{mJ} (°C)*
Yamal and Gydan Peninsulas, north of western Siberia	–21 to –24	–21 to –24	–32 to –36 (–22 to –28)
Bykovsky Peninsula, mouth of Lena River, western Yakutia	–30 to –34	–30 to –34	–45 to –49 (–32 to –34)
Upper Kolyma River, northeastern Yakutia	–29 to –33	–29 to –33	–43 to –49 (–30 to –34)
Vilyui and Aldan Rivers, central Yakutia	–29 to –31	–29 to –31	–43 to –46 (–37 to –45)
Ayon Island, northern Chukotka	–29 to –32	–29 to –32	–44 to –46 (–27 to –29)
Anadyr' and Mayn Rivers, southern Chukotka	–21 to –29	–21 to –29	–31 to –43 (–21 to –27)

*Present mean January temperatures in parentheses for comparison

Using the relationship between the mean winter temperatures and oxygen isotope records obtained by Vasil'chuk (1992), it is possible to say that the winter climate was cold, stable and unchangeable in northern Eurasia from 40 to 10 ka ago.

Seasonal Climatic Conditions During the Time of the Mammoths

Mammoth remains are usually treated as indicators of very cold climatic conditions. The extinction of mammoths is one of the most often discussed problems in the paleogeography of the Late Quaternary. One of the most important causes of their extinction is connected with the change of climatic conditions and, therefore, the composition and production of biomass. The paleotemperature record obtained immediately from mammoth habitats, *i.e.*, detailed records of syngenetic ice wedges, which have been dated as Late Pleistocene and Early Holocene, give valuable information about the mammoths' environment. The oxygen isotope and pollen data from the same sections make it possible to reconstruct separately winter and summer temperatures. This approach is of great significance. Comparing the trends of winter and summer temperatures, we can see that winter temperatures changed especially abruptly at the Pleistocene/Holocene boundary.

An analysis of all information obtained indicates that mammoths were excellently adapted to Late Pleistocene long and cold winters without any thaws. They had long, shaggy coats and underwool, a thick layer of subcutaneous fat, tiny ears and short tails. Underwool is characterized by thick hair, which was four times thicker than that of present-day cold-adapted animals. Mammoths did not have adipose glands in their skin, so their wool would get wet when it was raining or foggy. Large tusks came in handy for scraping snow and ice both for drinking purposes (like present-day elephants) and to expose buried forage. Their large size and spreading cushioned feet on which they distributed their weight may have enabled them to cope with snow better than most large herbivores in arctic and subarctic environments. The survival of such large animals in regions with a marked seasonal temperature range requires not only abundant summer herbage but also large quantities of winter feed, probably including dead grasses and bark from shrubs and trees.

At the Pleistocene/Holocene transition, winter temperatures changed sharply. Increasing Atlantic influences caused an increase in winter temperatures and the appearance of winter thaws. If thaws occurred in February or March, they could be fatal for mammoth herds, because the resulting multilayered ice crust made it impossible to find food and to move. The animals could not move because their legs were adapted to friable and relatively shallow snow cover but not to multilayered ice crust. Moreover, mammoth hair would have quickly become covered with ice, making the animals look like terrestrial icebergs.

We have reconstructed the environment in the mammoths' time applying different methods. The oxygen isotope data in ice wedges enabled us to determine that during the interval from 40 to 10 ka BP, mean January temperatures in northern Siberia were *ca.* 8–12°C lower (in Chukotka up to 17–18°) than the modern ones (Table 2). We have established that the interval from 40 to 10 ka BP was a single cryochron (Vasil'chuk 1992, 1993) with severe winters when the oscillations of temperatures were rather small, thawing was rare and the snow cover, as a rule, quite friable. Such winters permitted mammoths to dig out the grass easily from under the snow. Interpretation of pollen data enabled us to reconstruct the mean July temperatures for the period 40–10 ka BP. They were *ca.* 1–4°C lower than the contemporary ones (almost 7°C lower in the Chukotka Peninsula). During short periods of warming, the July temperatures could have been by 1–3°C higher than modern ones (Vasil'chuk and Vasil'chuk 1995).

Use of Mammoth Fossils for Dating the Host Sediments

Mammoth remains have been used widely in the dating of host sediments. The high degree of validity of ^{14}C dates of mammoth bones (Sulerzhitskij 1995), enables us to determine the lower limit of the host sediment age. In several sequences (Duvannyj Yar, Zelyonyj Mys and Kular in northern Yakutia) we have produced a series of ^{14}C dates on different kinds of organic matter—plant remains, peat, roots and wood, and bones. In many cases, the ^{14}C ages of plant remains were younger than the ages of bones from the same layers. For example, the ages of plant remains from Zelyonyj Mys sequences were in the interval from 27 to 37 ka BP and those of bones from the same depth from 43.7 to >50 ka BP (Vasil'chuk 1992). The same situation occurred in the Duvannyj Yar natural exposure, where the series of ^{14}C dates of plant remains lies in the interval from 40 to 20 ka BP, with three dates of mammoth bones in a normal sequence (28.6, 33.8, 34.7) and two inversion dates of >50 and 53 ka BP (Vasil'chuk 1992). We received non-inversion dates on tusk (15.1 ka BP) in the Ledovyj Obryv natural exposure in Chukotka, which were between the dates on plant remains of 34 and 14 ka BP (Vasil'chuk 1992). These data show that the dating of the host sediments by the use of mammoth bones is, in principle, possible; however, redeposition of separate bones is typical and must be taken into account in determining the host sediments' age.

Because whole carcasses are, as a rule, not redeposited, their ^{14}C dates conform better with the age of the host formation. However, there are some exceptions. For example, the Kirgilyakh baby mammoth (which is ^{14}C-dated to 38–41 ka BP) had been redeposited together with frozen host sediments into the younger (^{14}C-dated as Late Holocene) permafrost complex.

Mammoth Fossils and Reconstruction of Environmental Conditions

Some important regularities in the distribution of mammoth fossils appear within the Eurasian territory. First, the temporal distribution of the mammoth remains found in Eurasia is rather even for the whole period from 10 ka BP to the older limit of the ^{14}C method (Fig. 2). Second, the spatial distribution of dated fossils shows that the southern boundary of the mammoths' distribution is very close to the southern boundary of the ice wedge cast distribution, which is located *ca.* 45°N (Fig. 1). It may be assumed that the Late Pleistocene mammoth habitat corresponds to the severe permafrost area characterized by vast polygonal ice wedge landscapes. Third, as no breaks occur in the series of data from northern Asia, the European part of Russia and western Europe including Great Britain, it seems that the mammoths lived everywhere over this vast area. Therefore, the series of ^{14}C dates from 40 to 10 ka BP on mammoth fossils from Scandinavia gives reason for critical evaluation of the scale and dynamics of the Late Pleistocene Glaciation in this region. Mammoth remains in South Sweden (from 13 to >30 ka BP), Norway (from 19 to 32 ka BP), Finland (from 15 to >43 ka BP) and Denmark (from 13 to 32 ka BP) suggest that large parts of Scandinavia were ice-free in Middle and Late Weichselian time (Donner, Jungner and Kurten (1979) reached similar conclusions).

So, for the period of the last glaciation, ^{14}C dates on mammoth remains have been obtained from the entire territory of the supposed last glaciation area. ^{14}C dates for the period of the last glaciation have been obtained in North America as well. Weber *et al.* (1981) received six ^{14}C dates from bone fragments from Canyon Creek in interior Alaska—*ca.* 28, 32, 38, 39, 39 and 40 ka BP. In Canyon Creek, a portion of a tooth plate and bone fragments of *Mammuthus primigenius* and many bones of *Equus, Alces, Lepus, Canis, Ovis, Bison, etc.,* were sampled (Weber *et al.* 1981). Assuming that the ^{14}C dates are trustworthy, the finds of mammoth remains show that our knowledge about the glaciation environment needs essential supplements.

Conclusion

Comprehensive analyses of ^{14}C, pollen, oxygen isotope and geological data enable us to draw some conclusions about the development of the mammoth fauna and their environment. In particular our data show that:

1. Mammoth remains from frozen ground are a very suitable material for ^{14}C dating.
2. The temporal distribution of the ^{14}C dates of fossils from the vast Eurasian territory is even for the whole period from 40 to 10 ka BP.
3. No time breaks appear in the series of dates in northern Asia, nor in eastern and western Europe.
4. The southern boundary of mammoths' distribution is close to the southern boundary of the ice wedge cast distribution (and therefore close to the southern limit of severe permafrost). This demonstrates that the mammoth fauna is a typical component of Late Quaternary permafrost environments.

Acknowledgments

We should like to thank L. D. Sulerzhitskij from the Geological Institute of the Russian Academy of Sciences for field assistance at the Kolyma River, for interesting discussions on ^{14}C dating of mammoth remains, for ^{14}C analyses and helpful comments on the manuscript. We acknowledge our debt to T. Kaare for the revision of the English text. Sincere thanks are due to A. Long, C. V. Haynes and an anonymous reviewer for critically reading and correcting the manuscript.

REFERENCES

Aaris-Sorensen, K., Petersen, K., Strand, L. and Tauber, H. 1990 Danish finds of mammoth (*Mammuthus primigenius* (Blumenbach)); stratigraphical position, dating and evidence of Late Pleistocene environment. *Danmarks Geologiske Undersogelse* B14: 1–44.

Agenbroad, L. D. and Mead, J. I. 1989 Quaternary geochronology and distribution of *Mammuthus columbi* on the Colorado Plateau. *Geology* 17(9): 861–864.

Belaya, B. V. and Kisterova, I. B. 1978 Palynological data received in connection with finding a mammoth in summer 1977. *Materials on Geology and the Use of Full Minerals in the Northeast of the USSR* 24: 250–250 (in Russian).

Belorusova, J. M., Lovelius, N. V. and Ukraintseva, V. V. 1977 Paleogeography of the Late Pleistocene and Holocene in the area of the Selerican horse find. *Proceedings of the Zoological Institute* (Moscow) 63: 265–276 (in Russian).

Berglund, B. E., Hakansson, S. and Lagerlund, E. 1976 Radiocarbon-dated mammoth (*Mammuthus primigenius* Blumenbach) finds in South Sweden. *Boreas* 5(3): 177–191.

Coope, G. R. and Lister, A. M. 1987 Late-glacial mammoth skeletons from Condover, Shropshire, England. *Nature* 330(6147): 472–474.

Donner, J., Jungner, H. and Kurten, B. 1979 Radiocarbon dates of mammoth finds in Finland compared with radiocarbon dates of Weichselian and Eemian deposits. *Bulletin of the Geological Society of Finland* 51(1–2): 45–54.

Follestad, B. A. and Olsson, I. U. 1979 The ^{14}C age of the "Toten" mammoth, Eastern Norway. *Boreas* 8 (3): 307–312.

Gorlova, R. N. 1982 The plant macroremains found in the enteron tract of the Yuribeyskiy mammoth. *In* Sokolov, V. E., ed., *The Yuribeyskiy Mammoth.* Moscow, Nauka: 37–43 (in Russian).

Grant, V. 1985 *The Evolutionary Process: A Critical Review of Evolutionary Theory.* New York: Columbia University Press: 499 p.

Guthrie, R. D. 1990 *Frozen Fauna of the Mammoth Steppe: The Story of Blue Babe.* Chicago, University of Chicago Press: 323 p.

Hakansson, S. 1976 University of Lund radiocarbon dates IX. *Radiocarbon* 18(3): 290–320.

Haynes, C. V. 1993 Contributions of radiocarbon dating to the geochronology of the peopling of the New World. *In* Taylor, R. E., Long, A. and Kra, R. S., eds., *Radiocarbon After Four Decades: An Interdisciplinary Perspective.* New York, Springer-Verlag: 355–374.

Heintz, A. N. and Garutt, V. E. 1965 Determination of the absolute age of the fossil remains of mammoths and wooly rhinoceros from the permafrost in Siberia. *Norsk Geologisk Tidsskrift* 45: 73–79.

Johnson, D. L. 1978 The origin of island mammoths and the Quaternary land bridge history of the Northern Channel Island, California. *Quaternary Research* 10(2): 204–225.

Jungner, H. and Sonninen, E. 1983 *Radiocarbon Dates 2.* Helsinki, Radiocarbon Dating Laboratory, University of Helsinki: 121 p.

Kurten, B. 1968 *Pleistocene Mammals of Europe.* London, Weidenfeld & Nocolson: 317 p.

Kupriyanova, L. A. 1957 The analyses of pollen and plant remains from the stomach of the Beryosovka River mammoth (on the question of vegetation character in the epoch of the Beryosovka River mammoth). In *Articles Devoted to the Memory of A. N. Krishtofovich.* Vol. 4. Moscow–Leningrad. Academy of Science of the USSR: 331–358 (in Russian).

Lister, A. M. and Sher, A. V. 1995 Ice cores and mammoth extinction. *Nature* 378: 23–24.

Long, A., Sher, A. and Vartanyan, S. 1994 Holocene mammoth dates. *Nature* 369: 364.

Maarleveld, G. C. 1976 Periglacial phenomena and the mean annual temperature during the last glacial time in Netherlands. *Bulletin Periglacjalniy* 26: 57–78.

Meltzer, D. J. and Mead, J. I. 1985 The timing of Late Pleistocene mammalian extinctions in Northern America. *Quaternary Research* 19: 130–135.

Semken, H. A. 1983 The Holocene mammalian record of the eastern and central United States. *In* Wright, H. E., Jr., ed., *Late Quaternary Environments of the United States.* Vol. 2, *The Holocene.* Minneapolis, University of Minnesota Press: 182–207.

Shilo, N. A., Lozhkin, A. V., Titov, E. E. and Shumilov, Yu. V. 1983 *The Kirgilyakh Mammoth.* Moscow, Nauka: 214 p. (in Russian).

Sokolov, V. E., ed. 1982 *The Yuribeyskiy Mammoth.* Moscow, Nauka: 160 p. (in Russian).

Solonevich, N. G., Tikhomirov, B. A. and Ukraintseva, V. V. 1977 The preliminary results of the study of plant remnants from the enteron of Shandrin mammoth (Yakutia). In *Proceedings of the Zoological Institute,* (Moscow) 63: 277–280.

Stafford, T. W., Jr., Jull, A. J. T., Brendel, K., Duhamel, R. C. and Donahue, D. 1987 Study of bone radiocarbon dating accuracy at the University of Arizona NSF Accelerator Facility for Radioisotope Analysis. *Radiocarbon* 29(1): 24–44.

Stuart, A. J. 1991 Mammalian extinctions in the Late Pleistocene of Northern Eurasia and North America. *Biological Reviews* 66: 453–562.

Sulerzhitskij, L. D. 1995 Features of radiocarbon chronology of the mammoths (*Mammutus primigenius*) of Siberia and Northeastern Europe. *In* Baryshnikov, G., ed., Studies of Pleistocene and Recent Mammals. *Proceedings of the Zoological Institute* (St. Petersburg) 263: 163–183 (in Russian).

Sukachev, V. N. 1914 The study of the plant remnants from food of the mammoth found at Beryosovka

River, Yakutia area. In *Scientific Results of the Expedition of the Imperator Academy of Science for Excavation of the Mammoth Found at Beryosovka River in 1901*. Petersburg: 1–18.

Tikhomirov, B. A. and Kupriyanova, L. A. 1954 The study of pollen from plant remains from food of Beryosovka River mammoth. *Transactions of the Academy of Science of the USSR* 95(6): 1312–1315 (in Russian).

Ukraintseva, V. V. 1979. The vegetation of warm intervals of the Late Pleistocene and the extinction of some large herbivorous mammals. *Botanical Journal of the Academy of Science of the USSR* 64(3): 318–330 (in Russian).

Vartanyan, S. L., Arslanov, Kh. A., Tertychnaya, T. V. and Chernov, S. B. 1995 Radiocarbon dating evidence for mammoths on Wrangel Island, Arctic Ocean, until 2000 BC. *Radiocarbon* 37(1): 1–6.

Vartanyan, S. L., Garutt, V. E. and Sher, A. V. 1993 Holocene dwarf mammoths from Wrangel Island in the Siberian Arctic. *Nature* 362: 337–340.

Vasil'chuk, Yu. K. 1992 *Oxygen Isotope Composition of Ground Ice (Application to Paleogeocryological Reconstructions)*. Vols. 1 and 2. Moscow, Theoretical Problems Department, Russian Academy of Science (in Russian).

____1993 Northern Asia cryolithozone evolution in Late Quaternary. In *Permafrost. Sixth International Conference, Beijing, China. Proceedings*. Vol. 1. Wushan, Guangzhou, South China University of Technology Press: 945–950.

Vasil'chuk, Yu. K. and Vasil'chuk, A. C. 1995 Climate variations during last Late Pleistocene cryochron 40–10 Kyr BP in Northern Eurasia. In *International Conference on Past, Present and Future Climate. Proceedings of the SILMU Conference Held in Helsinki, Finland*: 67–70.

Vereshchagin, N. K. 1979 *Why Did the Mammoths Become Extinct?* Leningrad, Nauka: 195 p. (in Russian).

Weber, F. R., Hamilton, T. D., Hopkins, D. M., Repenning, C. A. and Haas, H. 1981 Canyon Creek: A Late Pleistocene vertebrate locality in interior Alaska. *Quaternary Research* 16 (2): 167–180.

Zaklinskaya, E. D. 1954 On plant cover in the epoch of the Taimyr Peninsula mammoth. *Transactions of the Academy of Science of the USSR*. 98(3): 471–474 (in Russian).

APPENDIX: RADIOCARBON DATES OF MAMMOTH REMAINS IN EURASIA

No.	^{14}C date (yr BP), Lab code	Material dated	Site
Eastern Europe			
1	9780 ± 260 (TA-12)	Bone	Kunda Settlement
2	11,000 ± 200 (GIN-93)	Bone	Kostenki Settlement
3	12,200 ± 300 (IGAN-282)	Molar	TimonovkaI Settlement
4	12,630 ± 360 (GIN-4137)	Molar	Eliseevichi Settlement
5	12,900 ± 200 (OxA-709)	Molar	Mezhirichi Settlement
6	12,970 ± 140 (LU-102)	Molar	Eliseevichi Settlement
7	13,650 ± 180 (LU-153)	Molar	Yudinovo Settlement
8	13,680 ± 60 (GIN-6209)	Tusk	Sevsk Town
9	13,900 ± 200 (IGAN-78)	Bone	Avdeevo Settlement
10	13,950 ± 70 (GIN-5778)	Bone	Sevsk Town
11	14,100 ± 400 (GIN-4139)	Molar	Eliseevichi Settlement
12	14,290 ± 120 (GIN-2356)	Tusk	Or'ya Settlement
13	14,320 ± 270 (QC-897)	Molar	Mezhirichi Settlement
14	14,360 ± 150 (GIN-2913)	Bone	Shatrishche Settlment
15	14,400 ± 250 (OxA-712)	Molar	Mezhirichi Settlement
16	14,470 ± 100 (LU-126)	Molar	Eliseevichi Settlement
17	14,590 ± 140 (GIN-4136)	Molar	Eliseevichi Settlement
18	14,600 ± 200 (OxA-717)	Molar	Gontsy Settlement
19	14,700 ± 250 (OxA-715)	Molar	Chulatovo Settlement
20	14,700 ± 500 (GIN-2593)	Molar	Kintu Lake
21	15,100 ± 200 (OxA-719)	Molar	Mezin Settlement
22	15,100 ± 250 (OxA-716)	Molar	Berdyzh Settlement
23	15,110 ± 530 (LU-358)	Bone	Timonovka I Settlement
24	15,660 ± 180 (LU-127)	Molar	Yudinovo Settlement
25	15,245 ± 1080 (QC-900)	Molar	Mezhirichi Settlement
26	16,300 ± 700 (GIN-2002)	Molar	Timonovka I Settlement
27	16,850 ± 120 (GIN-4138)	Molar	Eliseevichi Settlement
28	17,340 ± 170 (LU-360)	Molar	Eliseevichi Settlement
29	17,930 ± 100 (LE-1432A)	Molar	Gagarino Settlement
30	18,300 ± 200 (GIN-3727)	Molar	Zaraisk Town
31	18,320 ± 280 (TA-121)	Bone	Byzovaya Settlement

32	18,690 ± 770 (LU-361)	Molar	Pogon Settlement
33	19,000 ± 300 (OxA-697)	Molar	Radomyshl' Settlement
34	19,200 ± 350 (OxA-718)	Molar	Kirillovka Settlement
35	19,200 ± 200 (LE-2946B)	Molar	Leski Settlement
36	19,280 ± 600 (KI-1058)	Bone	Mezhirichi Settlement
37	19,800 ± 350 (OxA-698)	Molar	Novgorod-Severski Town
38	20,150 ± 100 (LE-1432B)	Molar	Gagarino Settlement
39	20,300 ± 200 (LE-1602)	Molar	Sagaidak I Settlement
40	20,620 ± 100 (LE-1432C)	Molar	Gagarino Settlement
41	21,240 ± 200 (LE-1602a)	Molar	Sagaidak I Settlement
42	21,600 ± 2200 (GIN-4)	Molar	Mezin Settlement
43	22,000 ± 300 (GIN-3698)	Molar	Zaraisk Town
44	22,200 ± 300 (GIN-3634)	Bone	Kostenki Settlement
45	22,600 ± 300 (GIN-3633)	Bone	Kostenki Settlement
46	22,800 ± 300 (GIN-3632)	Bone	Kostenki Settlement
47	23,430 ± 180 (LU-104)	Molar	Berdyzh Settlement
48	23,660 ± 270 (LU-359)	Molar	Khotylevo Settlement
49	23,770 ± 1540 (LE-2946A)	Molar	Leski Settlement
50	24,600 ± 150 (LE-2624)	Molar	Anetovka II Settlement
51	24,950 ± 400 (IGAN-73)	Molar	Khotylevo Settlement
52	25,000 ± 300 (GIN-2463)	Bone	Nizhniy Novgorod Region
53	25,300 ± 400 (GIN-6143)	Molar	Lower Kama River
54	26,470 ± 420 (LU-125)	Molar	Yurovichi Settlement
55	27,500 ± 800 (KI-1051)	Molar	Mezin Settlement
56	27,700 ± 500 (GIN-5880)	Bone	Sungir', Vladimir Region
57	30,500 ± 900 (LU-60)	Bone	Tver' Region
58	32,100 ± 500 (GIN-6146)	Molar	Lower Kama River
59	35,100 ± 1000 (GIN-6633)	Soft tissue	Starun Town
60	37,000 ± 500 (GIN-6141)	Molar	Lower Kama River
61	37,300 ± 1000 (GIN-6142)	Molar	Lower Kama River
62	37,600 ± 400 (GIN-3231)	Molar	Viliya River (Neman)
63	38,400 ± 1000 (GIN-6148)	Molar	Lower Kama River
64	42,200 ± 300 (GIN-6410)	Tusk	Novopetrovskoe Settlement, Moscow Region
65	43,600 ± 1000 (GIN-6145)	Molar	Lower Kama River
66	44,000 ± 1000 (GIN-6144)	Molar	Lower Kama River
67	44,200 ± 1000 (GIN-6147)	Molar	Lower Kama River
68	>47,700 (GIN-7075)	Bone	Pavlovsk, Voronezh Region
North of European Russia			
69	18,320 ± 280 (TA-121)	Bone	Pechora River
70	29,300 ± 300 (GIN-7575)	Molar	Bol'shezemel'skaya tundra
71	>36,000 (IEMAE)	Tusk	Kanin Peninsula
Western Siberia			
72	12,860 ± 90 (SOAN-1283)	Bone	Irtysh River, W.S.
73	13,350 ± 60 (GIN-7539)	Bone	Krasnoyarsk Town
74	13,930 ± 80 (GIN-7541)	Bone	Krasnoyarsk Town
75	14,240 ± 160 (SOAN-78)	Bone	Volch'ya Griva Settlement
76	18,600 ± 2000 (GIN-2862)	Bone	Middle Enisey River
77	19,500 ± 200 (GIN-2859)	Bone	Middle Enisey River
78	19,700 ± 200 (GIN-2861)	Tusk	Middle Enisey River
79	19,960 ± 80 (GIN-3016)	Bone	Chulym River
80	20,100 ± 100 (GIN-2863)	Tusk	Middle Enisey River
81	20,100 ± 300 (GIN-3017)	Bone	Middle Enisey River
82	20,400 ± 240 (SOAN-1513)	Tusk	Mogochino Settlement
83	20,200 ± 100 (GIN-2860)	Bone	Chulym River
84	41,900 ± 800 (GIN-5337)	Molar	Tavda River
North of Western Siberia			
85	9600 ± 300 (VSEGINGEO)	Soft tissue	Yuribey River
86	9730 ± 100 (MGU-763)	Stomach contents	Yuribey River
87	10,000 ± 70 (LU-1153)	Stomach contents	Yuribey River
88	10,350 ± 50 (GIN-6386)	Molar	Seyakha Mutnaya River
89	14,400 ± 80 (GIN-7292)	Bone	Seyakha Zelyonaya River
90	17,500 ± 300 (GIN-7576)	Molar	Parisento River
91	25,400 ± 300 (GIN-2210)	Bone	Upper Yuribey River

92	27,200 ± 500 (GIN-2021b)	Molar	Yambuto Lake, Gydan
93	29,300 ± 300 (GIN-6386A)	Bone	Seyakha Mutnaya River,
94	30,250 ± 1800 (T-298)	Skin	Gyda River
95	34,500 ± 300 (GIN-6475A)	Tusk	Shchushch'ya River, Yamal
96	31,500 ± 600 (GIN-2201)	Bone	Yekaryauyakha River, Gydan
97	33,500 ± 1100 (T-298)	Blubber	Gyda River
98	34,500 ± 300 (GIN-6475A)	Tusk	Shchushch'ya River, Yamal
99	35,500 ± 1100 (T-298)	Blubber	Gyda River
Taimyr Peninsula			
100	9670 ± 60 (GIN-1828)	Tusk	Nizhnaya Taimyra River
101	9860 ± 50 (GIN-1495)	Molar	Nizhnaya Taimyra River
102	10,100 ± 100 (GIN-1489)	Molar	Engel'gard Lake
103	10,300 ± 100 (GIN-1828k)	Bone.	Nizhnaya Taimyra River
104	10,680 ± 70 (GIN-3768)	Bone	Nganasanskaya River
105	11,140 ± 180 (GIN-3067)	Molar	Taimyr Lake
106	11,450 ± 250 (T-297)	Soft tissue	Mamont River, Shrenk
107	12,100 ± 80 (GIN-1783)	Bone	Taimyr Lake, Baskura
108	12,260 ± 120 (GIN-2943r)	Bone	Severnaya River
109	12,450 ± 60 (GIN-3242)	Bone	Severnaya River
110	12,780 ± 80 (GIN-2677)	Bone	Bikada River
111	13,340 ± 240 (GIN-2758a)	Bone	Bolshaya Balachnya River
112	16,330 ± 100 (GIN-3130)	Mandible	Bolshaya Balachnya River
113	18,680 ± 120 (GIN-5046)	Tusk	Boderbo-Tarida River
114	20,400 ± 100 (GIN-3952)	Tusk	Dudypta River
115	22,750 ± 150 (GIN-3089)	Bone	Taimyr Lake, Baskura
116	23,500 ± 300 (GIN-2763a)	Tusk	Bolshaya Balachnya River
117	23,800 ± 400 (GIN-1296B)	Bone	Taimyr Lake, Sabler
118	24,900 ± 500 (GIN-2160)	Pelvis	Taimyr Lake, Baskura
119	25,100 ± 550 (LE-612)	Soft tissue	Pyasina River
120	26,700 ± 700 (GIN-1216)	Tusk	Gulya River
121	27,300 ± 200 (GIN-3836)	Tusk	Logata River
122	27,500 ± 300 (GIN-3929)	Tusk	Kubalakh River
123	27,500 ± 200 (GIN-3505)	Scalpula	Lygiy-Yurege River
124	28,800 ± 600 (GIN-952)	Tusk	Shrenk River
125	29,400 ± 400 (GIN-3310)	Tusk	Chaidachtar Lake
126	29,500 ± 300 (GIN-2155)	Tusk	Taimyr Lake, Matuda
127	31,800 ± 500 (GIN-3240a)	Bone	Severnaya River
128	31,900 ± 300 (GIN-5726)	Bone	Sualema River
129	32,000 ± 200 (GIN-3117)	Femur	Balakhnya River
130	32,000 ± 500 (GIN-2151)	Limb bone	Taimyr Lake, Matuda
131	35,000 ± 500 (GIN-3821)	Bone	Logata River
132	35,800 ± 2700 (T-169)	Skin	Mokhovaya River
133	36,200 ± 500 (GIN-3822)	Tusk	Logata River
134	36,800 ± 500 (GIN-3122)	Tusk	Bolshaya Balachnya River
135	36,950 ± 4300 (T-169)	Skin	Mokhovaya River
136	38,000 ± 1500 (GIN-942)	Tusk	Khatanga River
137	38,300 ± 600 (GIN-3817)	Tusk	Logata River
138	38,400 ± 700 (GIN-3118)	Tusk	Bolshaya Balachnya River
139	38,500 ± 500 (GIN-3136)	Bone	Boderbo-Tarida River
140	38,500 ± 500 (GIN-2763B)	Molar	Boderbo-Tarida River
141	38,800 ± 400 (GIN-3476)	Tusk	Nemudikatarida River
142	38,800 ± 1300 (GIN-1491)	Tusk	Trautfetter River
143	38,900 ± 600 (GIN-3831)	Tusk	Logata River
144	39,100 ± 700 (GIN-3120P)	Bone	Bolshaya Balachnya River
145	39,300 ± 500 (GIN-3121P)	Bone	Bolshaya Balachnya River
146	39,300 ± 500 (GIN-3071)	Bone	Taimyr Lake, Baykura
147	39,800 ± 600 (GIN-3135)	Bone	Boderbo-Tarida River
148	40,200 ± 600 (GIN-3804)	Tusk	Logata River
149	40,500 ± 800 (GIN-1818P)	Bone	Engel'gard Lake
150	40,800 ± 2000 (GIN-1835)	Bone	Taimyr Lake, Gofman
151	41,200 ± 1000 (GIN-2744B)	Bone	Boderbo-Tarida River
152	41,400 ± 2000 (GIN-3941)	Tusk	Shaitan Lake
153	42,800 ± 800 (GIN-3946)	Tusk	Massonov, Khatanga Riverbasin

154	43,500 ± 1000 (GIN-3072)	Bone	Taimyr Lake, Baykura
155	45,000 ± 1000 (GIN-766)	Bone	Kheta River
156	46,100 ± 1200 (GIN-3073)	Bone	Taimyr Lake, Baykura
157	47,900 ± 1600 (GIN-3118a)	Tusk	Bolshaya Balachnya River
158	>49,500 (GIN-3080)	Tusk	Taimyr Lake, Baykura
159	>49,500 (GIN-3092a)	Tusk	Bolshaya Balachnya River
160	>52,700 (GIN-2764B)	Bone	Boderbo-Tarida River
161	>53,170 (LU-1057)	Bone	Khatanga River
Central Siberia			
162	20,700 ± 150 (GIN-7709)	Bone	Belaya River (Angara)
163	21,600 ± 200 (GIN-7708)	Bone	Belaya River (Angara)
164	23,600 ± 200 (GIN-5886)	Bone	MiddleAngara River
165	41,100 ± 1500 (GIN-7707)	Bone	Belaya River (Angara)
166	49,700 ± 1100 (GIN-689)	Tusk	Maimechya River, Putoran
Northern Yakutia			
167	10,370 ± 70 (SOAN-327)	Bone	Berelyokh River
168	12,000 ± 130 (LU-149)	Tusk	Berelyokh River
169	12,240 ± 160 (LU-139)	Tusk	Berelyokh River
170	12,530 ± 60 (SOAN-2203)	Humerus	Achchaika-Allaikha River
171	12,570 ± 80 (MAG-826)	Humerus	Achchaika-Allaikha River
172	12,850 ± 110 (LU-1055)	Tusk	Berelyokh River
173	13,700 ± 800 (MAG-114)	Soft tissue	Berelyokh River
174	14,340 ± 50 (GIN-4115)	Tusk	Lena River
175	14,800 ± 50 (GIN-3518)	Tusk	Ulakhan-Yuryakh
176	17,780 ± 80 (GIN-5042)	Molar	Lower Lena River
177	18,680 ± 120 (GIN-5046)	Tusk	Bur, Olenyok River Basin
178	18,700 ± 100 (GIN-6099)	Tusk	Amydai, Olenyok Basin
179	21,260 ± 310 (LU-786)	Mandible	Lower Lena River
180	21,630 ± 240 (LU-1328)	Carpal	Bykovski Peninsula
181	22,000 ± 200 (GIN-5574)	Molar	Anabar River, Popigay
182	23,100 ± 200 (GIN-3232)	Pelvis	Tyung, Lena River
183	24,000 ± 1100 (GIN-7176)	Tusk	Kular Settlment
184	25,300 ± 600 (GIN-3502)	Bone	Yarasalakh River
185	26,000 ± 1600 (Mo-215)	Hair	Lena River, Chekurovka
186	28,600 ± 300 (GIN-3867)	Limb Bone	Duvanniy Yar, Kolyma River
187	28,900 ± 300 (GIN-5573)	Tusk	Anabar River, Popigay
188	29,400 ± 400 (GIN-3310)	Tusk	Anabar River
189	29,500 ± 3000 (T-170)	Soft tissue	Lena River, Sanga-Yuryakh
190	29,600 ± 500 (GIN-3234)	Vertebrae	Tyung River, Lena basin
191	30,400 ± 300 (GIN-6023a)	Bone	Khamus-Yuryakh River, Kolyma
192	31,500 ± 2000 (T-170)	Soft tissue	Lena River, Sanga-Yuryakh
193	31,750 ± 2500 (T-299)	Soft tissue	Beryosovka River
194	31,900 ± 300 (GIN-5726)	Ribs	Anabar Gulf, Sualema River
195	32,200 (500 (SOAN-1006B)	Stomach contents	Shandrin River
196	32,300 ± 400 (GIN-5074)	Tusk	Popigay River
197	32,650 ± 2500 (T-170)	Soft tissue	Lena River, Sanga-Yuryakh
198	33,800 ± 500 (GIN-3861)	Bone	Duvanny Yar, Kolyma River
199	34,450 ± 2500 (T-171)	Soft tissue	Lena River (Bykovskaya)
200	34,700 ± 400 (GIN-4434)	Bone	Duvanny Yar, Kolyma River
201	35,000 ± 300 (GIN-3503)	Bone	Laptev Sea coast
202	35,800 ± 1200 (T-171)	Soft tissue	Lena River (Bykovskaya)
203	35,830 ± 630 (LU-504)	Skin	Tirekhtyakh River
204	36,450 ± 420 (SOAN-1005)	Soft tissue	Shandrin River
205	36,600 ± 500 (GIN-5751)	Molar	Anabar River, Popigay
206	37,000 ± 500 (GIN-5750)	Molar	Semiriskai River, Popigay
207	39,400 ± 1000 (GIN-3517)	Bone	Laptev Sea coast
208	40,100 ± 500 (GIN-5726A)	Molar	Anabar Gulf
209	40,300 ± 400 (GIN-5025)	Molar	Anabarka River, Popigay
210	40,350 ± 880 (LU-595)	Stomach contents	Shandrin River
211	41,750 ± 1290 (LU-505)	Soft tissue	Shandrin River
212	41,900 ± 800 (GIN-5224)	Tusk	Anabarka River, Popigay
213	42,400 ± 800 (GIN-6310)	Molar	Khamus-Yuryakh Riv, Kolyma
214	43,200 ± 400 (GIN-6100)	Bone	Amydai, Olenyok Basin

215	43,700 ± 800 (GIN-3849)	Bone	Zelyoniy Mys Settlement
216	44,000 ± 3500 (T-170)	Soft tissue	Lena River, Sanga-Yuryakh
217	44,000 ± 3500 (T-299)	Soft tissue	Beryosovka River
218	44,540 ± 1900 (LU-1050)	Bone	Tirekhtyakh River
219	45,500 ± 1200 (GIN-6105)	Tusk	Amydai, Olenyok Basin
220	46,100 ± 1000 (GIN-3206)	Bone	Lower Kolyma River
221	49,500 (GIN-6101)	Tusk	Nekyu, Olenyok Basin
222	>50,000 (GIN-359)	Bone	Lower Lena River
223	>50,000 (GIN-5731)	Molar	Anabarka River, Popigay
224	>50,000 (SOAN-813)	Soft tissue	Tirekhtyakh River
225	>50,000 (GIN-3848)	Bone	Zelyoniy Mys Settlement
226	>50,000 (GIN-3866)	Bone	Duvanniy Yar, Kolyma River
227	50,400 ± 1300 (GIN-4114)	Tusk	Lower Lena River
228	>53,000 (GIN-3857)	Tusk	Duvanniy Yar, Kolyma River
229	>53,170 (LU-1057)	Skin	Tirekhtyakh River
Magadan Region			
230	21,600 ± 200 (GIN-6309)	Tusk	Tanon River
231	28,400 ± 300 (GIN-5696)	Tusk	Srednekan River
232	39,570 ± 870 (LU-718A)	Soft tissue	Kirgilyakh River
233	39,590 ± 770 (LU-718B)	Soft tissue	Kirgilyakh River
234	40,600 ± 700 (MAG-366A)	Soft tissue	Kirgilyakh River
235	41,000 ± 1100 (MAG-366B)	Soft tissue	Kirgilyakh River
236	41,000 ± 900 (MAG-576)	Soft tissue	Kirgilyakh River
Chukotka Peninsula			
237	14,380 ± 70 (GIN-7289)	Tusk	
238	15,100 ± 70 (GIN-5370)	Tusk	Mayn River
239	31,370 ± 900 (MAG-1000A)	Soft tissue	Enmynveem River
240	31,100 ± 900 (MAG-1000B)	Soft tissue	Enmynveem River
241	32,800 ± 720 (MAG-1001A)	Soft tissue	Enmynveem River
242	32,850 ± 900 (MAG-1000)	Soft tissue	Enmynveem River
243	32,890 ± 1200 (MAG-1001B)	Soft tissue	Enmynveen River
244	32,000 ± 3000 (MAG-1124)	Soft tissue	Enmynveem River
Kamchatka Peninsula			
245	12,630 ± 50 (GIN-3420)	Tusk	Kamchatka River, Urz
246	21,300 ± 400 (GIN-2224)	Skull	Pakhtcha River
247	21,750 ± 150 (GIN-5299b)	Tusk	Kamchatka River
248	30 000 ± 300 (GIN-3415)	Tusk	Kamchatka River
249	36,000 ± 500 (GIN-3425)	Tusk	Kamchatka River
250	39,600 ± 1600 (GIN-3411)	Molar	Kamchatka River
251	40,600 ± 600 (GIN-3407)	Tusk	Kamchatka River
Arctic Islands			
252	3730 ± 40 (LU-2741)	Tusk	Wrangel Island
253	3920 ± 30 (GIN-6980)	Tusk	Wrangel Island
254	4010 ± 50 (LU-2798)	Molar	Wrangel Island
255	4040 ± 30 (LU-2808)	Tooth	Wrangel Island
256	4400 ± 40 (LU-2756)	Tusk	Wrangel Island
257	4410 ± 50 (LU-2768)	Tusk	Wrangel Island
258	4740 ± 40 (LU-2556)	Tibia	Wrangel Island
259	4900 ± 40 (LU-2740)	Tusk	Wrangel Island
260	5110 ± 40 (LU-2794)	Molar	Wrangel Island
261	5200 ± 30 (LU-2745)	Tusk	Wrangel Island
262	5250 ± 40 (LU-2744)	Tusk	Wrangel Island
263	5310 ± 90 (LU-2742)	Tusk	Wrangel Island
264	5480 ± 50 (LU-2535)	Tusk	Wrangel Island
265	6260 ± 50 (LU-2799)	Molar	Wrangel Island
266	6360 ± 60 (AA-11529)	Molar	Wrangel Island
267	6610 ± 50 (LU-2558)	Tusk	Wrangel Island
268	6760 ± 50 (LU-2736)	Tusk	Wrangel Island
269	6890 ± 50 (LU-2810)	Tooth	Wrangel Island
270	7040 ± 60 (LU-2746)	Tusk	Wrangel Island
271	7250 ± 60 (LU-2809)	Molar	Wrangel Island
272	7295 (95 (AA-11530)	Molar	Wrangel Island
273	7360 ± 50 (LU-2559)	Tusk	Wrangel Island

274	7390 ± 30 (LU-2444)	Tusk	Wrangel Island
275	7710 ± 40 (GIN-6995)	Tusk	Wrangel Island
276	11,500 ± 60 (LU-610)	Tusk	Severnaya Zemlya
277	12,010 ± 110 (LU-2823)	Molar	Wrangel Island
278	12,750 ± 50 (GIN-6987)	Tusk	Wrangel Island
279	12,980 ± 80 (LU-2792)	Molar	Wrangel Island
280	15,420 ± 100 (LU-1671)	Tusk	Kotel'niy Island
281	19,270 ± 300 (LU-654B)	Tusk	Severnaya Zemlya
282	19,970 ± 110 (LU-688)	Molar	Severnaya Zemlya
283	19,990 ± 110 (LU-1790)	Tusk	Kotel'niy Island
284	20 000 ± 110 (LU-2807)	Molar	Wrangel Island
285	20,900 ± 100 (GIN-5760)	Tusk	Faddeevskiy Island
286	25,030 ± 210 (LU-749B)	Tibia	Severnaya Zemlya
287	25,800 ± 200 (GIN-4710B)	Tusk	Faddeevskiy Island
288	28,000 ± 200 (GIN-4710)	Tusk	Faddeevskiy Island
289	29,020 ± 190 (LU-1791)	Tusk	Kotel'niy Island
290	29,100 ± 400 (GIN-4330)	Bone	Faddeevskiy Island
291	29,100 ± 1000 (GIN-4711)	Tusk	Faddeevskiy Island
292	32,100 ± 900 (MAG-316)	Skin	Lyakhovskiy Bolshoiy Island
Denmark			
293	13,240 +760/−690 (K-3697)	Tusk	Rosmos 1
294	21,530 ± 430 (K-3703)	Bone	Myrup Banke
295	24,190 ± 420 (K-3806)	Tusk	Munke Bjergby
296	25,110 ± 440 (K-3699)	Tusk	Hadsund
297	25,480 +560/−520 (K-3809)	Tusk	Ostrupgard
298	25,520 +920/−830 (K-3805)	Tusk	Ny Stengaard
299	25,760 +840/−770 (K-3805)	Tusk	Ny Stengaard
300	26,270 +1400/−1210 (K-3805)	Tusk	Ny Stengaard
301	27,810 ± 610 (K-4192)	Tusk	Stengardens Grusgrav 2
302	28,120 +760/−680 (K-3808)	Tusk	Ronninge 1
303	29,570 ± 950 (K-3807)	Tusk	Saxkobing
304	31,840 +1010/−870 (K-3696)	Tusk	Kiskelund
305	32,460 +970/−870 (K-4190)	Tusk	Lundebjerg 1
306	>37,900 (K-4191)	Tusk	Sonder Kollemorten
307	>39,500 (K-4188)	Tusk	Sonder Omme
308	>39,600 (K-4587)	Tusk	Rosmos 2
Germany			
309	15,810 ± 410 (HV-1961)	Molar	Kelsterbach
310	30,300 +2500/−1900 (Fra-5a)	Femur	Kelsterbach
Switzerland			
311	12,270 ± 210 (Ly-877)	Tusk	Praz Rodet
312	34,600 +2700/−1800 (Ly-751)	Tusk	Bioley-Orjulaz
Poland			
313	20,200 ± 350 (OxA-635)	Bone	Spadzista Street, Krakow
314	20,600 ± 1050 (Ly-631)	Bone	Spadzista Street, Krakow
315	21,000 ± 900 (Ly-2542)	Bone	Spadzista Street, Krakow
316	23,040 ± 170 (GrN-6636)	Bone	Spadzista Street, Krakow
France			
317	12,000 ± 220 (Ly-1351)	Scapula	Etiolles
318	14,330 ± 260 (Ly-357)	Bone	La Croze-sur-Suran 1
319	14,390 ± 300 (Ly-433)	Bone	La Columbière rockshelter
320	14,850 ± 350 (Ly-434)	Bone	La Croze-sur-Suran 2
321	25,800 ± 700 (Ly-1863)	Tusk	La Mère Clochette Grotto
Ireland			
322	33,500 ± 1200 (D-122)	Molar	Castlepook Cave, Cork
Great Britain			
323	11,650 ± 130 (OxA-2155)	Ivory rod	Kent's Cavern
324	12,080 ± 130 (OxA-1457)	Skull	Condover, Shropshire
325	12,170 ± 130 (OxA-1890)	Ivory rod	Cough's Cave
326	12,300 ± 180 (OxA-1316)	Molar	Condover, Shropshire
327	12,320 ± 120 (OxA-1462)	Tusk	Robin Hood's cave
328	12,330 ± 120 (OxA-1456)	Molar	Condover, Shropshire

329	12,400 ± 160 (OxA-1455)	Tusk	Condover, Shropshire
330	12,460 ± 160 (OxA-1204)	Calcaneum	Condover, Shropshire
331	12,480 ± 96 (Birm-1273com.)	Tusk	Condover, Shropshire
332	12,700 ± 160 (OxA-1021)	Tusk	Condover, Shropshire
333	12,920 ± 390 (Birm-1273)	Tusk	Condover, Shropshire
334	18,000 +1400/−1200 (Birm-146)	Bone	Cae Gwyn Cave, Wales
335	19,300 ± 700 (Gif-1110)	Bone	Condover, Shropshire
336	26,700 ± 550 (OxA-1205)	Bone	Pin Hole Cave, Creswell
337	33,200 ± 1300 (OxA-1069)	Bone	Conningbrook, Kent
338	34,500 ± 500 (Birm-466)	Bone	Little Rissington
339	34,850 ± 1500 (OxA-1654)	Molar	King Arthur's Cave
340	35,200 ± 1600 (OxA-1610)	Bone	Conningbrook, Kent
341	37,020 +1900/−1350 (Q-2500)	Tusk	Farnham, Surrey
342	37,300 ± 1900 (OxA-1644)	Bone	Conningbrook, Kent
343	38,500 ± 2300 (OxA-1565)	Molar	King Arthur's Cave
344	38,600 ± 2400 (OxA-1611)	Bone	Conningbrook, Kent
345	38,600 +1720/−1420 (NPL-1628)	Tusk	Oxbow, Leeds
346	>39,500 (OxA-1566)	Molar	King Arthur's Cave
Finland			
347	15,500 ± 200 (Hel-1074)	Humerus	Herttoniemi
348	25,200 ± 500 (Hel-1075)	Femur	Lohtaja
349	>43,000 (Hel-1076)	Molar	Espoo
Norway			
350	19,000 ± 1200 (U-4214)	Tusk	Toten, Opland
351	20 000 ± 250 (K-3703)	Tusk	Favang
352	22,370 ± 980 (K-3703)	Tusk	Favang
353	24,400 ± 900 (K-3806)	Tusk	Kvam
354	28,100 +2300/−1800 (U-2766)	Tusk	Toten, Opland
355	32,100 +3100/−2300 (U-4214)	Tusk	Toten, Opland
Sweden			
356	13,090 ± 120 (Lu-796, 2)	Tusk	Lockarp
357	13,260 ± 110 (Lu-865)	Tusk	Lockarp
358	13,360 ± 95 (Lu-796)	Tusk	Lockarp
359	19,150 ± 390 (Lu-887E)	Tusk	Arrie
360	22,000 +900/−800 (Lu-887)	Tusk	Arrie
361	31,200 +3050/−2650 (Lu-746)	Tusk	Orsjo
362	36,000 +1550/−1300 (Lu-879)	Tusk	Dosebacka
363	36,100 +2000/−1600 (Lu-880)	Tusk	Orsjo

References: Berglund, Hakansson and Lagerlund 1976; Follestad and Olsson 1979; Orlova 1979; Jungner and Sonninen, 1983; Aaris-Sorensen *et al.* 1990; Stuart 1991; Vasil'chuk 1992; Svezhentsev and Popov 1993; Vartanyan, Garutt and Sher 1993; Vartanyan *et al.* 1995; Sulerzhitskij 1995.

[RADIOCARBON, VOL. 39, NO. 1, 1997, P. 19–26]

RADIOCARBON AMS DATING OF POLLEN CONCENTRATED FROM EOLIAN SEDIMENTS: IMPLICATIONS FOR MONSOON CLIMATE CHANGE SINCE THE LATE QUATERNARY

WEIJIAN ZHOU,

National Laboratory of Loess and Quaternary Geology, Xi'an 710054 China

DOUGLAS DONAHUE and A. J. T. JULL

NSF-Arizona AMS Facility, University of Arizona, Tucson, Arizona 85721 USA

ABSTRACT. Dating pollen concentrated from eolian sediments provides a new way to establish a chronological framework on the Loess Plateau of China. We show that pollen deposited simultaneously with sediment in a stable environment can provide reliable ages. We suggest that the reliability of pollen dating can be evaluated by comparison with wood cellulose or charcoal ages from the same stratigraphic level. Dating pollen concentrates from the various profiles indicates paleomonsoon precipitation variability at the loess/desert transitional belt from the late Pleistocene to the early Holocene.

INTRODUCTION

Loess-paleosol ^{14}C dating in the loess Plateau of China has been limited by the lack of suitable dating material. Previously, datable materials included mainly organic matter in soil, which generally provides a minimum age, owing to the presence of younger organic materials brought in by agriculture or atmospheric carbon incorporated through plant growth (Head, Zhou and Zhou 1989).

In this paper, we evaluate the use of fossil pollen as a dating material. Pollen concentrated from sediments can be dated on the basis of the following postulates. 1) Pollen is produced annually and deposited *in situ* in sediment; its exine or outer layer is composed of sporopollenin, which is very stable and does not exchange carbon with sediment. 2) Pollen undergoes limited translocation in loess-paleosol, <10 cm (Wu *et al.* 1992), because at the loess/desert belt (which belongs to the arid steppe environment, with low annual precipitation and scarce vegetation cover), soil development is very weak, although mixing and percolation occur in the pedogenic process (Dimbleby 1985). 3) Pollen is an abundant plant fossil, well preserved in sediment, and accelerator mass spectrometry (AMS) technology allows the analysis of <500 μg of carbon. 4) Pollen is predominantly of terrestrial origin, and its age should not be influenced by reservoir effects (Regnell 1992).

Brown *et al.* (1989, 1992) showed that separation of pollen and pollen concentrates from lake sediments provides a dating material that is potentially superior to any sediment components used previously. Long, Davis and Lanois (1992) developed procedures for physically removing non-pollen contaminants from pollen concentrates, achieving high-precision dates. Based on their work, we developed and modified a procedure suitable for the extraction of pollen concentrate from eolian sediments.

DESCRIPTIVE BACKGROUND

This study focused on five profiles at the present northwestern margin of the Loess Plateau (Fig. 1), *i.e.,* at the loess/desert transitional belt. Loess-mantled hills, sandy loess platforms (*yuan*) and seasonally flowing streams characterize the landscape of this area. In winter, the area has predominantly northerly and northwesterly winds, generating frequent dust storms. In summer, the main winds are southeasterly, moving inland off the ocean and producing 80% of the annual precipitation that falls as rainstorms (Zhang and Lin 1992). Mean annual temperature is 8°C; mean annual precipitation is *ca.* 200–400 mm.

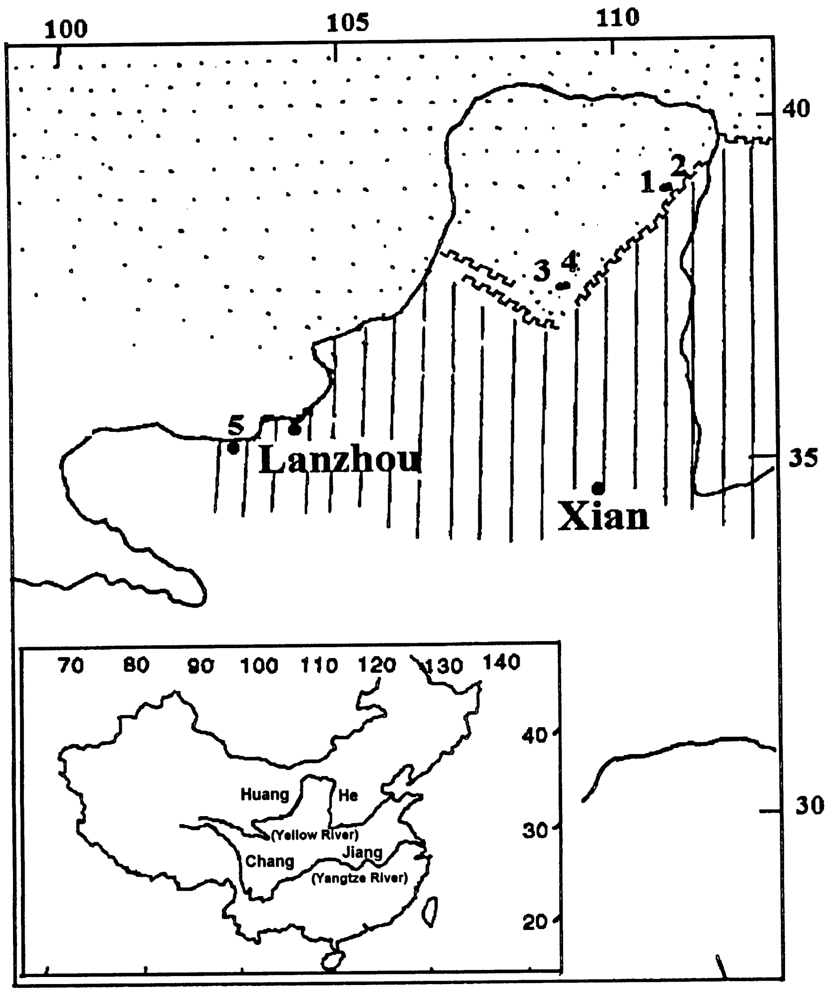

Fig. 1. Map showing study sites and the northern margin of the Loess Plateau. 1. Shiyaowan; 2. Yangtaomao; 3. Xuanheze; 4. Midiwan; 5. Baxie at the loess/desert transitional belt. The inset map shows China and the Yellow River.

The Xuanheze profile (37°39′N,108°37′E, at a mean elevation of 1400 m) has a 500-cm exposure of sediment (Figs. 1 and 2a). It is located on the second terrace of Xuanhe, a seasonal tributary of the Heiheze River, which is a second-order tributary of the Huanghe (Yellow River). The lowest 60 cm is a grayish-green silty mud. From 440 to 200 cm depth it is characterized by an eolian sand. Grayish-white marl occurs between 200 and 50 cm from the top of the sediment column. The top 50 cm consists of a grayish-green silty mud. The Midiwan profile (Fig. 1) occurs *ca.* 500 m to the east, located on the first terrace of Xuanhe River, with 1380 cm of peat sediment. Based on the ^{14}C chronology, peat deposition in the lake basin began *ca.* 13,000 BP, reflecting the onset of a warm-moist climate in the last deglaciation. Peat deposition reached maximum thickness *ca.* 10,000–7500 BP, during the Holocene Optimum. The section of the Midiwan profile is high-resolution and appears to be continuous. A detailed study of this profile has been given elsewhere (Zhou *et al.* 1996; Zhou 1995).

The Yangtaomao profile (38°48′N, 110°27′E, at a mean elevation of 1400 m) consists of sand and interstratified paleosol exposed by wind erosion at the top of a loess-mantled hill (Zhou *et al.* 1996). The section of the studied profile (Figs. 1 and 2c) consists of the upper 350 cm, below which loess is found. From 350–315 cm is an immature sandy paleosol. Pale-yellow eolian sand at 315–157 cm depth contains a 38-cm-thick immature sandy paleosol (242–204 cm depth). The top 157 cm consists of a dark grayish-brown paleosol complex interstratified with an eolian sand layer 40-cm thick (78–38 cm depth). This soil complex consists of well-developed sandy steppe-type paleosol and is poorly consolidated. Located *ca.* 500 m to the west of the Yangtaomao section is a 2-m-thick exposure of the Shiyaowan profile (Figs. 1 and 2b). This section consists of eolian sand (200–150 cm) and grayish-brown paleosol (150–0 cm).

The Baxie loess section is located at the southwest margin of the Loess Plateau, 65 km southwest of Lanzhou (35°33′N, 103°35′E, 2000 m elevation), The stratigraphy of this profile was studied in detail by Zhou *et al.* (1992) and An *et al.* (1993). Here, we tried to redate one sample from the Baxie paleosol (where there was evidence for an increase of precipitation during the Younger Dryas interval), in order to compare dating of pollen concentrate with that of humic acid.

Methods

Separation of the pollen concentrates is based on both particle size and specific gravity (Table 1). Pollens from semi-arid to arid zones are mostly silt-sized. Before removing sand grains (> 40 μm) from the silt fraction by sieving, we used 5% HCl to disaggregate carbonate clay. The mesh size of the sieve was also selected to eliminate organic detritus larger than most pollen. Then, we further

TABLE 1. Flowchart for Pollen Concentrate Preparation

200 g paleosol or 10 g peat
↓
Hot 5% HCl for 30 min
↓
Sieving at 40 μm
↓
Hot 40% HF for 30 min
↓
Hot 10% HCl for 10 min repeated
↓
Hot 5% NaOH for 20 min repeated
→
Hot 10% HCl for 10 min. Rinsed with distilled H_2O
↓
Floating selection with 2.2 gm cm^{-3}, centrifuge at 5000 rpm min^{-1} for 5 min.
↓
5% HCl for 24 h
↓
$NaClO_2$ bleaching for 3 min
↓
10% HCl, then rinsed with H_2O
↓
Pollen concentrate for AMS dating

removed $CaCO_3$ with 5% HCl, humic acid with 10% NaOH, and silica with 40% HF. Because pollen from semi-arid to arid zones ranges in specific gravity from 2.2 to 1.5, we floated pollen out of the sediment using a heavy liquid (KI + HI + Zn) with a specific gravity (sp. gr.) of 2.2 g cm^{-3}. The liquid was then diluted with water to sp. gr. of < 1.5 to sediment the material. To increase pollen recovery, the extraction step was repeated twice, as sand, loess and paleosol are low in pollen compared to other sediments. Ke (1994) pointed out that flotation with a heavy liquid of sp. gr. *ca.* 2.2 is especially efficient for pollen extraction from loess-paleosol samples. Before we carried out the flotation method with a heavy liquid of sp. gr. 2.2, we tried the method proposed by Brown *et al.* (1992), but failed to extract enough pollen from eolian sand and paleosol for dating. Therefore, we developed a method combining particle size separation with floating in a heavy liquid, which enabled successful extraction of pollen from sand and paleosol. After pollen extraction, we found that our pollen concentrates consisted of 50% pollen (mainly *Artemisia* and Chenopodiaceae), 45% phytoliths (considered to be a reliable alternative source for ^{14}C dating (Wilding 1967; Mulholland 1992)) and 0–5% organic fragments. Careful microscope identification showed no soil fungi spores in the samples we studied. Because spores of soil fungi are the products of humid forest soil, generally they adhere to residues of higher plants (Cao 1980). Since the objective is to date the original carbon, any younger material adhering to the pollen particles must be removed. We used an oxidizer of 2% $NaClO_2$ for cleaning pollen concentrates. Because $NaClO_2$ is a very strong oxidizer and destroys lignin and humic acids, but is also corrosive to pollen grains, we used the weak solution for a short period, *e.g.*, no longer than 5 min. Pollen samples were then treated further with 10% HCl, rinsed with distilled water and dried.

Ca. 500 mg of extracted pollen concentrates was combusted in a sealed tube with CuO. The CO_2 was reduced to graphite (Slota *et al.* 1987) for AMS dating (Donahue, Jull and Zabel 1984).

Results and Discussion

Pollen dating results from the various profiles are shown in Tables 2–4. In order to evaluate the reliability of pollen concentrate dating, we re-collected four samples. Three samples are from the well-dated Midiwan peat profile (Zhou *et al.* 1996), containing wood, charcoal, and peat (Table 2) and the others from Baxie paleosol for pollen concentrate dating. We can compare ages of wood cellulose and pollen (958 cm, 10,370 ± 70 (AA-12190); 10,360 ± 65 (AA-12186)), peat and pollen (1112 cm, 11,755 ± 95 (AA-16691); 11,765 ± 80 (AA-12188)), and charcoal and pollen (1143 cm, 12,750 ± 95

TABLE 2. AMS Result Comparison of Pollen Concentrates with Other Dating Material from Midiwan Peat and Baxie Loess Profiles

Lab Code*	Depth (cm)	Material dated	^{14}C age (yr BP)
AA-12190	958	Wood cellulose	10,370 ± 70
AA-12186†	958	Pollen concentrate	10,360 ± 65
AA-16691	1112	Fine peat	11,755 ± 95
AA-12188†	1112	Pollen concentrate	11,765 ± 80
AA-12196†	1143	Pollen concentrate	12,390 ± 100
AA-16393	1143	Charcoal	12,750 ± 95
AA-16389	973	Charcoal	10,610 ± 80
AA-6442	925	Humic acid	9695 ± 95‡
M12566†	925	Pollen concentrate	10,630 ± 70‡

*AA- = NSF-AMS Facility, The University of Arizona
†Re-collected samples for pollen dating research
‡from Baxie loess profile

(AA-16393); 12,390 ± 100 (AA-12196)). These values are in good agreement and indistinguishable within each pair within one standard deviation, indicating that pollen concentrate dating is reproducible. As for the Baxie paleosol (An *et al.* 1993), which indicates a precipitation increase during the Younger Dryas on the Loess Plateau, the new pollen-concentrate age (935 cm depth, 10,630 ± 70 BP (AA-12566)) is *ca.* 900 yr older than the previous humic-acid age (925 cm depth, 9695 ± 95 (AA-6442)), although there is 10 cm difference in sample depth. The new pollen concentrate age on Baxie paleosol agrees with a recent charcoal age on the Midiwan peat, which is regarded as an indicator of increased precipitation in the mid Younger Dryas (AA-16389, 10,610 ± 80; Zhou *et al.* 1996). This obviously suggests that pollen concentrate dating improves upon the age of humic acid from paleosol.

We applied this method to the chronology of these various profiles, with very interesting results (Tables 3 and 4; Fig. 2). Terrace two in the Xuanheze profile (Fig. 2a) shows that pollen concentrate ages form a good age sequence, except for one date from eolian sand: at 330 cm depth, AA-16120, the pollen concentrate dated *ca.* 10,000 yr younger than the one above at 200 cm depth, AA-16119. Since the sand layer generally deposits rapidly, it is hard to believe that it took *ca.* 10,000 yr for the deposition of *ca.* 250 cm-thick sand. Accordingly, sample AA-16120 must contain younger pollen or organic detritus, and it should be discarded. The silty mud layer of the profile may correspond to the mud layer of the Beizhuangcun profile from the Loess Plateau (28,400 ± 340 BP, XLLQ28, Zhou, Zhou and Head 1990) and possibly further to the later oxygen isotope stage 3 of deep sea cores (Imbrie *et al.* 1984), reflecting cool and wet climatic conditions in East Asia. Moreover, we expect that dating of pollen concentrates from the Shiyaowan paleosol (Fig. 2b and Table 4) should provide reliable ages. These results generally agree with those from Midiwan peat (Zhou *et al.* 1996), indicating that warm and moist monsoon climate was favorable to paleosol development between *ca.* 11,680 and 13,700 BP, during the climatic conditions of the last deglaciation.

TABLE 3. AMS Dating Result of Pollen from Xuanheze Eolian Sand-Paleosol Profile

Lab code	Depth (cm)	Material dated	^{14}C age (yr BP)
AA-16118	170	Pollen concentrate	27,910 ± 330
AA-16119	200	Pollen concentrate	27,540 ± 320
AA-16120	330	Pollen concentrate	17,315 ± 130
AA-16121	490	Pollen concentrate	28,730 ± 790

Table 4 and Figure 2c show pollen concentrate ages obtained from Yangtaomao paleosol and eolian sand. One sample at 158 cm depth gives a pollen concentrate age *ca.* 3000 yr too old, and another one at 258 cm depth is *ca.* 1600 years too young, again providing evidence that pollen concentrated from eolian sand contains either younger or older materials. However, the rest of the six dates from paleosol have a good age sequence with depth and can be regarded as reliable. Microscopic examination combined with dating shows that pollen concentrate consists of two fractions: 1) pollen deposited simultaneously with sediment, and 2) reworked pollen including older (fossilized) spore pollen preceding sediment deposition *in situ*, or younger pollen transported through hydrological or agricultural activities; both younger and older pollen may come from either distant or local regions. Pollen reworking is generally an indicator of an unstable environment (Zhou *et al.* 1996).

The history of Asian monsoon variation at the loess/desert transitional belt at the end of the last glaciation has been reconstructed on the basis of the ^{14}C chronostratigraphy in Yangtaomao. The period from *ca.* 11,200 to 10,000 BP (interpolated age) was dominated by a climate marked by cold and dry

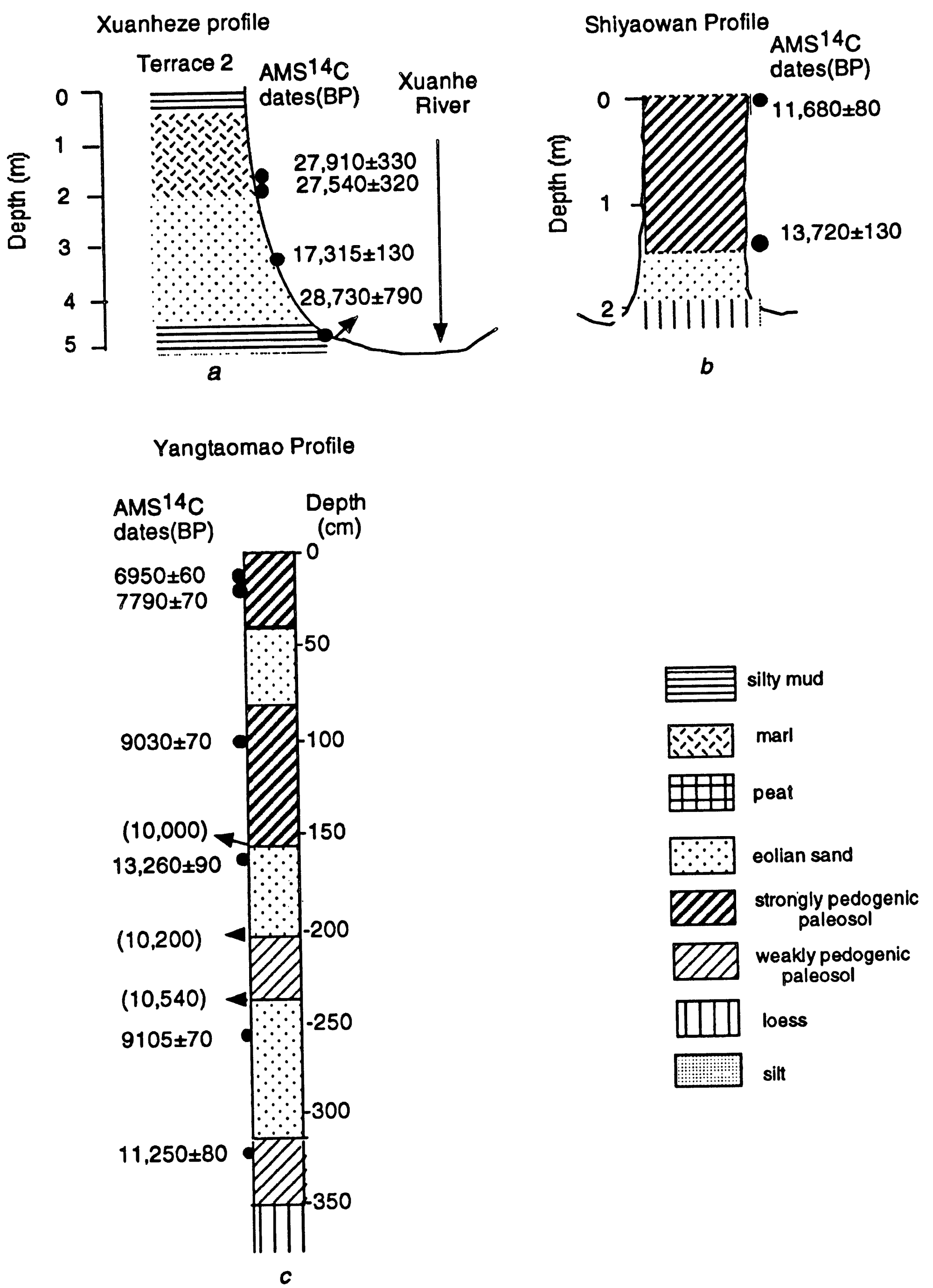

Fig. 2. (a) Xuanheze mud-eolian sand, (b) Shiyaowan loess-paleosol, and (c) Yangtaomao eolian sand-paleosol profiles, with AMS ^{14}C dates of pollen concentrate (*Artemisia*, Chenopodiaceae, *Pinus*, and organic residues). Ages in brackets are derived by interpolation. Dating of pollen concentrates extracted from paleosol or mud creates good age sequences with depth, except on those from eolian sand. Based on dating and lithology, several wet phases are marked by mud or paleosol around the late Pleistocene, last deglaciation, mid Younger Dryas and early Holocene.

TABLE 4. AMS Dating Results of Pollen from Yangtaomao and Shiyaowan Eolian Sand-Loess-Paleosol Profiles

Lab code	Depth (cm)	Dating material	^{14}C age (yr BP)
AA-12317	11	Pollen concentrate	6950 ± 60
AA-12311	22	Pollen concentrate	7790 ± 70
M-12313	102	Pollen concentrate	9030 ± 70
AA-12315	158	Pollen concentrate	13,260 ± 90
AA-12312	258	Pollen concentrate	9105 ± 70
AA-12316	325	Pollen concentrate	11,250 ± 80
AA-12306*	12	Pollen concentrate	11,680 ± 80
M-12307*	140	Pollen concentrate	13,720 ± 130

*Samples collected from Shiyaowan profile

winter monsoon during which 167 cm of eolian sand was deposited. However, the continued influx of an accretionary sandy soil suggests the continuation of strong winter monsoon conditions and increased precipitation. From 10,000–9000 BP, the well-developed paleosol reflects strengthening summer and weakening winter monsoon climates. A rapid decrease in the strength of the summer monsoon from *ca.* 9000 until 8000 BP, as recorded in the deposition of an eolian sand unit, indicates the return of the strong winter monsoon. After *ca.* 7000 BP, the profile was eroded. The late-glacial climatic oscillation evidence described here supports the pollen analysis results obtained from Midiwan profile (Zhou *et al.* 1996).

CONCLUSION

1. The comparison of ^{14}C ages of pollen concentrate with wood, charcoal, peat and paleosol humic acid clearly demonstrates that pollen dating provides useful age information for the Loess Plateau chronology. The newly obtained dating of pollen concentrate from the Baxie paleosol (10,630 ± 70 BP) agrees with charcoal dating of Midiwan peat (10,610 ± 80 BP). Our study shows that pollen concentrates may be a better material for dating paleosol than humic acid on the condition that pollen was deposited simultaneously with sediment in a stable sedimentary environment, such as pollen from paleosol or peat, whereas pollen preserved in an unstable environment (*e.g.*, pollen from eolian sand or loess in an area where the winter monsoon is predominant and strong) does not necessarily provide reliable data. Therefore, a reliable chronology of the loess-paleosol sequence cannot be established without pollen separation, where suitable dating materials such as wood and charcoal are lacking. We intend to experiment further with loess-paleosol sequences for which detailed stratigraphic work has been done in order to improve the chronology of the Loess Plateau.

2. Four major wet phases have been dated from the Late Pleistocene to the early Holocene. Phase 1 is marked by lacustrine mud, which developed in Xuanheze *ca.* 29,000 yr BP; a similar sedimentary phase can be found in many locations on the Loess Plateau, reflecting a wet-cool climate (based on finding pollen of *Abies* and *Pinus* in Beizhuangcun mud (Zhou, Zhou and Head 1990)). In phase 2, *ca.* 13,700 BP, paleosol started to develop as shown in Shiyaowan, indicating the arrival of the last deglaciation. Phase 3 is recorded in Yangtaomao sandy paleosol (10,500–10,200 BP) during the Younger Dryas interval from 11,200 to 10,000 BP, indicating increased precipitation. In phase 4, from 10,000 to 9000 BP, paleosol was well developed, reflecting warm-moist climatic conditions and arrival of the Holocene.

Precipitation variability is especially important for the understanding of paleomonsoon climate change at the loess/desert transitional belt of East Asia and can be used as a historic analog for climate prediction.

Acknowledgments

This study was supported by the Chinese National Science Foundation and U.S. National Science Foundation. The research staff of the NSF-Arizona AMS laboratory at the University of Arizona provided generous help in many ways.

References

An, Z. S., Porter, S. C., Zhou, W. J., Lu, Y. C., Donahue, D. J., Head, M. J., Wu, X. H., Ren, J. Z., and Zheng, H. B. 1993 Episode of strengthened summer monsoon climate of Younger Dryas age on the Loess Plateau of central China. *Quaternary Research* 39: 45–54.

Brown, T. A., Nelson, D. E., Mathewes, R. W., Vogel, J. S. and Southon, J. R. 1989 Radiocarbon dating of pollen by accelerator mass spectrometry. *Quaternary Research* 32: 205–212.

Brown, T. A., Farwell, G. W., Grootes, P. M., and Schmidt, F. H. 1992 Radiocarbon AMS dating of pollen extracted from peat samples. *In* Long, A. and Kra, R. S., eds., Proceedings of the 14th International ^{14}C Conference. *Radiocarbon* 34(3): 550–556.

Cao, S. G., 1980 *Guidelines for Soil Micromorphology Study.* Beijing, Agriculture Press (in Chinese).

Dimbleby, G. W. 1985 *The Palynology of Archaeological Sites.* New York, Academic Press: 176 p.

Donahue, D. J., Jull, A. J. T., and Zabel, T. H. 1984 Results of radioisotope measurements at the National Science Foundation / University of Arizona tandem accelerator mass spectrometer facility. *Nuclear Instruments and Methods in Physics Research* 219(B): 162–166.

Head, M. J., Zhou, W., and Zhou, M. 1989 Evaluation of the ^{14}C ages of organic fractions from loess paleosol sequences near Xian, China. *In* Long, A., Kra, R. S. and Srdoč, D., eds, Proceedings of the 13th International ^{14}C Conference. *Radiocarbon* 31(3): 680–694.

Imbrie, J., Hays, J. D., Martinson, D. G., McIntyre, A., Mix, A. C, Morley, J. J., Pisias, N. G., Prell, W. L. and Shackleton, N. J. 1984 The orbital theory of Pleistocene climate: Support from a revised chronology of the marine ^{18}O record. *In* Berger, A., Imbrie, J., Hays, J., Kukla, G. and Saltzman, B., eds., *Milankovitch and Climate (Part 1).* Dordrecht, Reidel: 269–305.

Ke, M. H. 1994 A method of pollen-spore analysis in loess. *Acta Botanica Sinica* 36(2): 144–147.

Long, A., Davis, O. K., and Lanois, J. D. 1992 Separation and ^{14}C dating of pure pollen from lake sediments: Nanofossil AMS dating. *In* Long, A. and Kra, R. S., eds., Proceedings of the 14th International ^{14}C Conference. *Radiocarbon* 34(3): 557–560.

Mulholland, S. C. and Prior, C. 1992 Processing of phytoliths for radiocarbon dating by AMS. *Phytolitharian Newsletter* 7(2): 7–9.

Regnell, J. 1992 Preparing pollen concentrates for AMS dating: A methodological study from a hard-water lake in southern Sweden. *Boreas* 21: 373–377.

Slota, P. J., Jull, A. J. T., Linick, T. W. and Toolin, L. J. 1987 Preparation of small samples for ^{14}C accelerator targets by catalytic reduction of CO. *Radiocarbon* 29(2): 303–306.

Wilding, L. P. 1967 Radiocarbon dating of biogenetic opal. *Science* 156: 66–67.

Wu, N. Q., Lu, H. Y., Nie, G. Z., Wang, Y. J., Meng, Y. and Gu, G. A. 1992 The study of phytoliths in C_3 and C_4 grasses and its paleoecological significance. *Quaternary Sciences* 3: 241–251 (in Chinese).

Zhang, J. C., and Lin, Z. G. 1992 *Climate of China.* Trans. Tan, D. New York, John Wiley: 376 p.

Zhou, W. J., Zhou, M. F., and Head, M. J. 1990 ^{14}C Chronology of Beizhuangcun sedimentation sequence since 30,000 years B.P. *Chinese Science Bulletin* 35(7): 567–572.

Zhou, W. J., An, Z. S., Lin, B. H., Xiao, J. Zhang, J. Z., Xie, J., Zhou, M. F., Porter, S. C., Head, M. J. and Donahue, D. J. 1992 Chronology of the Baxie loess profile and the history of monsoon climates in China between 17,000 and 6000 years BP. *In* Long, A. and Kra, R. S., eds. Proceedings of the 14th International ^{14}C Conference. *Radiocarbon* 34(3): 818–825.

Zhou, W. J., Donahue, D. J., Porter, S. C., Jull, A. J. T., Li, X. Q. Stuiver, M., An, Z. S., Matsumoto, E., and Gong, G. R. 1996 Variability of monsoon climate in East Asia at the end of last glaciation. *Quaternary Research*, in press.

Zhou, W. J. (ms.) 1995 Monsoon climate change in the environmentally sensitive zone of inland China in the last 13,000 yr and its ^{14}C chronology. Ph.D dissertation, Northwest University, Xian, China.

[RADIOCARBON, VOL. 39, NO. 1, 1997, P. 27–32]

CALIBRATION OF RADIOCARBON DATES FOR THE LATE PLEISTOCENE USING U/Th DATES ON STALAGMITES

JOHN C. VOGEL

Council for Scientific and Industrial Research, Box 395, Pretoria, South Africa 0001

and

JOEL KRONFELD

Department of Geophysics, University of Tel Aviv, Ramat Aviv, Israel

ABSTRACT. Twenty paired ^{14}C and U/Th dates covering most of the past 50,000 yr have been obtained on a stalagmite from the Cango Caves in South Africa as well as some additional age-pairs on two stalagmites from Tasmania that partially fill a gap between 7 ka and 17 ka ago. After allowance is made for the initial apparent ^{14}C ages, the age-pairs between 7 ka and 20 ka show satisfactory agreement with the coral data of Bard *et al.* (1990, 1993). The results for the Cango stalagmite between 25 ka and 50 ka show the ^{14}C dates to be substantially younger than the U/Th dates except at 49 ka and 29 ka, where near correspondence occurs. The discrepancies may be explained by variations in ^{14}C production caused by changes in the magnetic dipole field of the Earth. A tentative calibration curve for this period is offered.

INTRODUCTION

At the International Radiocarbon Conference in Bern in 1978, it was pointed out that certain ^{14}C dates for the Late Pleistocene appear to be several thousand years too young when compared with corresponding uranium series dates (Vogel 1980; Barbetti 1980). This prompted us to undertake a more detailed comparison of the two dating techniques using a slender 2.8 m stalagmite from the Cango Caves in the Cape Province of South Africa. This specimen, which stood at the far end of Cave II, was sawed into sections and removed during several visits over a period of four years. It proved to be ideal for the purpose since it had a coarse crystalline nonporous structure that ensured closed-system conditions. Its base turned out to date back nearly 50,000 yr; water was dripping onto the tip so that it was still growing at the time of removal. Preliminary results for the comparison were reported at the next Radiocarbon Conference in Seattle in 1982 (Vogel 1983).

Unfortunately there is a gap in the sequence, because the stalagmite's growth halted between *ca.* 17,000 and 7000 yr ago. This gap could partially be filled by samples of two similarly crystalline stalagmites from Lynd's Cave in Tasmania (Vogel 1987; Goede and Vogel 1991).

METHOD

We cut samples along the growth axis of the three stalagmites and performed the ^{14}C and U/Th analyses using the same pieces in each case. Carbon dioxide for measurement of the ^{14}C in a CO_2 proportional counter was generated by adding acid, and the remaining solution was processed for the U/Th isotope analysis, using standard α-counting techniques.

RESULTS

The results for the Cango stalagmite are given in Table 1, and those for Lynd's Cave are listed in Table 2. Two adjustments need to be made to the dates.

1. The ^{14}C ages must be corrected for the apparent initial age of the calcite when it is precipitated from the dripping groundwater.

As previously shown (Vogel 1983), the first six ^{14}C dates for the upper 95 cm of the Cango stalagmite show complete concordance with the U/Th dates if 1450 yr are subtracted from the initial age and the results are calibrated with the tree-ring calibration curve (*e.g.*, Stuiver and Pearson 1993). This correction of 1450 yr is thus adapted for the older sections, too. It is, of course, possible that the apparent initial age varied with differing climatic conditions, but the shift would not have been more than a few hundred years, since this figure has been found to apply to groundwater in limestone areas worldwide. The adjustment for the Lynd's Cave stalagmites is less certain. 1500 yr are subtracted from these ^{14}C dates, but an error of ±500 should be assumed. When these results were first presented (Vogel 1987) 2160 yr was subtracted, based on a comparison with parallel electron spin resonance (ESR) dates, but subsequent tree-ring calibration data for the early Holocene (Kromer and Becker 1993) have shown this correction to be too large.

2. The U/Th ages need to be corrected for any initial ^{230}Th that may have been incorporated into the stalagmite during formation.

   Most of the samples had very small amounts of ^{232}Th. For those that did show measurable amounts of the isotope, the adjustment was <230 yr, assuming an initial $^{230}Th/^{232}Th$ activity ratio of 1 ± 0.5. An exception was the Lynd's Cave stalagmite L1, which had a very low uranium content (*ca.* 0.02 ppm) and consequently required a correction of 620 yr in one case. The U/Th results from this specimen are therefore less precise than the rest.

TABLE 1. ^{14}C and U/Th data for Cango stalagmite V3. Column 2 gives the distance of the sample from the tip of the stalagmite; column 4 the apparent ^{14}C age adjusted for isotope fractionation using the $^{13}C/^{12}C$ ratio. Columns 7, 8 and 9 list the activity ratios of the U and Th isotopes and column 10 the U-series ages adjusted for initial Th.

Sample	Distance (mm)	Lab code (Pta-)	Apparent ^{14}C age (yr BP)	Anal. no.	U cons (ppm)	$\frac{^{234}U}{^{238}U}$	$\frac{^{230}Th}{^{232}Th}$	$\frac{^{230}Th}{^{234}U}$	U/Th age (yr BP)
V3/1a	5	2256	1530 ± 50	U-003	0.068	3.70	--	--	recent
V3/1b	14	2435	1490 ± 55	--	--	--	--	--	
V3/1c	314	2579	3270 ± 45	U-107	0.062	3.43	10	0.019	1870 ± 220
V3/1d	492	2289	4660 ± 60						
V3/2a	715	2580	5730 ± 50	U-108	0.098	3.61	28	0.044	4710 ± 350
V3/2b	887	2581	6380 ± 60	U-109	0.109	3.59	101	0.057	6240 ± 400
V3/2c	974	2436	15,400 ± 140	U-112	0.091	3.14	217	0.152	17,400 ± 800
V3/6a	989	3081	15,790 ± 50	U-263	0.109	3.15	>>	0.166	19,300 ± 800
V3/6b	1157	3087	19,180 ± 50						
V3/6c	1304	3090	21,610 ± 70	U-242	0.140	2.65	>>	0.227	27,200 ± 3000
V3/3m	1517	3084	26,710 ± 110	U-265	0.078	3.18	103	0.227	27,200 ± 1300
V3/3b	1598	3277	28,380 ± 150	U-282	0.101	3.10	256	0.264	32,100 ± 2100
V3/4a	1679	2657	30,300 ± 610	U-118	0.106	3.02	>>	0.242	29,200 ± 800
V3/4c	1759	3078	30,130 ± 180	U-264	0.083	3.22	>>	0.243	29,300 ± 3000
V3/4d	1842	3077	30,170 ± 180	U-266	0.073	2.99	153	0.282	34,400 ± 2200
V3/4b	2030	2658	30,110 ± 500	U-119	0.083	3.18	173	0.287	35,200 ± 1000
V3/5a	2101	3279	32,670 ± 330	U-269	0.077	3.03	>>	0.294	36,400 ± 1800
V3/5c	2181	3893	33,870 ± 330	U-325	0.087	3.05	155	0.305	37,700 ± 1200
V3/5b	2288	2689	35,900 ± 280	U-136	0.058	3.11	255	0.311	38,700 ± 900
V3/7a	2409	3278	36,520 ± 300	U-270	0.109	2.84	254	0.329	41,300 ± 1200
V3/7d	2491	3887	37,580 ± 490	U-324	0.117	2.85	200	0.348	44,100 ± 1400
V3/7c	2589	3884	41,330 ± 630	U-323	0.107	2.90	200	0.352	44,700 ± 1400
V3/7b	2698	3280	47,660 ± 1120	U-283	0.119	2.73	420	0.381	49,200 ± 1300

TABLE 2. ^{14}C and U/Th data for the Tasmanian stalagmites. (See Table 1 for explanation.)

Sample	Distance (mm)	Lab code (Pta-)	Apparent ^{14}C age (yr BP)	Anal. no.	U cons (ppm)	$\frac{^{234}U}{^{238}U}$	$\frac{^{230}Th}{^{232}Th}$	$\frac{^{230}Th}{^{234}U}$	U/Th age (yr BP)
Lynd's Cave stalagmite L2									
L2/1	717	3792	10,980 ± 110	U-305	0.307	3.12	171	0.104	11,740 ± 500
L2/2	515	3791	11,800 ± 100						
L2/4	334	3707	12,770 ± 100	U-293	0.262	2.97	236	0.117	13,300 ± 360
L2/3	120	3708	13,450 ± 130	U-294	0.305	2.85	442	0.128	14,570 ± 420
Lynd's Cave stalagmite L1									
L1/3	1380	3762	8320 ± 90	U-301	0.019	2.32	12	0.069	7070 ± 570
L1/6	980	3731	10,970 ± 100	U-299	0.016	2.69	64	0.099	11,080 ± 800
L1/7	614	3797	12,400 ± 110						
L1/9	79	3713	14,170 ± 60	U-295	0.024	2.80	44	0.114	12,840 ± 750

DISCUSSION

With these two adjustments to the ages, the results for the Cango stalagmite are plotted (Fig. 1.) against the distance from the tip. A few of the U/Th analyses had relatively large margins of error, but on the whole they show a nearly linear growth of the stalagmite between 44 ka and 18 ka ago, with a somewhat slower growth rate between 49 ka and 44 ka. The ^{14}C ages, on the other hand, show major deviations from this linear growth curve, especially for the period beyond 30,000 yr BP, where they are consistently several thousand years younger than the uranium series dates.

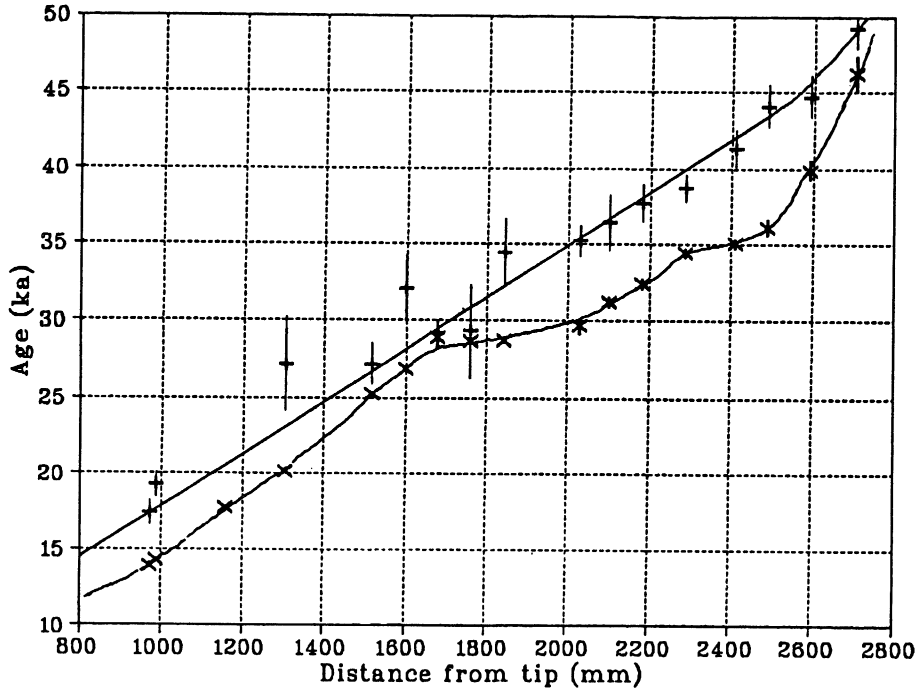

Fig. 1. ^{14}C dates (×) adjusted for initial age of 1450 yr and parallel U-series dates (+) for the Cango stalagmite showing the large discrepancy between age-pairs between 30 ka and 45 ka

Now, it is well known that samples older than 30,000 yr are prone to produce ^{14}C ages that are too young due to contamination by small amounts of more recent carbon. The fact that the ^{14}C date for the bottommost sample agrees with the U/Th age to within 1σ if the correct ^{14}C half-life (5730 yr) is used (49,200 ± 1300 (U/Th) – 47,550 ± 1120 (^{14}C) = 1650 ± 1720), indicates, however, that contamination cannot in this case explain the discrepancies between the two methods. Of special significance is near identity between the ^{14}C and U/Th ages *ca.* 29,000 yr ago. This will be discussed briefly below.

For the period between 10 and 20 ka we need to consider the age-pairs derived from the two Lynd's Cave stalagmites (Table 2). As previously noted (Vogel 1987), these data also show considerable discrepancies between the ^{14}C ages and the U/Th ages.

More recently, a comprehensive set of age comparisons has been published using coral from Barbados (Bard *et al.* 1990, 1993), which confirm that ^{14}C dates between 12 ka and 22 ka are several thousand years too young. The U/Th dates were produced by thermal ionization mass spectrometry (TIMS), which gives greater precision than the conventional α-counting technique. In Figure 2 these results are presented together with our measurements in this time range; two pairs from Cango (V3) are also included to extend the age range. All except two of our data points correspond to the TIMS results to within one sigma, thus confirming that the ^{14}C age discrepancy is a worldwide phenomenon and that the stalagmite data do represent the actual situation.

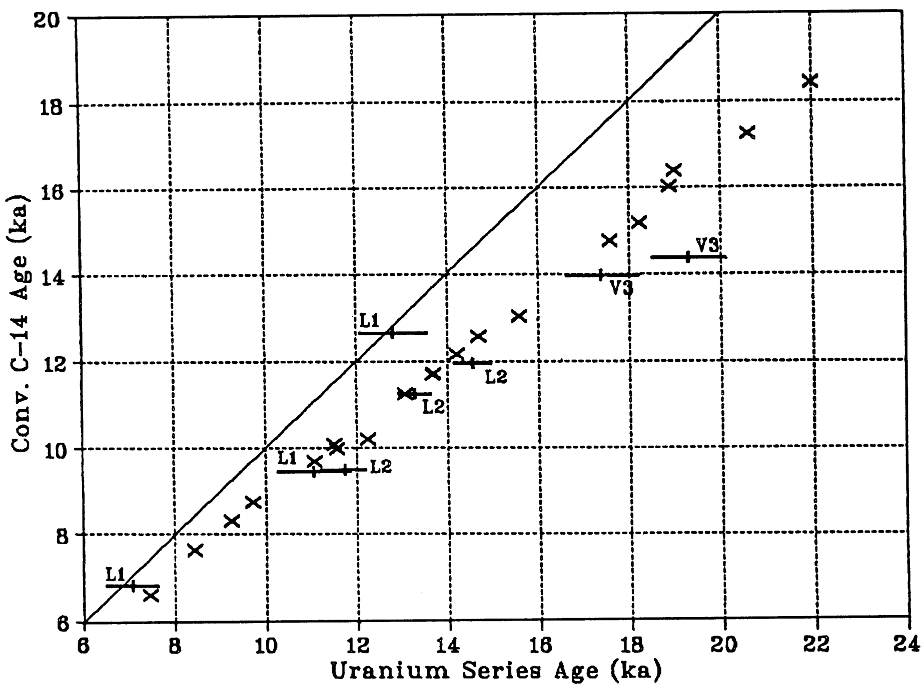

Fig. 2. Calibration curve for conventional ^{14}C dates after Bard *et al.* (1993) (✕) with our age-pairs for the Lynd's Cave stalagmites (L1 and L2) (Table 2) and the two Cango Cave (V3) age-pairs in this time range (Table 1)

Using the comparisons obtained from the Cango Cave stalagmite, a calibration curve for the period 25 ka to 50 ka is plotted in Figure 3. The four samples with U/Th error margins greater than ± 2000 yr (V3/6c, V3/3b, V3/4c and V3/4d) are not included in the figure because they are not very meaningful. The margins of error of this curve are still relatively large, but for the present it can be used in cases where absolute date estimates are required rather than ^{14}C ages. It is evident from this figure that ^{14}C dates between 35 ka and 45 ka are *ca.* 5000 yr too young. Recently, one additional age comparison has been published (Bischoff *et al.* 1994) that confirms this discrepancy.

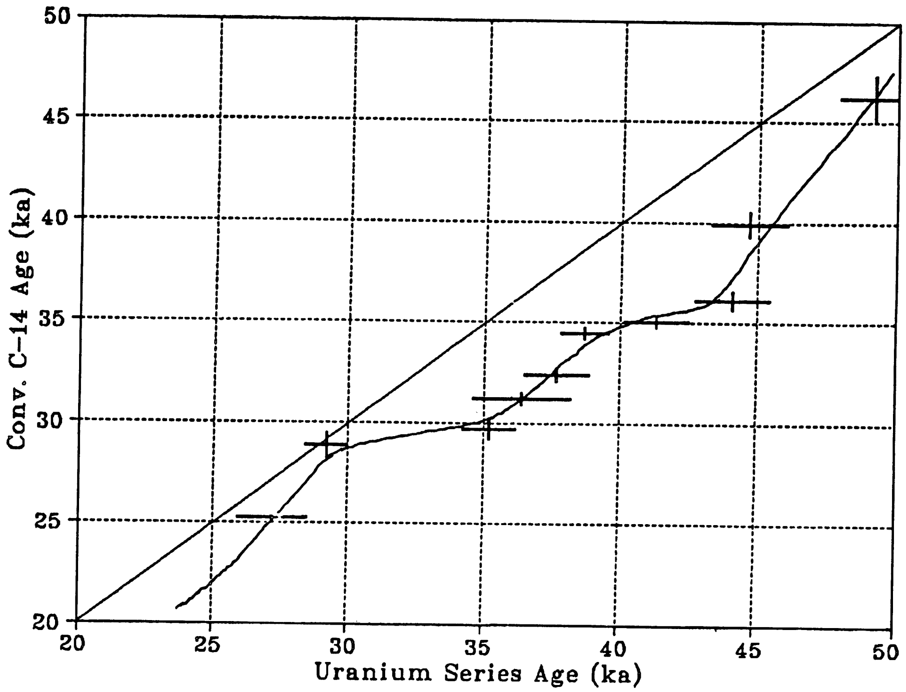

Fig. 3. Calibration curve for conventional ^{14}C dates between 20 ka and 50 ka using the data for the Cango Cave stalagmite, V3 (Table 1)

The authors find that their ^{14}C ages on charcoal (37 ± 1 ka) are much younger than U/Th ages on bracketing flowstone (42.6 ± 1.1 ka) in a cave near Barcelona, Spain. If the ^{14}C date is calibrated, using Figure 3, it overlaps with the U/Th date.

Not shown in Figure 2 is the isolated coral sample of Bard *et al.* (1993) that gave an age-pair at variance with our results at *ca.* 30 ka (Figure 3). Their measurements show the ^{14}C date to be 4780 ± 380 (2σ) yr younger than the U/Th date of 30,225 ± 160 yr, whereas our age-pair at 29,000 yr shows almost no difference between the two techniques: at 29,200 ± 800 yr (U/Th) the ^{14}C age is only 350 yr younger. Other age-pairs in this time range, on the other hand, do seem to support our finding: the five comparisons listed by Barbetti (1980) between 26,000 yr and 32,000 yr individually and collectively show virtually no discrepancy between U/Th and ^{14}C ages. The weighted averages for these six samples give:

$$29{,}690 \pm 680 \text{ yr (U/Th)} - 29{,}800 \pm 760 \text{ yr } (^{14}C) = -110 \pm 1020 \text{ yr}.$$

Conclusion

If ^{14}C dating gives the correct age at 29,000 yr, it implies that a drastic decrease in the ^{14}C levels of the atmosphere occurred. This seems to be indicated by the very slow decrease in the ^{14}C ages between the U/Th dates of 35,000 and 29,000 yr (Fig. 1). The effect could have been caused by a major increase in the strength of the Earth's dipole field, and there is some evidence that this did happen. Most estimates of the global dipole field intensity during the last 120,000 yr indicate considerably lower values than today, but at least one of them (Tric *et al.* 1992) shows near-normal dipole intensity between 55 and 47 ka, between 33 and 25 ka and after 12 ka, with distinctly lower values in between. The geomagnetic modulation of the ^{14}C production rate could thus explain qualitatively, at least, the general trend of the data presented here.

Acknowledgments

We especially thank Professor Hilary Deacon for originally arranging permission to remove the Cango stalagmite for our investigations. Albert Goede supplied the Tasmanian samples. We thank Ebbie Visser for her careful monitoring of the radiocarbon measurements.

References

Barbetti, M. 1980 Geomagnetic strength over the last 50,000 years and changes in atmospheric ^{14}C concentration: Emerging trends. *In* Stuiver, M. and Kra, R., eds., Proceedings of the 10th International ^{14}C Conference. *Radiocarbon* 22(2): 192–199.

Bard E., Arnold, M., Fairbanks, R. G. and Hamelin, B. 1993 ^{230}Th–^{234}U and ^{14}C ages obtained by mass spectrometry on corals. *In* Stuiver, M., Long, A. and Kra, R. S., eds., Calibration 1993. *Radiocarbon* 35(1): 191–199.

Bard, E., Hamelin, B., Fairbanks, R. G. and Zinder, A. 1990 Calibration of the ^{14}C timescale over the past 30,000 years using mass spectrometric U-Th ages from Barbados corals. *Nature* 345: 405–410.

Bischoff, J. L., Ludwig, K., Garcia, J. F., Carbonell, E., Stafford, T. W., Jr. and Jull, A. J. T. 1994 Dating of the basal Aurignacian sandwich at Abric Romani (Catalunya, Spain) by radiocarbon and uranium-series. *Journal of Archaeological Science* 21: 541–551.

Goede, A. and Vogel, J. C. 1991 Trace element variations and dating of a Late Pleistocene Tasmanian Speleothem. *Palaeogeography, Palaeoclimatology, Palaeoecology* 88: 121–131.

Kromer, B. and Becker, B. 1993 German oak and pine ^{14}C calibration, 7200–9439 BC. *In* Stuiver, M., Long, A. and Kra, R. S., eds., Calibration 1993. *Radiocarbon* 35(1): 125–135.

Stuiver, M. and Pearson, G. W. 1993 High-precision bidecadal calibration of the radiocarbon time scale, AD 1950–500 BC and 2500–6000 BC. *In* Stuiver, M., Long, A. and Kra, R. S., eds., Calibration 1993. *Radiocarbon* 35(1): 1–23.

Tric, E., Valet, J. P., Tucholka, P., Paterne, M., Labeyrie, L., Guichard, F., Tauxe, L. and Fontugne, M. 1992 Paleointensity of the geomagnetic field during the last eighty thousand years. *Journal of Geophysical Research* 97: 9337–9351.

Vogel, J. C. 1980 Accuracy of the radiocarbon time scale beyond 15,000 BP. *In* Stuiver, M. and Kra, R., eds., Proceedings of the 10th International ^{14}C Conference. *Radiocarbon* 22(2): 210–218.

____1983 ^{14}C variations during the Upper Pleistocene. In Stuiver, M. and Kra, R., eds., Proceedings of the 11th International ^{14}C Conference. *Radiocarbon* 25(2): 213–218.

____1987 Calibration of radiocarbon dates beyond 10 000 BP. *In* Aurenche, O., Evin, J., and Hours, F., eds., *Chronologies in the Near East*. BAR International Series 379(i). Oxford, BAR: 319–322.

[RADIOCARBON, VOL. 39, NO. 1, 1997, P. 33–48]

BOMB ^{14}C RECORDED IN LAMINATED SPELEOTHEMS: CALCULATION OF DEAD CARBON PROPORTION

DOMINIQUE GENTY and MARC MASSAULT

Université de Paris-Sud, Laboratoire d'Hydrologie et de Géochimie Isotopique, URA 723, CNRS, bâtiment 504, F-91405 Orsay Cedex, France

ABSTRACT. We performed radiocarbon measurements using accelerator mass spectrometry (AMS) on 6 stalagmites, 3 stalactites and 7 seepage waters from four different caves in Southwest France and Belgium in order to calculate the dead carbon proportion (dcp). All the speleothems studied are modern and annually laminated, which offers the advantage of an accurate chronology, with better than one-year resolution. Coupled with the fact that very little calcite is necessary for an AMS measurement (between 1.5 and 7 yr of calcite deposit), we obtained dead carbon values within an uncertainty limit of ± 1.5%. Results show that the dead carbon proportion varies from 9.2% to 21.9% for calcite deposits and from 3.6% to 21.9% for water. In each sampling site, the dcp is homogeneous. Although the inter-site dcp varies by >11%, its average value of 15.5% ± 4.4 still lies within the uncertainty range of the accepted value of 15% ± 5 (dilution factor of 0.85 ± 0.5). We compare the average dcp of each site with the local geology, vegetation and climate. Given similar geology and temperature, the highest dcp values are found under forest cover; dcp difference is up to 9%. However, the Belgian site, which is also under a forest, shows a dcp very close to the dcp found under grassland sites of Southwest France, which proves that other unknown factors may play an important role in dissolution processes. Secondary calcite deposition and redissolution in the soil zone or more likely in the fracture system before reaching the cave itself could also explain the inter-site differences. The IAEA isotopic model (Pearson model adapted for open systems) is in good agreement with the measured activities.

INTRODUCTION

Recent studies have shown that many speleothems possess annually deposited growth laminae; they can be visible (Genty 1993; Genty and Quinif 1996) or luminescent (Baker *et al.* 1993; Shopov and Dermendjiev 1990). The alternation of white porous and dark compact laminae represents the calcite deposit of one year, which gives modern laminated speleothems a very accurate chronology. It is not rare to have speleothems with continuous laminae for >100 yr, but in the case of longer durations, laminae are frequently interrupted by discontinuities. The search for paleoclimatic signals from these laminae has already started: correlation has been found between the laminae thickness and the pluviometry (Genty and Quinif 1996; Railsbak *et al.* 1994), and a stable isotopic seasonal signal has been observed in several stalagmites (Genty, Quinif and Keppens 1995).

Speleothem carbon has two principal sources: 1) the CO_2 of the soil above the cave; 2) the carbonate of the limestone where the cave developed and/or of secondary calcite deposits of the unsaturated zone. The soil CO_2 comes from root respiration and microbial decomposition of organic matter; it is thus linked to atmospheric CO_2 (Dörr and Münnich 1986). Carbon from limestone is generally so old as to have a negligible ^{14}C activity; however, if it comes from secondary deposits, its activity can be significant.

The determination of speleothem ^{14}C activity has at least two essential purposes:

1. To estimate the age of the deposit. Even if it is not now the most appropriate method precisely because of the unknown dead carbon proportion, it has been the only feasible method for a long time (Broecker and Olson 1960; Geyh and Franke 1970). It is still used because of its cost advantage over the U/Th mass spectrometric method and because it is a means of checking U/Th ages for the last 40 ky (Bastin and Gewelt 1986; Brook and Nickmann 1996; Genty *et al.* 1996; Gewelt, 1985; Geyh and Henning 1986; Goede and Vogel 1991; Holmgren, Lauritzen and Possnert 1994; Issar *et al.* 1992; Pazdur, Pazdur and Pawlyta 1995; Railsback *et al.* 1996; Talma and Vogel 1992; Vogel 1983).

2. To reconstruct atmospheric ^{14}C activity through time; in this case, the chronology is given by U/Th ages (Holmgren, Lauritzen and Possnert 1994; Vogel 1983). Atmospheric ^{14}C wiggles observed during the Holocene in tree-ring dated wood (Wigley and Kelly 1990) are probably due to the Earth's geomagnetic field changes (Bard, Hamelin and Fairbanks 1990; Mazaud *et al.* 1991; Vogel 1983), solar activity variations (Suess and Linick 1990) and the capacity of the ocean to absorb CO_2 (Goslar *et al.* 1995). During historical time, ^{14}C variations include an abrupt increase between AD 1500 and 1700 (the de Vries effect), a slight decrease of 2% since the beginning of the industrial period (AD 1850; the Suess effect), and finally, a massive production of ^{14}C in the atmosphere because of nuclear bomb tests (maximum increase of >100% in 1963–1964; Levin *et al.* 1992).

There are major problems in both cases: 1) the initial activity is not known; in other words the dcp must be estimated (or the dilution factor q that is its complement; Gewelt 1986); 2) the dcp possibly varies with time.

The dcp has been calculated in several different ways (Table 1):

- by measurement of the ^{14}C activity on the top of still-dripping stalagmites (Vogel 1983; Gewelt 1985, 1986; Bastin and Gewelt 1986); using the classical β-counting method, one must sample >20 g of calcite (more often between 30 and 100 g); thus, the error margin is large because sampling takes into account deposits of different ages (*e.g.*, a dcp of 30% was found on the top of three active Belgian stalagmites, whereas the value taken into account was 15% (Gewelt 1986));
- by age-distance interpolation up to the top of the stalagmite (linear least-square fit); the hypothesis of a constant growth rate must be considered critically here, because stalagmite growth rates are highly variable even over short periods (*i.e.*, from 0.1 to 1.0 mm yr^{-1}; Genty and Quinif 1996; Genty *et al.* 1996);
- by comparison with pollen extracted from the speleothem; this technique can be used in areas where the emergence or disappearance of a taxon is abrupt (*i.e.*, emergence of *Tilia* at the Atlantic in Belgium; Bastin and Gewelt 1986); but this is not an accurate method because there is very little pollen in speleothem calcite (up to 5 grains gm^{-1} of $CaCO_3$) and a great quantity of calcite is required (>100 g);
- by comparison with U/Th ages (Vogel 1983; Holmgren, Lauritzen and Possnert 1994); the accuracy depends on the U/Th errors, which are great for recent deposits (very little thorium).

In order to attempt more accurate dead carbon inferences we have combined these methods, using 1) annually laminated speleothems, which give an excellent chronology for the last few decades, and 2) AMS techniques that permit the analysis of *ca.* 10 mg of calcite, which is, in the most favorable cases, 1 yr of deposits, and more often, 2–7 yr.

Our purpose is to compare dcp's in modern deposits and water from four sites and to explain the observed variability in relation to the geology, vegetation and climate.

Site and Sample Descriptions

Samples come from caves at Han-sur-Lesse cave (Belgium; 50°08'N, 5°10'E, elevation 180 m); Villars (Dordogne, France; 45°30'N, 0°50'E, elevation 175 m), La Faurie (Dordogne, France; 45°08'N, 1°11'E, elevation 225 m) and Proumeyssac (Dordogne, France; 44°55'N, 0°56'E, elevation 155 m).

TABLE 1. Examples of Dilution Factors Found in Speleothems

Speleothem type, locale	Dilution factor q*	Method	Reference
Stalagmites – Belgium	0.85 ± 0.05	Pollen correlation	Bastin and Gewelt 1986
Stalagmite crust on a bone (called travertine) – Moaning Cave, California, USA	0.915	^{14}C age-distance interpolation (linear least square fit)	Broecker and Olson 1960
Stalagmites and stalactites – Red Spider Cave, Georgia, USA	0.85	Bibliography†	Brook and Nickmann 1996
Stalagmites and flowstones – Belgium	0.85	Pollen correlation, bibliography	Gewelt 1985
Stalagmites and flowstones – Belgium	0.85 (est.); 0.69; 0.72; 0.69 (measured)	Pollen correlation, bibliography	Gewelt 1986
Stalagmite – Central Europe	0.85	Bibliography	Geyh and Franke 1970
Flowstone – Heggen Cave, Germany	0.81	^{14}C age-distance interpolation (linear least square fit)	Geyh and Hennig 1986
Stalagmite – Tasmania	0.83 ± 0.05	Bibliography	Goede and Vogel 1991
Stalagmites – Galilee, Israel	0.89	Bibliography	Issar *et al.* 1990
Speleothems – Cracow–Wielun, Poland	0.83	Bibliography	Pazdur *et al.* 1995
Stalagmite – Drotsky's Cave, Botswana	0.86	^{14}C age-distance interpolation (linear least square fit)	Railsback *et al.* 1994
Stalagmite – Cango Cave, South Africa	0.83	^{14}C age-distance interpolation (linear least square fit)	Talma and Vogel 1992
Stalagmite – Cango Cave, South Africa	0.83	^{14}C age of the still active top, comparison with U/Th ages	Vogel 1983

*q = 1 – (dead carbon proportion) / 100; note that all values are between 0.81 and 0.91, meaning that the dead carbon proportion is between 9 and 19%.

†"Bibliography" = author(s) used former works for their dilution factor q.

All these caves are horizontal and developed in hilly areas. Their entrances are on hill flanks, which explains the low thickness of the terrain above them (<50 m). Each site has characteristic geology, vegetation type and density, soil and limestone thicknesses and climate (Table 2). Examination of aerial photographs and of maps permitted us to estimate the grassland/forest ratio of the watershed above the caves; the Han-sur-Lesse and Villars caves are under forest while La Faurie and Proumeyssac are under grassland.

AMS ^{14}C activity measurements were performed on 6 stalagmites, 3 stalactites and 7 seepage waters. Except for Proumeyssac (station #1), waters and calcite deposits are from different systems (different places inside the cave). In the Han-sur-Lesse cave, the two stalactites studied correspond to the two stalagmites, which permits the comparison of the isotopic content of stalactite and stalagmite.

TABLE 2. Comparison of the Dead Carbon Proportion with the Geology, Vegetation and Climate Characteristics of the Four Studied Sites

Site	dcp (%) in: **speleothems** *(waters)*	Stratigraphy	Limestone thickness above cave (m)	Cave air pCO_2 (%)	Vegetation types and tree density of forest cover	Grassland/ forest ratio (%)	Soil thickness above cave (cm)	Mean annual precipitation (mm)	Mean temp., Jan, May, Sept (°C)
Han-sur-Lesse (Belgium)	**13.8 ± 1.5** (n = 4)	Givetian (Devonian)	50	0.03 (50 m near the entrance, large gallery)	Hornbeams, limes, oaks, hazels	0	5–30	787 (6 yr)	2.5 - 9.1 - 14.8
Villars (Dordogne, France)	**21.1 ± 1.5** (n = 3) *(20.0 ± 1.5; n = 3)*	Bajocian (Jurassic)	10–40	0.16 (n=2; 3 Jan 1997)	Oaks (13 oaks / 100 m^2; mean dia. = 17 cm), hazels, junipers, mosses, grass	5 ± 2	0–15	1048 (10 yr)	4.1 - 14.0 - 16.0
La Faurie (Dordogne, France)	**12.2 ± 1.5** (n = 1) *(3.7 ± 1.5; n=2)*	Bajocian (Jurassic)	15	0.08 (n=1; 31 Dec 1996)	Grass, mosses, oaks (20 oaks / 100 m^2; mean dia. = 10 cm)	90 ± 5	0–20	861 (10 yr)	4.6 - 14.1 - 16.2
Proumeyssac (Dordogne, France)	**9.2 ± 1.5** (n = 1) *(5.5 ± 1.5; n = 2)*	Maastrichtian (Cretaceous)	20	0.04 (n=1; 2 Jan 1997)	Grass, mosses, oaks (9 oaks / 100 m^2; mean dia. = 24 cm)	85 ± 5	10–30	889 (23 yr)	4.6 - 14.1 - 16.2

METHODS

Analytical Procedures

Between 19 and 82.3 mg of $CaCO_3$ were sampled with a microdrill for measurements on speleothems. This corresponds to 1.5 to 7 annual alternations. Laminae counting determined the exact date of the deposition of each sample (Table 3). Water analysis was performed on volumes of 100 to 200 ml.

Calcite powders were reacted with H_3PO_4 in order to obtain CO_2. The CO_2 gas was graphitized on iron with hydrogen at 650°C for 100 min; residual gas was used for stable isotope measurements on a SIRA spectrometer. Carbon atoms were counted with an accelerator mass spectrometer (Tandetron) at Gif-sur-Yvette (Centre des Faibles Radioactivités, France). Water samples were reacted with H_3PO_4 and degassed CO_2 was used as above for ^{14}C activity and $\delta^{13}C$ measurements.

Analytical errors, including laboratory errors, are ±0.1% for $\delta^{13}C$ and between 0.6 and 0.9 pMC for ^{14}C activity. Calcite powders are from seasonal laminae, and because two laminae deposit in one year, accuracy of sampling is less than one year.

Dead Carbon Calculation

Dead carbon calculation requires three values: 1) the deposit ^{14}C activity; 2) the deposit age; 3) the atmospheric ^{14}C activity during the deposit formation. Because the latter has varied greatly during recent decades, due to nuclear bomb tests, it is necessary to have the most accurate date for the calcite deposits ($\Delta^{14}C$ varied from 200‰ in 1960 to >1000‰ in 1963 in the Northern Hemisphere; Levin *et al.* 1992). This is possible with annually laminated speleothems. One must be cautious in attributing an age to a karst water because the latter may be composed of waters of different residence times: typically, a rapid transit occurs a few hours to a few days after a storm event, whereas in dry periods water comes mostly from porous media storage whose age is difficult to know (Ford and Williams 1989). Spring hydrographic analysis can tell us about the storage characteristics of an aquifer (Mangin 1975). Models with different water flow characteristics have been developed: porous (or diffuse), fissure and conduit flows permit plotting of a karst aquifer on a three end-member diagram (Atkinson 1985; Hobbs and Smart 1986). However, very little is known about stalactite flow characteristics; the few published measurements also show the existence of a fast and a slow component (Pitty 1966; Baker *et al.* 1997; Destombes *et al.* 1997; Genty *et al.* in press; Reicher and Trimborn 1995), but only the continuous dripping flow rate and the chemistry under several stalactites will permit quantification of these two components (work in progress). For all the waters, it is assumed that the sampling date corresponds to the water age because of the low thickness of the terrain above the caves and because it has been observed that after a rain storm, flow rate increases in the caves after a few hours or a few days. However, we must keep in mind that dilution with older water is possible.

Because the calcite samples correspond to a depositional time span between 1.5 and 7 yr, we have considered the mean atmospheric ^{14}C activity of the corresponding period. No direct atmospheric ^{14}C activity measurements near the studied sites are available. This is why we used the published results of European sites, particularly those from Germany (Levin *et al.* 1992; Levin, Graul and Trivett 1995). For the most recent years, we have extrapolated data from the modeling, with an exponential representation of the decrease of the atmospheric ^{14}C activity measured at Schauinsland (Germany; Levin, Graul and Trivett 1995).

TABLE 3. ^{14}C Activity and ^{13}C Results of Speleothems and Seepage Waters*

Sample	Type	Position	Quantity	Duration covered by sample	$a^{14}C_m$ (pMC)	Error (pMC)	$\delta^{13}C$ (‰ PDB ±0.1)
Vil-stm1 14C-C	Stalagmite	Under the top	19 mg	1985–1992; 7 alternations	96.6	0.6	–8.9
Vil-stm5 14C-A	Stalagmite	Growth surface	59.9 mg	1991–1995; 3–4 alternations	91.1	0.6	–9.7
Vil-stm4 14C-A	Stalagmite	Under the top	31.5 mg	1958–1965 (?); 7 alternations	118.6	0.6	–10.1
Vil-eau 14C-A	*Water*	*Station #1B*	*200 ml*	*2 Sep 1995; <3 h*	*89.7*	*0.6*	*–11.8*
Vil-eau 14C-B	*Water*	*Station #4*	*100 ml*	*22 Aug 1996; < 3 h*	*93.7*	*0.8*	*–9.7*
Vil-eau 14C-C	*Water*	*Station #1B*	*100 ml*	*22 Aug 1996; < 3 h*	*91.6*	*0.8*	*–10.9*
Fau-stt1 14C-A	Stalactite	Tip (6 mm), thin wall	59 mg	1990–1996; 6 alternations	102.6	0.8	–10.9
Fau-eau 14C-A	*Water*	*Station #2*	*120 ml*	*24 Aug 1996; < 48 h*	*110.3*	*0.8*	*–11.7*
Fau-eau 14C-B	*Water*	*Station #12*	*120 ml*	*24 Aug 1996; < 48 h*	*110.0*	*0.7*	*–11.7*
Prou-pot1 14C-A	Stalagmitic crust	Growth surface, station #1	63 mg	Apr 1996 – Aug 1996	104.0	0.9	–11.2
Prou-eau 14C-B	*Water*	*Station #1*	*120 ml*	*26 Aug 1996; < 0.3 h*	*108.2*	*0.7*	*–10.7*
Prou-eau 14C-A	*Water*	*Station #2*	*120 ml*	*26 Aug1996; < 0.5 h*	*108.2*	*0.7*	*–14.0*
Han-stm4 14C-A	Stalagmite	Growth surface	72.8 mg	Jan 94 – Jun 95; 1.5 alternations	98.9	0.8	–9.3
Han-stm5 14C-A	Stalagmite	Growth surface	44.1 mg	Jun 94 – Nov 95; 1.5 alternations	100.5	0.6	–9.1
Han-stt4 14C-A	Stalactite	Tip (6 mm), thin wall	56.2 mg	1989–1995; 6 alternations	102.1	0.9	–10.2
Han-stt5 14C-A	Stalactite	Tip (4 mm), soda-straw 2/3 filled	62.3 mg	1991–1995; 4 alternations	99.6	0.8	–10.8

TABLE 3 – *continuation*

Sample	$\Delta^{14}C_{atm}$ (‰)	$a^{14}C_{atm}$ (pMC ±0.7)	dcp (% ±1.5)	$\delta^{18}O$ (‰ PDB ±0.1)	$a^{14}C_g$ (pMC)	CO_2/DIC frac. (pMC)	$a^{14}C_{DIC}$ (pMC)	Avg. cave temp. (°C ±0.2)	CO_2/DIC frac. (‰PDB ±0.1)	IAEA model (pMC ±1.5)
Vil-stm1 14C-C	171.0	121.2	20.3	–4.8	117.4	3.0	120.4	--	--	--
Vil-stm5 14C-A	127.0	116.7	21.9	–5.1	112.9	2.8	115.8	--	--	--
Vil-stm4 14C-A	450.0	150.1	21.0	–4.1	145.3	2.7	148.1	--	--	--
Vil-eau 14C-A	*109.0*	*114.8*	*21.9*	--	*111.1*	*2.3*	*113.5*	*11.3*	*–9.45*	*104.7*
Vil-eau 14C-B	*106.0*	*114.5*	*18.2*	--	*110.8*	*2.8*	*113.7*	*11.3*	*–9.45*	*85.4*
Vil-eau 14C-C	*106.0*	*114.5*	*20.0*	--	*110.8*	*2.6*	*113.4*	*11.3*	*–9.45*	*95.8*
Fau-stt1 14C-A	129.0	116.9	12.2	–4.8	113.1	2.6	115.7	--	--	--
Fau-eau 14C-A	*106.0*	*114.5*	*3.6*	--	*110.8*	*2.4*	*113.2*	*12.9*	*–9.26*	*101.5*
Fau-eau 14C-B	*106.0*	*114.5*	*3.9*	--	*110.8*	*2.4*	*113.2*	*12.9*	*–9.26*	*101.5*
Prou-pot1 14C-A	106.0	114.5	9.2	–5.3	110.8	2.5	113.3	--	--	--
Prou-eau 14C-B	*106.0*	*114.5*	*5.5*	--	*110.8*	*2.6*	*113.4*	*13.0*	*–9.25*	*92.8*
Prou-eau 14C-A	*106.0*	*114.5*	*5.5*	--	*110.8*	*1.8*	*112.7*	*13.0*	*–9.25*	*121.7*
Han-stm4 14C-A	116.0	115.5	14.4	–5.9	111.8	2.9	114.8	--	--	--
Han-stm5 14C-A	116.0	115.5	13.0	–4.9	111.8	3.0	114.8	--	--	--
Han-stt4 14C-A	137.0	117.7	13.2	–5.5	114.0	2.7	116.7	--	--	--
Han-stt5 14C-A	128.0	116.8	14.7	–5.9	113.0	2.6	115.6	--	--	--

*$a^{14}C_m$ = sample measured ^{14}C activity; $a^{14}C_{atm}$ = atmospheric ^{14}C activity (calculated with $\Delta^{14}C$ published data and an atmospheric CO_2 $\delta^{13}C$ = –8.2‰); $a^{14}C_g$ = soil CO_2 ^{14}C activity; CO_2/DIC frac. = soil CO_2 / DIC fractionation factors; $a^{14}C_{DIC}$ = DIC ^{14}C activity, IAEA model = initial DIC ^{14}C activity calculated with the IAEA model.

The dcp is calculated using the measured ^{14}C activity of the deposit ($a^{14}C_m$) and the mean atmospheric ^{14}C activity of the period covering the calcite formation ($a^{14}C_{atm}$; Table 3):

$$dcp = \left(1 - \frac{a^{14}C_m}{a^{14}C_{atm}}\right) 100\ \% \ . \tag{1}$$

Because we compare only groundwaters, no normalization (for a $\delta^{13}C$ of –25‰; Stuiver and Polach 1977; Mook 1980) was done (Wigley and Muller 1981).

The dilution factor (q) connected to the "hard water effect" and used by several authors (Thorpe, Otlet and Sweting 1980; Vogel 1983; Gewelt 1985; Bastin and Gewelt 1986; Fontes 1992) is

$$q = (100 - dcp) / 100 \ . \tag{2}$$

From $a^{14}C_m$ and $\delta^{13}C$ uncertainties (average uncertainty of ±0.7 pMC and ±0.1‰, respectively) and assuming an average error of ±0.7‰ for the $a^{14}C_m$, we estimated the total dcp error at ±1.5%.

Dead carbon calculation, as presented above, is actually an apparent proportion because it is deduced from direct atmospheric and carbonate or water ^{14}C activity measurements and does not take into account fractionation processes. The decrease of the seepage water ^{14}C activity due to limestone dissolution (the actual "dead carbon effect") should lie between the dissolved inorganic carbon (DIC) ^{14}C activity of the water before and after dissolution. Before dissolution, DIC activity is in equilibrium with the soil CO_2; after dissolution, DIC activity is similar to the measured activity of water bicarbonates and of calcite, within uncertainties due to fractionation processes. Thus, it would be more rigorous to consider isotopic fractionations that occur at different stages (Fig. 1):

1. exchange between atmospheric and soil CO_2;
2. CO_2 dissolution and bicarbonate formation;
3. limestone dissolution (dead carbon injection);
4. seepage;
5. CO_2 degassing and $CaCO_3$ precipitation at the time of seepage into the cave.

Based on this simplified course, the dead carbon arrives in the water during the third stage and it is necessary to know the processes during the two previous stages.

Exchange between Atmospheric and Soil CO_2

A global formula takes into account ^{14}C fractionation due to photosynthesis, decarboxylation and diffusion (Fontes 1992):

$$a^{14}C_g = a^{14}C_{atm}\left(\frac{1 - 2.3(\delta^{13}C_{atm} - \delta^{13}C_g)}{1000}\right) pMC \ , \tag{3}$$

where "g" signifies soil CO_2 and "atm" atmospheric CO_2. The latter is known ($a^{14}C_{atm}$ is variable and $\delta^{13}C_{atm}$ = –8.2‰, from Levin, Graul and Trivett (1995)), so we must estimate $\delta^{13}C_g$. Above the caves studied, vegetation consisting of oak trees and Graminaceae is typical of the C_3 type (Calvin-Benson photosynthetic pathway) which produces a $\delta^{13}C_g$ between –20 and –25‰ (Fritz *et al.* 1978; Dörr and Münnich 1986, etc.). Direct measurements on soils above limestone yield values between –20.8 and –23.1‰ for Moulis (Pyrenees, France; Fleyfel 1979) and –22‰ for the Champagne area

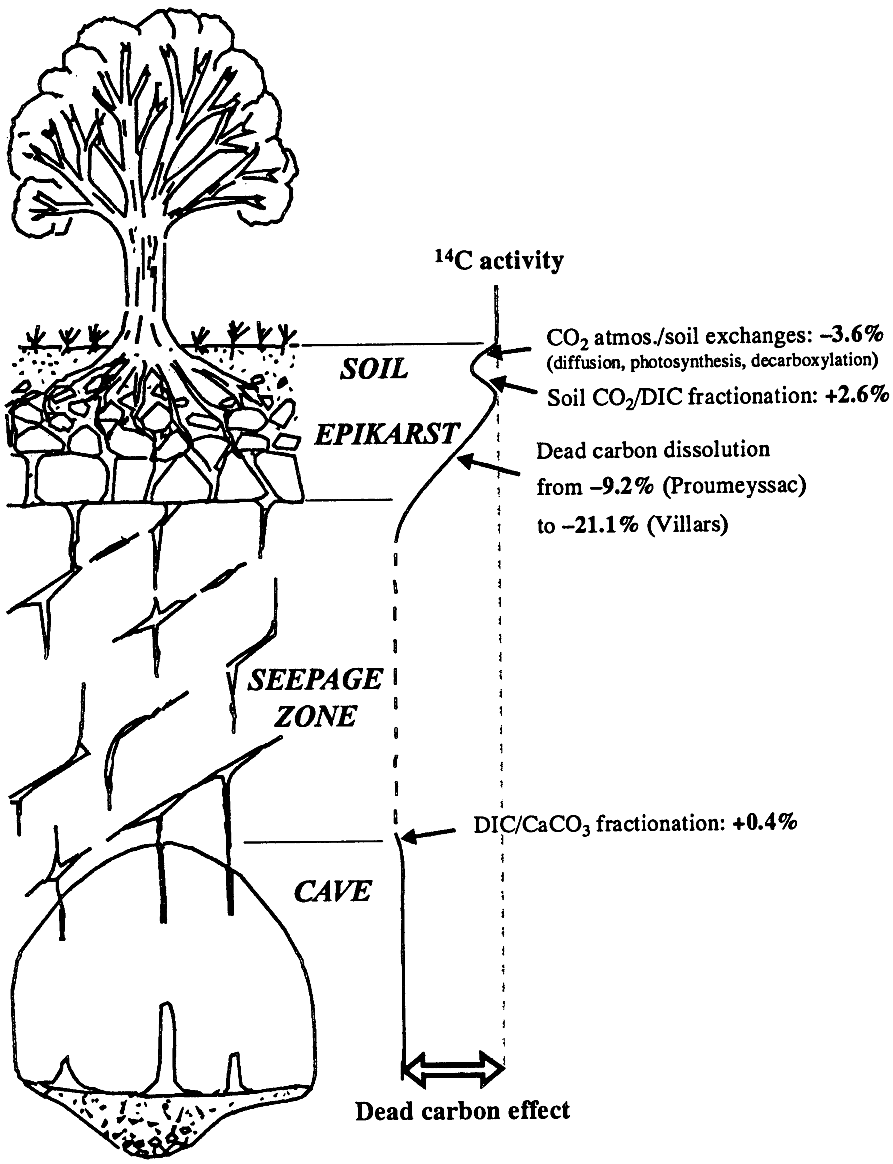

Fig. 1. Schematic ^{14}C activity evolution from atmosphere toward cave deposit. Numbers in % represent the average relative ^{14}C activity variations due to fractionation processes (see text and Table 3). Note that the ^{14}C activity decrease due to soil/atmosphere exchange is compensated by the CO_2/DIC fractionation within the uncertainty limits (± 1.5%).

(France; Dever *et al.* 1982). We can reasonably consider a mean value of –22‰. Results show that soil CO_2 activity is, on average, 3.6 pMC lower than atmospheric activity (Table 3). Karstic soils are generally very thin, and it can be assumed that there is no significant delay between atmosphere and soil CO_2 (Dever *et al.* 1982).

CO_2 Dissolution and Bicarbonate Formation

Assuming equilibrium between soil CO_2 and the DIC, the activity of the latter is given by (Saliège and Fontes 1984):

$$a^{14}C_{DIC} = a^{14}C_g + 0.23(\delta^{13}C_{DIC} - \delta^{13}C_g)\ \text{pMC}\ . \quad (4)$$

Results show an average $^{14}C_{DIC}$ enrichment of 2.6 pMC (Table 3).

The net isotopic balance of stages 1 and 2 is a decrease of about 1 pMC between atmosphere and DIC activities, which is similar to the uncertainty range ±1.5 pMC. Thus, depending on whether we consider atmospheric activity or DIC activity, it is very likely that we will obtain similar values for the dead carbon proportion.

Several models have been developed in order to estimate the hard water effect (connected to the dead carbon effect by Equation (2)) by the calculation of correction for initial water activity: *e.g.*, Tamers's chemical model (1967), Pearson's isotopic model (1965), the IAEA isotopic model (Salem *et al.* 1980), Plummer's chemical and isotopic model (1977) and Fontes and Garnier's chemical and isotopic model (1979). We have applied the IAEA model, which corresponds to the Pearson model corrected by the CO_2/DIC fractionation factor εg-b. This authorizes its use for open systems, which is more adapted to the karstic unsaturated zone:

$$a^{14}C_{DIC} = (a^{14}C_g - a^{14}C_c) \cdot (\delta^{13}C_{DIC} - \delta^{13}C_c) / (\delta^{13}C_g - \varepsilon g\text{-}b - \delta^{13}C_c)\ \text{pMC}\ , \quad (5)$$

where $a^{14}C_c$ and $\delta^{13}C_c$ relate to the limestone of the rock formation,
and $\varepsilon g\text{-}b = -9483\ T^{-1} + 23.89‰$
with T = temperature in K (Mook, Bommerson and Staverman 1974).

Results and Discussion

^{13}C Results

Measured $\delta^{13}C$ values (Table 3) are typically in the range of published results for speleothems and demonstrate that the main source of carbon from dissolved inorganic carbon comes from an equilibration with soil CO_2 (*i.e.*, with $\delta^{13}C_g = -22‰$ and $T = 15°C$, the enrichment factor = $-9‰$, then $\delta^{13}C_{DIC} = -13‰$; Mook, Bommerson and Staverman 1974; Schwarcz 1986; Dulinski and Rozanski 1990; Gascoyne 1992). Calcite values are slightly higher than water values. Average differences are 1.2‰ for Villars, 0.8‰ for La Faurie and 1.1‰ for Proumeyssac. For the cave temperatures (between 10.5 and 15°C), the enrichment factor between DIC and calcite is much lower than the observed difference (between 0.41 and 0.18‰; Mook 1980). However, these differences cannot be interpreted in terms of isotopic equilibrium because waters and calcite do not come from the same systems, and we know that variations from place to place in the same cave can be very great, as noticed in Lower Cave in England (variations up to 4.7‰ between modern deposits; Baker *et al.* 1996). Another possibility is seasonal variation: because calcite develops over several years, mostly in winter when the drip rate is high (Genty *et al.* 1996, 1997), and because all the waters studied were sampled in summer, it may be possible that the observed differences reflect seasonal variations in the isotopic content of seepage water. Similar variations have been observed in the seasonal growth laminae of stalagmites in Belgium, possibly due to the isotopic content variation of the seepage water (Genty, Quinif and Keppens 1995). The other possibility is that water is lighter than calcite because of a slight kinetic fractionation due to a fast CO_2 degassing during $CaCO_3$ precipitation; however, if this is the case here, it would provoke a negligible ^{14}C fractionation (Hendy 1971).

In the Han-sur-Lesse cave, analyzed samples consist of two pairs of stalagmites and stalactites; each pair belongs to the same system. A ^{13}C enrichment of 0.9‰ and 1.7‰ is observed between stalactites and stalagmites for both stations, respectively. Differences up to 2.8‰ have been observed between stalactites and stalagmites of Lower Cave, England (Baker, Barnes and Smart 1996); evaporation could be one of the causes. Here, the $\delta^{18}O$ results do not testify in favor of evaporation, at least for the Han-stt4/Han-stm4 couple where the difference is –0.4‰ (Table 3); then kinetic isotopic fractionation due to a fast CO_2 escape could explain these differences (Hendy 1971). In any case, differences here are small and will have no important consequences on ^{14}C fractionation (*i.e.*, if we assume a ^{14}C fractionation twice that of the ^{13}C fractionation, maximum ^{14}C enrichment will be 3.4‰, which is within the ^{14}C activity measurement uncertainty).

^{14}C Results

Calcite and DIC AMS ^{14}C contents are between 89.7 and 118.6 pMC (Table 3). These high values confirm the continued importance of bomb ^{14}C contamination. The dead carbon proportion is between 9.2% and 21.9% for the calcite deposits and between 3.6% and 21.9% for the DIC of seepage waters. From these results we can make two important inferences: 1) for the same sampled site, waters have a systematically lower dead carbon proportion than calcite; 2) for the same site and where we analyzed several calcite samples, the dead carbon proportion is homogeneous.

^{14}C Activity Comparison between Water (DIC) and Calcite

Villars cave samples show the lowest dcp difference between water and calcite (avg. = 1.1%), which is within the uncertainty limits (± 1.5%). For the La Faurie and Proumeyssac caves, the difference is greater: 8.5% and 3.7%, respectively. Table 4 includes factors capable of having an influence on ^{14}C content in water. These show that:

- Neither the time elapsed between sampling and analysis, nor the time during which water was sampled, has any effect on dcp: *i.e.*, similar dcp is found for a low drip rate (La Faurie) and for a high drip rate (Proumeyssac);
- $\delta^{13}C$ values do not show any possible equilibrium with cave air, whose composition must be similar to that of the atmosphere, but are characteristic of DIC that has been in equilibrium with soil CO_2 (according to the pCO_2, which is close to that of the atmosphere; however, measurements will be necessary to verify this);
- pH values are typical of karstic waters; note, however, the higher pH (8) in the Proumeyssac cave.

Explanation of water-calcite ^{14}C activity differences must be found elsewhere. Seasonal variations in the ^{14}C content of soil CO_2 have been detected in Germany: it is lower in winter because of more intense organic matter decomposition and it is higher in summer because plant root respiration is the dominant factor; the winter/summer $\Delta^{14}C$ variation varies from 50‰ under grassland to 100‰ under forest (Dörr and Münnich 1986). Water that feeds speleothems in temperate areas like Europe infiltrates mostly in winter between November and March (Genty *et al.* 1997); then it is likely that calcite deposits more closely reflect the winter season. Conversely, water that has been collected in August must reflect the summer season. Thus, the differences observed between the ^{14}C activity of water and calcite could be explained by a simple seasonal variation in the ^{14}C content of the soil above the cave; but more measurements are needed to confirm this hypothesis.

TABLE 4. Factors Capable of Influencing Content of ^{14}C in Water

Sample and station numbers	dcp (%)	Type of bottle	ND*	TE†	MFR‡	pH	$\delta^{13}C$ (‰ PDB)	Cave air pCO_2 (%)§
Vil-eau 14C-A - #1B	21.9	Plastic 250ml	10	<3	4.7	?	−11.8	0.16
Vil-eau 14C-B - #4	18.2	Plastic 250ml	49	<3	3.8	7.5	−9.7	0.16
Vil-eau 14C-C - #1B	20.0	Plastic 250ml	49	<4	6	7.5	−10.8	0.16
Fau-eau 14C-A - #2	3.6	Glass 150ml	47	<48	95	7.1	−11.7	0.08
Fau-eau 14C-B - #12	3.9	Glass 150ml	47	<48	100	7.1	−11.7	0.08
Prou-eau 14C-B - #1	5.5	Glass 150ml	47	<0.3	continuous water flow	8.0	−10.7	0.04
Prou-eau 14C-A - #2	5.5	Glass 150ml	47	<0.5	<2	8.0	−14.0	0.04

*ND = No. of days between sampling and analysis
†TE = Time elapsed during dripping sampling, hours
‡MFR = Mean flow rate, seconds/drip
§Measured January 1997

Inter-Site ^{14}C Activity Comparison

For each site, and where at least several analyses have been made, it appears that the calcite dcp is homogenous (Fig. 2). Villars shows the highest values (avg. = 21.1%, σ = 0.8%; n = 3), followed by Han-sur-Lesse (avg. = 13.8%, σ = 0.8%; n = 4), La Faurie (12.2%; n = 1) and Proumeyssac (9.2%; n = 1). Comparison of these results with environmental conditions—vegetation type and density, soil thickness, geology and limestone formation thickness, pluviometry and temperature (Table 2)—leads to the following remarks:

- Rock formation thickness does not correlate with dcp; moreover, in the same cave a similar dcp was found for two samples taken at a 10 m altitude difference (Villars, #1B and #4);
- soil thicknesses, which are typical of karstic areas, also do not correlate with dcp;
- the lowest dcp (calcite and water) is found under grassland (La Faurie and Proumeyssac), whereas the highest is found under forest (Villars and Han-sur-Lesse);
- however, the Han-sur-Lesse site (Belgium), also covered by a continuous forest, shows a calcite dcp close to the dcp found under grassland in Southwestern France sites; note also that this site is about 3°C colder than the French ones;
- the difference observed between La Faurie and Villars, which are 60 km apart and have similar geology and climate, is possibly due to the forest cover of the Villars site.

The dcp is theoretically linked to the dissolution intensity: the more intense the dissolution, the higher the dcp. Factors that control carbonate dissolution are temperature and, most importantly, soil CO_2 partial pressure (Dever *et al.* 1982; Dörr and Münnich 1986, *etc.*). Soil CO_2 has two major sources: root respiration and microbial organic matter decomposition. Both sources will be higher in a forest soil than under a grassland. This can explain, for the most part, why dcp is higher under forest covers like the Villars and Han-sur-Lesse caves. It is possible that the 3°C lower temperature of the Belgian site yields a lower vegetation activity and thus a lower dissolution and dcp.

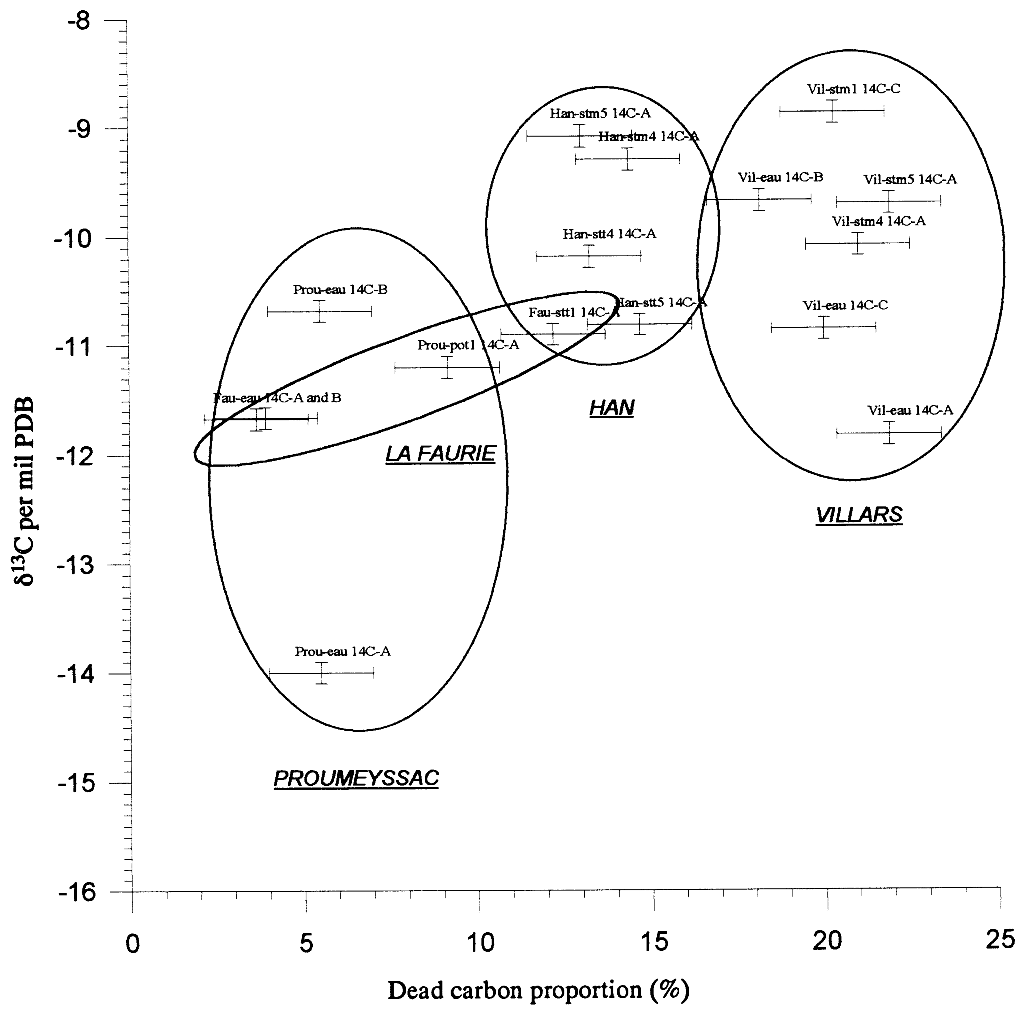

Fig. 2. Dead carbon proportion (dcp) *vs.* $\delta^{13}C$. Note that all samples from the same site are grouped together; Villars cave has the highest dcp, followed by Han-sur-Lesse cave, both under a forest cover. La Faurie and Proumeyssac, which are under grassland, show the lowest dcp.

But we must consider that other unquantified factors may possibly intervene. The possible mixing of fast and slow transit waters can change the theoretical ages that we have considered; only the hydrographic analysis of stalactite dripping flows in the different sites studied will inform us as to the possible age spectrum of the waters (work in progress). Another complicating factor can be the fracture density in the rock formation through which water infiltrates. During seepage, both water and gas infiltrate (two-phase seepage) as has been shown in a Southern France karstic area (Mangin 1975; Fleyfel 1979; Fleyfel and Bakalowicz 1980). Such a flow, combined with an intense fracture system, will favor dissolution-reprecipitation processes and thus secondary calcite deposits before reaching the cave itself (not to mention the higher possibility of isotope exchanges). This will have major consequences on speleothem isotope measurements, particularly in modern deposits. For example, a period of intense dissolution will have opposite effects on dcp:

- a decrease in the DIC ^{14}C activity, and consequently a higher dcp, if the dissolved carbonate is old limestone;
- an increase in the DIC ^{14}C activity, and consequently a lower dcp, if the dissolved carbonate is a secondary calcite deposit that was precipitated in the 1960s, when the atmospheric ^{14}C activity was very high.

The actual process probably occupies a midpoint between these two hypotheses: both old limestone with 0 pMC activity and secondary calcite deposits with a significant ^{14}C activity are dissolved during infiltration.

Comparison Between Measured ^{14}C Activity and the IAEA Model Initial Activity Calculation

Water mixing models could be helpful in understanding dissolution processes. Because we do not have enough chemical data, we have only tested the corrected Pearson isotopic model, known as the IAEA model (Salem *et al.* 1980), on three sites: La Faurie, Villars and Proumeyssac (Table 3). Because the original Pearson model is designed for closed systems (Pearson 1965) and because the karstic unsaturated zone cannot be considered as a closed system (CO_2 is mostly dissolved in the presence of carbonates, at least in our sites where the soil thickness is only a few centimeters; Krajcar-Bronić *et al.* 1986, 1992; Ek, Hilaire-Marcel and Trudel 1981; Fontes 1992), it must be corrected by the CO_2/DIC fractionation factor. Considering a soil CO_2 $\delta^{13}C = -22‰$ and a 0 pMC ^{14}C activity for the limestone formation, the average calculated DIC activities show quite good agreement (±15 pMC) with measured activities (Table 3). The average difference between the IAEA and the measured activities is −1.2 pMC ($\sigma = 12.0$), which confirms the validity of this model in different geological contexts (Fontes, 1985).

Conclusions

1. Thanks to annually laminated speleothems, the dcp due to old limestone dissolution can be calculated within an uncertainty range of ±1.5%.
2. The dcp varies from 9.2% to 21.9% for calcite deposits and from 3.6% to 21.9% for DIC in water.
3. At the same sampling site, and where several measurements were made, the dcp is homogeneous.
4. Inter-site dcp variations are up to 11%; the average dcp in our sites is 15.5% ± 4.4, within the uncertainty range of former measurements and assumptions (15% ± 5; equivalent to a dilution factor of 0.85 ± 0.5).
5. For the same site, water has a lower dcp than calcite deposits (mean differences are between 1.1 and 8.5%); this could be because all the waters studied were sampled in summer, when soil CO_2 activity is higher, while speleothems mostly develop in winter and spring when soil CO_2 activity is lower; but more measurements are needed to confirm this hypothesis.
6. For a similar environment, the dcp is higher under forest cover (*e.g.*, at the Dordogne sites, dcp = 21.1% under forest and dcp = 12.2% under grassland); this may be the consequence of more intense dissolution processes due to root respiration and microbial organic matter decomposition. However, the Belgian site, also under a forest cover, shows a dcp very close to Southwestern France sites that are under grassland; the 3°C lower temperature may be one of the causes. The possible mixing of rapid and slow (old) water flows must also be considered as playing a role in dcp results; only stalactite hydrographic analyses in each site will bring insight into the nature of the drainage.

7. The IAEA isotopic water mixing model (Pearson model corrected for an open system) is in good agreement with measured activities.

If dcp is as varied as we observed from one site to another, and if those variations are due to vegetation and soil conditions, it is very likely that dcp changed at any given site during the past when vegetation altered because of human activities and/or climate changes. From our study, dcp can vary by 11%; this yields an age difference of 970 yr, which is not negligible for the Holocene or Late Glacial chronology. Thus it is highly recommended to calculate the dcp at the sample site first before doing any age calculation based on ^{14}C method.

If vegetation seems to be a factor that influences the dcp, it is likely that environmental factors that favor secondary calcite precipitation in the unsaturated zone, such as fracture density, also play an important role. The high measured activities could accordingly be explained by the dissolution of secondary calcite deposits that precipitated in the 1960s or 1970s, when the atmospheric activity was very high. Thus, the dcp can be tied both to vegetation and to the local potential of secondary calcite deposit. The possible existence of such a process greatly complicates the interpretation of the dcp; work in progress on a single laminated stalagmite will help shed light on the importance of dissolution-precipitation processes above a cave.

ACKNOWLEDGMENTS

This study was funded by specific research programs of the Centre National de la Recherche Scientifique: DBT, DYTEC and GDR 970. It is part of IGCP 379 and PAGES PEPIII programs. We are grateful to Thierry Baritaud, Yves Quinif and Guy Deflandre, who helped us in sampling, and to the cave owners, Hubert Versaveau, Alain Frances, and Mesdames Duret and Trapp. All AMS measurements were performed at the Tandetron at the Centre des Faibles Radioactivités, Gif-sur-Yvette, France. We thank Andy Baker for his help in pCO_2 measurements and are grateful to Bogomil Obelić and Niel L. Plummer for helpful comments.

REFERENCES

Atkinson, T. C., 1985 Present and future directions in karst hydrogeology. *Annales de la Société Géologique de Belgique* 108: 293–296.

Baker, A., Smart, P. L., Edwards, R. L. and Richards, D. A. 1993 Annual growth bandings in a cave stalagmite. *Nature* 364: 518–520.

Baker, A., Barnes, W. and Smart, P.1996 Luminescence and discharge variations in stalagmite drip waters. In *Climate Change: The Karst Record.* Proceedings of the symposium in Bergen, Norway, August 1–4th 1996. Bergen, Norway, University of Bergen Karst Water Institute: 36–39.

Baker A., Ito, E., Smart, P. L. and McEvan, R., in press, Elevated 13-C in speleothem and implications for palaeovegetation studies. *Chemical Geology (Isotope Geoscience).*

Bard, E., Hamelin, B. and Fairbanks, R. G. 1990 U-Th ages obtained by mass spectrometry in corals from Barbados: Sea level during the past 130,000 years. *Nature* 346: 456–458.

Bastin, B. and Gewelt, M. 1986 Analyse pollinique et datation ^{14}C de concrétions stalagmitiques holocènes: Apports complémentaires des deux méthodes. *Géographie Physique et Quaternaires* 15(2): 185–196.

Broecker, W. S. and Olson, E. A. 1960 Radiocarbon measurements and annual rings in cave formations. *Nature* 185: 93–94.

Brook, G. A. and Nickmann, R.J. 1996 Evidence of Late Quaternary environments in Northwestern Georgia from sediments preserved in Red Spider Cave. *Physical Geography* 17(5): 465–484.

Destombes, J. L., Cordonnier, M., Gadat, J. Y. and Delannoy J. J. 1997 Periodic and aperiodic forcing of water flow through sodastraw stalactites (Choranche, Vercors, France). *In* Union International de Spéléologie, eds., *Proceedings of the 12th International Speleological Congress of Chaud-Les-Fonds, Neuchâtel, Switzerland*: in press.

Dever, L., Durand, R., Fontes, J. C. and Vachier, P. 1982 Géochimie et teneurs isotopiques des systèmes saisonniers de dissolution de la calcite dans un sol sur craie. *Geochimica et Cosmochimica Acta* 46: 1947–1956.

Dörr, H. and Münnich, K.O. 1986 Annual variations of the ^{14}C content of soil CO_2. *In* Stuiver, M. and Kra, R., eds., Proceedings of the 12th International ^{14}C Conference. *Radiocarbon* 28(2A): 338–345.

Dulinski, M. and Rozanski, K. 1990 Formation of $^{13}C/^{12}C$ isotope ratios in speleothems: A semi-dynamic model. *Radiocarbon* 32(1): 7–16.

Ek, C., Hilaire-Marcel, C. and Trudel, B. 1981 Sédimentologie et paléoclimatologie isotopique dans une grotte de Gaspésie, Québec. *Géographie Physique et Quaternaire* 34(2): 317–328.

Fleyfel, M. (ms.) 1979 Etude hydrologique, géochimique et isotopique des modalités de minéralisation et de transfert du carbone dans la zone d'infiltration d'un aquifère karstique: Le Baget (Pyrénées ariégeoises). Thèse de Docteur-Ingénieur Université P. et M. Curie, Paris: 221 p.

Fleyfel, M. and Bakalowicz M. 1980 Etude géochimique et isotopique du carbone mineral dans un aquifere karstique. *Colloque Société Géologique de France, Bordeaux 17–18 Novembre 1980:* 231–245.

Fontes, J. C. and Garnier, J. M. 1979 Determination of the initial ^{14}C activity of the total dissolved carbon: A review of the existing models and a new approach. *Water Resources Research* 15: 399–413.

Fontes, J. C. 1985 Some considerations on ground water dating using environmental isotopes. *In* Hydrogeology in the Service of Man, Memoirs of the 18th Congress of the International Association of Hydrologists. Cambridge, International Association of Hydrologists: 118–154.

Fontes, J. C. 1992 Chemical and isotopic constraints on ^{14}C dating of groundwater. *In* Taylor, R. E., Long, A. and Kra, R. S., eds., *Radiocarbon after Four Decades.* New York, Springer-Verlag: 242–261.

Ford, D. and Williams, P. 1989 *Karst Geomorphology and Hydrology.* London, Chapman & Hall: 601 p.

Fritz, P., Reardon, E. J., Barker, E. J., Brown, M., Cherry, A., Killey, W. D. and McNaughton, D. 1978 The carbon isotope geochemistry of a small groundwater system in north-eastern Ontario. *Water Resources Research* 14: 1059–1067.

Gascoyne, M. 1992 Paleoclimate determination from cave calcite deposits. *Quaternary Science Reviews* 11: 609–632.

Genty, D. 1993 Mise en évidence d'alternances saisonnières dans la structure interne des stalagmites. Intérêt pour la reconstitution des paléoenvironnements continentaux. *Comptes Rendus de l'Académie de Sciences* (Paris), ser. 2, 317: 1229–1236.

Genty, D., Baker, A., Barnes, W. and Massault, M. 1996 Growth rate, grey level and luminescence of stalagmite laminae. In *Climate Change: The Karst Record.* Proceedings of the symposium in Bergen, Norway, August 1–4th 1996. Bergen, Norway, University of Bergen Karst Water Institute: 36–39.

Genty, D., Deflandre, G., Quinif, Y. and Verheyden, S., in press, Les lamines de croissance des spéléothèmes: origine et intérêt paléoclimatique. *Annales de la Société Géologique de Belgique.*

Genty, D. and Quinif, Y. 1996 Annually laminated sequences in the internal structure of some Belgian stalagmites – Importance for paleoclimatology. *Journal of Sedimentary Research* 66: 275–288.

Genty, D., Quinif, Y. and Keppens, E. 1995 Les variations saisonnières des lamines de croissance mises en évidence par le dosage des isotopes stables de l'oxygène et du carbone. *Spéléochronos* (Faculté Polytechnique de Mons, Belgium) 6: 32–34.

Gewelt, M. 1985 Cinetique du concrétionnement dans quelques grottes belges: Apport des datations ^{14}C et $^{230}Th/^{234}U$. *Annales de la Société Géologique de Belgique* 108: 267–273.

Gewelt, M. 1986 Datation ^{14}C des concrétions de grottes belges: Vitesses de croissance durant l'Holocène et implications paléoclimatiques. *In* Paterson, K. and Sweeting, M. M. *New Directions in Karst: Proceedings of the Anglo-French Karst Symposium, September 1983.* Norwich, Geo Books: 293–322.

Geyh, M. A. and Henning G. J. 1986 Multiple dating of a long flowstone profile. *In* Stuiver, M. and Kra, R., eds., Proceedings of the 12th International ^{14}C Conference. *Radiocarbon* 28(2A): 503–509.

Geyh, M. A. and Franke, H. W. 1970 Zur Wachstumsgeschwindigkeit von Stalagmiten. *Atompraxis* 16: 46–48.

Goede, A. and Vogel, J. C. 1991 Trace element variation and dating of a Late Pleistocene Tasmanian speleothem. *Paleogeography, Paleoclimatology, Paleoecology* 88: 121–131.

Goslar, T., Arnold, M., Bard, E., Kuc, T., Pazdur, F., Ralska-Jasiewiczowa, M., Rozanski, K., Tisnerat, N., Walanus, A., Wicik, B. and Wieckowski, K. 1995 High concentration of atmospheric ^{14}C during the Younger Dryas cold episode. *Nature* 377: 414–417.

Hendy, C. H. 1971 The isotopic geochemistry of speleothems–I. The calculation of the effects of different modes of formation on the isotopic composition of speleothems and their applicability as paleoclimatic indicators. *Geochimica et Cosmochimica Acta* 35: 801–824.

Hobbs, S. L. and Smart, P. L. 1986 Characterization of carbonate aquifers: A conceptual base. *In* Union International de Spéléologie, ed., *Proceedings of the 9th International Speleological Congress of Barcelona* 1: 43–46.

Holmgren, K., Lauritzen, S. E. and Possnert, G. 1994 $^{230}Th/^{234}U$ and ^{14}C dating of a Late Pleistocene stalagmite in Lobatse II cave – Botswana. *Quaternary Geochronology* 13: 111–119.

Issar, A. S., Govrin, Y., Geyh, M. A., Wakshal, E. and Wolf, M. 1992 Climate changes during the Upper Holocene in Israel. *Israelian Journal of Earth Science* 40: 219–223.

Krajcar-Bronić, I., Horvatinčić, N., Srdoč, D. and Obelić, B. 1986 On the initial ^{14}C activity in karst aquifers with short mean residence time. *In* Stuiver, M. and Kra, R., eds., Proceedings of the 12th International ^{14}C Conference. *Radiocarbon* 28(2A) 436–440.

____1992 Experimental determination of the ^{14}C initial activity of calcareous deposits. *In* Long, A. and Kra, R. S., eds., Proceedings of the 14th International ^{14}C Conference. *Radiocarbon* 34(3): 593–601.

Levin, I., Bösiger, R., Bonani, G., Francey, R. J., Kromer, B., Münnich, K. O., Suter, M., Trivett, N. B. A. and Wölfli, W. 1992 Radiocarbon in atmospheric carbon dioxide and methane: Global distribution and trends. *In* Taylor, R. E., Long, A. and Kra, R. S., eds., *Radiocarbon after Four Decades*. New York, Springer-Verlag: 503–518.

Levin, I., Graul, R. and Trivett, N. B. A. 1995 Long-term observations of atmospheric CO_2 and carbon isotopes at continental sites in Germany. *Tellus* 47B: 23–34.

Mangin, A. (ms.) 1975 Contribution à l'étude des aquifères karstiques. Thèse de Doctorat, Université de Dijon.

Mazaud, A., Laj, C., Bard, E., Arnold, M. and Truic, E. 1991 Geomagnetic field control of ^{14}C production over the last 80 ky: Implications for the radiocarbon time-scale. *Geophysical Research Letters* 18: 1885–1888.

Mook, W. G. 1980 Carbon-14 in hydrogeological studies. *In* Fritz, P. and Fontes, J. Ch., eds., Handbook of Environmental Geochemistry 1A. Amsterdam, Elsevier Scientific Publishing Co.: 49–74.

Mook, W. G., Bommerson, J. C. and Staverman, W. H. 1974 Carbon isotope fractionation between dissolved bicarbonate and gaseous carbon dioxide. *Earth and Planetary Science Letters* 22: 169–176.

Pazdur, A., Pazdur, M. F. and Pawlyta J. 1995 Paleoclimatic implications of radiocarbon dating of speleothems from the Cracow-Wielun Upland Southern Poland. *In* Cook, G. T., Harkness, D. D., Miller, B. F. and Scott, E. M., eds., Proceedings of the 15th International ^{14}C Conference. *Radiocarbon* 37(2): 103–110.

Pearson, F. J. 1965 Use of $^{13}C/^{12}C$ ratios to correct radiocarbon ages of material initially diluted by limestone. *In* Chatters, R., ed., Proceedings of the 6th International Conference on Radiocarbon and Tritium Dating. Pullman, Washington, U.S. Atomic Energy Commission: 357–366.

Pitty, A. F. 1966 *An Approach to the Study of Karst Water.* University of Hull, Ocasional Papers in Geography 5: 70 p.

Plummer, L. N. 1977 Defining reactions and mass transfer in part of the Floridian aquifer. *Water Resource Research* 13: 801–812.

Railsback, L. B., Brook, G. A., Chen, J., Kalin, R. M. and Fleisher, C. J. 1994 Environmental controls on the petrology of a late Holocene speleothem from Botswana with annual layers of aragonite and calcite. *Journal of Sedimentary Research* A64 (1): 147–155.

Reicher, B. and Trimborn, P. 1995 Application of tracer techniques to characterize hydraulics and solute transport of the epikarst zone of a karst aquifer. In *Proceedings of the International Symposium on Isotopes in Water Resource Management.* Vienna, IAEA: 303–305.

Salem, O., Visser, J. H., Dray, M. and Gonfiantini, R. 1980 Groundwater flow patterns in the western Lybian Arab Jamahiriya. In *Arid-Zone Hydrology: Investigations with Isotope Techniques.* Vienna, IAEA: 165–179.

Saliege, J. F. and Fontes, J.-Ch. 1984 Essai de détermination expérimentale du fractionnement des isotopes ^{13}C et ^{14}C du carbone au cours de processus naturels. *International Journal of Applied Radiation and Isotopes* 35: 55–62.

Schwarcz, H. P. 1986 Geochronology and isotopic geochemistry of speleothems. *In* Fritz, P. and Fontes, J. Ch., eds., *Handbook of Environmental Geochemistry 2B.* Amsterdam, Elsevier Scientific Publishing Co.: 271–303.

Shopov, Y. Y. and Dermendjiev, V. 1990 Microzonality of luminescence of cave flowstones as a new indirect index of solar activity. *Compte Rendu de l'Académie Bulgare des Sciences* 43: 9–12.

Suess, H. E. and Linick, T. W. 1990 The ^{14}C record in bristlecone pine wood of the past 8000 years based on the dendrochronology of the late C. W. Ferguson. *Philosophical Transactions of the Royal Society of London* A330: 403–412.

Stuiver, M. and Polach, H. 1977 Discussion: Reporting of ^{14}C data. *Radiocarbon* 19(3): 355–363.

Talma, A. S. and Vogel J. C. 1992 Late Quaternary paleotemperatures derived from a speleothem from Cango Caves, Cape Province, South Africa. *Quaternary Reasearch* 37: 203–213.

Tamers, M. A. 1967 Radiocarbon ages of groundwater in an arid zone unconfined aquifer. In *Isotope Techniques in the Hydrological Cycle*. American Geophysical Union Monograph 11: 143–152.

Thorpe, P. M., Otlet, R. L. and Sweeting, M. M. 1980 Hydrological implications from ^{14}C profiling of UK Tufa. *In* Stuiver, M. and Kra, R. S., eds., Proceedings of the 10th International ^{14}C Conference. *Radiocarbon* 22(3): 897–908.

Vogel, J. C. 1983 ^{14}C variations during the Upper Pleistocene. *In* Stuiver, M. and Kra, R. S., eds., Proceedings of the 11th International ^{14}C Conference. *Radiocarbon* 25(2): 213–218.

Wigley, M. L. and Kelly, P. M. 1990 Holocene climatic change, wiggles and variations in solar irradiance. *Philosophical Transactions of the Royal Society of London* A330: 547–560.

Wigley, M. L. and Muller, A. B. 1981 Fractionation corrections in radiocarbon datings. *Radiocarbon* 23(2): 173–190.

[RADIOCARBON, VOL. 39, NO. 1, 1997, P. 49–59]

CHARACTERIZATION OF GROUNDWATER IN THE CARIRI (CEARÁ, BRAZIL) BY ENVIRONMENTAL ISOTOPES AND ELECTRIC CONDUCTIVITY

MARLUCIA F. SANTIAGO,[1] C. M. S. V. SILVA,[1] J. MENDES FILHO[1] and H. FRISCHKORN[2]

ABSTRACT. The Cariri region is the largest sedimentary basin in the state of Ceará, Brazil. Located in the southern portion of the state, it comprises the Araripe Plateau and the Cariri Valley on its northern foot. The region's groundwaters are being heavily exploited. Using electric conductivity (EC) and ^{18}O, ^{14}C and ^{3}H data, we differentiate groundwaters from various origins. We identified three horizons of springs on the slope of the Plateau through their geologic environment and the EC of their waters. Groundwaters from wells in the Cariri Valley are classified according to the aquifers exploited as indicated by the drilling profiles. However, strong tectonic features and intense fracturing in the Valley produce a great many horizontal discontinuities, which result in a mixing of groundwaters from different aquifers. Mixing systems are described in terms of $\delta^{18}O$–^{14}C and EC–^{14}C linear trends.

INTRODUCTION

The Cariri region is located in the southern portion of the state of Ceará in the semiarid northeast of Brazil. The area is a green "oasis" embedded in a barren landscape of mostly crystalline bedrock outcroppings. The region consists of a sedimentary plateau (the Araripe Plateau) with a mean elevation of 750 m and an area of *ca.* 7500 km^2, and a sedimentary basin (the Cariri Valley), measuring *ca.* 3500 km^2, on its northern foot.

Rich groundwater resources are the driving agents for the region's important economy, which is second only to that of the capital of the state. The resources provide an exclusive water source for cattle raising and domestic, industrial and agricultural water supplies and are being intensively exploited mainly for large-scale irrigation of sugar cane. However, the origin of the groundwater and its recharge areas are still largely unknown.

Our research in the Cariri was initiated because of popular complaints denouncing the environmental damage caused by deforestation at the top of the Araripe Plateau, as well as overexploitation of the Cariri Valley aquifers. The discharge from one of the major springs emerging from the cliffs of the Plateau has dropped during the period from 1920 to 1993 from *ca.* 1300 m^3 h^{-1} to 380 m^3 h^{-1} (Kemper *et al.* 1995). In years with poor rainfall the water table in the Valley lowered dramatically. A great number of private wells (with depths <20 m) fell dry and natural lakes disappeared without returning to their normal extension in the following years. Based on environmental isotope data (^{14}C, ^{18}O, ^{3}H) and EC measurements, we have characterized the waters from the different aquifers to evaluate regional groundwater dynamics.

DESCRIPTION OF THE AREA

The area of this study comprises mainly the townships of Crato, Juazeiro do Norte, Barbalha and Missão Velha (Fig. 1). In this part of the Cariri, mean annual rainfall is *ca.* 1000 mm, surpassing that of many coastal areas of the state. Differing from the rest of Ceará, where the southerly shifting of the Zone of Intertropical Convergence causes the single rainy period around April (lasting three to four months), the Cariri is favored with two distinct rainfall regimens that produce a two-humped distribution of precipitation: in addition to the main peak in April, a precursing one appears in January. This is due to cyclonic events penetrating from the south. Because of this, the growth period of vegetation is greatly increased as compared to the central and northern parts of Ceará.

[1]Department of Physics, Federal University of Ceará, PO Box 6030, 60451-970 Fortaleza, Brazil
[2]Department of Hydraulics, Federal University of Ceará, PO Box 6018, 60451-970 Fortaleza, Brazil

Structurally, the Cariri region is characterized by pronounced tectonic features. Mont'Alverne *et al.* (1995) describe successive grabens and horsts along sections AB and CD in Figure 1A. Chignone *et al.* (1986) individualized seven structural blocks in the Cariri Basin, the most important of which are: 1) the block of Crato/Corredores, with arched grabens and horsts; 2) the graben of the Serra das Cacimbas; and in between these, 3) the regional, central horst of Mauriti.

A drilling (P1 in Fig. 1B) by Petrobras in the township of Araripina/Pernambuco, on the Plateau, revealed the following sequence of formations (thicknesses are in parentheses): Exu (228 m), Arajara (165 m), Santana (112 m), Rio da Batateira (198 m), Abaiara (124 m), Missão Velha (190 m), Brejo Santo (431 m) and Mauriti (41 m). Exu, Arajara, Santana and Rio da Batateira are all from the Middle Cretaceous Period, Abaiara is from the Cretaceous, Missão Velha and Brejo Santo from the Upper Jurassic and, finally, Mauriti, which is in contact with the crystalline basement, is from the Silurian/Devonian Period. The first three formations constitute the Araripe Plateau and are absent in the Cariri Valley. Arajara, Santana and Brejo Santo formations are aquitards and the others are aquifers.

A drilling by the Departamento Nacional de Produção Mineral (DNPM) in the township of Bodocó/ Pernambuco, *ca.* 15 km southwest of the Petrobras, showed that the formations Abaiara, Missão Velha and Mauriti are absent at this location. Sequence and thicknesses are as follows: Exu (190 m), Arajara (40 m), Santana (242 m), Rio da Batateira (59 m), Brejo Santo (380 m) and Mauriti (32 m). The piezometric level for the Rio da Batateira Formation was 370 m by this drilling.

Due to sandy soils on top of the Plateau and, possibly, open fractures in the Exu Formation, infiltration occurs very quickly there. A surface drainage system is only faintly developed. Even several hours after heavy rainfall, no accumulation of surface water is found. There are no producing deep wells on the Plateau, with the exception of one in the Fazenda Janaguba, near the edge of the Plateau, that taps the saturated layer (possibly 60 m thick) at the contact of the formations Exu and Arajara. However, there are some localized perched aquifers, such as in a settlement called "Cacimbas". (The name refers to a type of shallow, dug well found in the area.)

The Exu/Arajara and Arajara/Santana contacts constitute discontinuities (from high to low) of hydraulic conductivity and define the horizons of some hundreds of springs that emerge at roughly half of the height of the Plateau above the Basin. They appear mainly in gorges and other locations affected by erosion where resistance to water flow is reduced. Their total discharge is roughly 50 m^3 min^{-1} (Gaspary 1967). The allocation and use of the waters from some of these springs have been legally established for over a century.

The exploitation of aquifers in the Cariri Basin is intense. The depths of wells studied range from 32 to 240 m, with pumping rates reaching 300 $m^3 h^{-1}$; their water generally derives from contributions from various aquifers. Wells are often arranged in batteries, specially along the alluvial zones of the rivers Rio da Batateira (in Crato), Riacho dos Macacos (in Juazeiro do Norte), Rio Salamanca (in Barbalha) and Riacho dos Porcos (in Milagres). Due to excessive pumping of wells, in some of these rivers during the dry season, the natural runoff has not been replaced by returning waste water from households and factories.

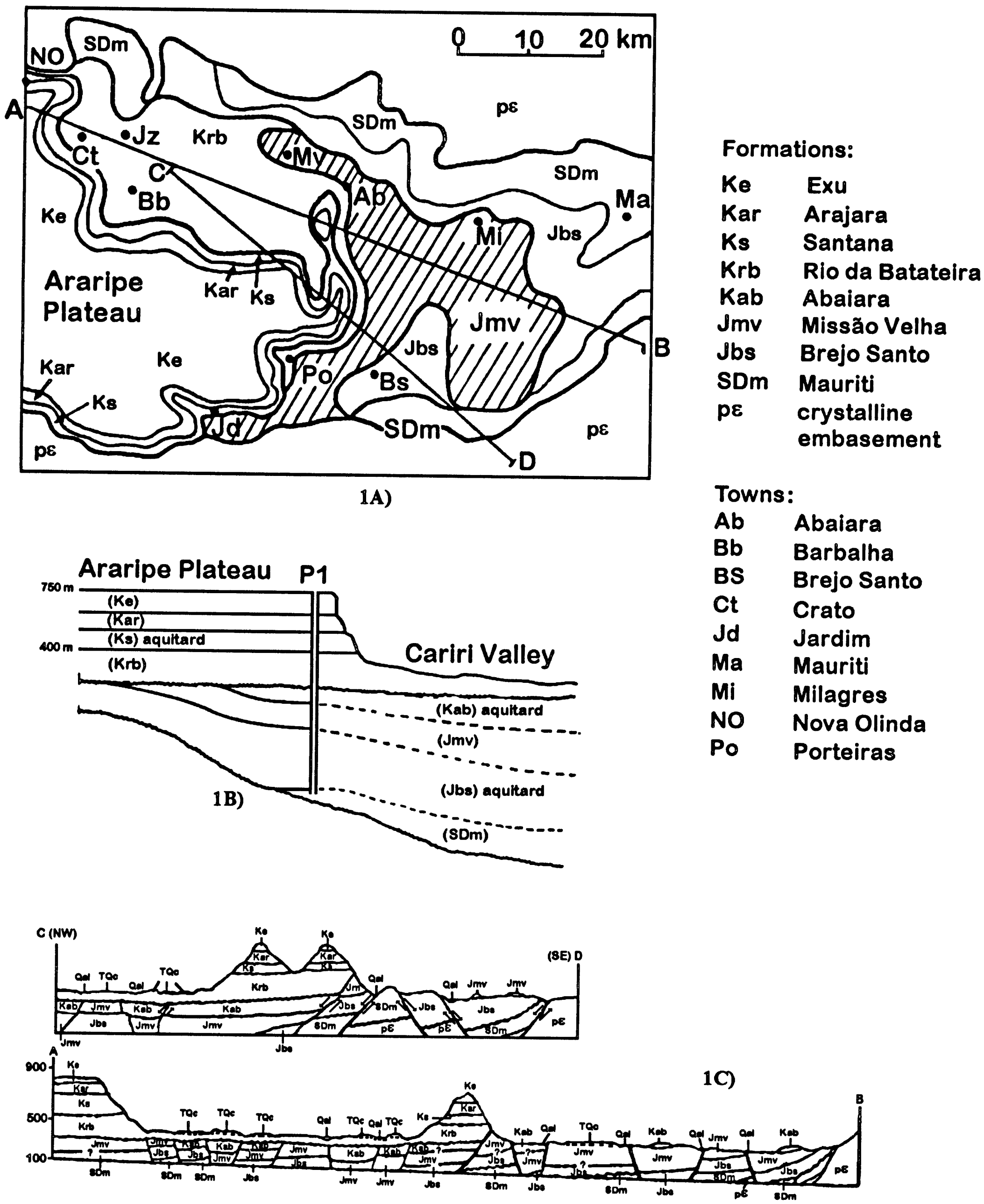

Fig. 1. A) The area of study; B) Geological sketch; C) Stratigraphic of the Araripe Plateau and Cariri Valley.

METHODS

^{14}C and ^{18}O measurements were made on groundwater, and ^{3}H and ^{18}O were analyzed in water from springs. The discharge from two springs was monitored for *ca.* 3 yr using NaCl dilution after instantaneous injection. ^{14}C and ^{3}H were measured in our (Physics Department) laboratory and ^{18}O was measured by Hydroisotop (Schweitenkirchen, Germany). Electric conductivity (EC) was measured in the field. Geographic coordinates were assigned through GPS.

^{14}C values were obtained by gas-proportional counting of acetylene (864 ml at 760 Torr, corresponding to *ca.* 1 g of carbon). The standard used was HOxI. An error of $\pm 1\ \sigma$ applies to the counting statistics of background, samples and modern standard. Some of the ^{14}C data were published previously (Santiago *et al.* 1994). Tritium was measured in our laboratory with a Packard Tri-Carb® 2000 CA/LL liquid scintillation spectrometer after electrolytic enrichment by a factor of 40, starting with a sample volume of 500 ml, and using Insta-Gel® as scintillator. The detection limit was 0.3 TU.

RESULTS

In Table 1, 19 springs are listed together with their locations (township, coordinates), EC, $\delta^{18}O$ (‰, SMOW) and the approximate discharge (*Q*). The last column indicates the environment (formation or interface of formations) as assigned by us using a spring's elevation together with the stratigraphic column. Three groups can be distinguished.

1. The first set comprises the first 12 springs (from Batateira through Santa Rita), listed in Table 1 in order of decreasing discharge. They originate from the Exu/Arajara contact. Their waters are very weakly mineralized, with EC $\leq 30\ \mu S\ cm^{-1}$.
2. The second set is made up of three minor springs from the Arajara Formation (Angélica, Olho d'água and Recanto). Their discharge is much smaller and diffuse and has therefore not been measured. Mineralization is significantly higher (EC from *ca.* $80\ \mu S\ cm^{-1}$ to $130\ \mu S\ cm^{-1}$) than in the first group.
3. The third set comprises the springs Solzinho and Macauba, which we attribute to the contact of the formations Arajara and Santana. Their EC is $234\ \mu S\ cm^{-1}$ and $266\ \mu S\ cm^{-1}$, which is two to three times that of the second set.

We added two springs to Table 1 that do not originate from the Plateau but are located in the Cariri Valley: Rosário and Ciciaca. Rosário is located on the cliff of the horst of Mauriti, and Ciciaca where the Mauriti Formation meets the crystalline basement. We measured $\delta^{18}O$ for some springs: Pendência in Missão Velha yielded −3.4‰; Boca da Mata and Solzinho in Jardim, −2.9‰ and −3.5‰, respectively. The two springs in the Valley, Rosário and Ciciaca, measured −3.4‰ and −2.9‰.

Results from wells in the Cariri Valley show a wide range of values reflecting the opulence of tectonic features of the region. We group them according to the main aquifers exploited as indicated by the drilling profiles. Tables 2–5 represent, respectively, wells in the aquifers Rio da Batateira, Rio da Batateira in combination with Missão Velha, Missão Velha, and, finally, Mauriti. However, we must emphasize that we deal with production wells where all water entries are utilized, irrespective of their origin. Thus, we cannot expect a clear-cut separation of the different groups. Nevertheless, EC is a fairly good parameter for characterizing the water produced by each group:

- The Rio da Batateira wells have EC below $200\ \mu S\ cm^{-1}$ if we eliminate a subgroup of five wells (at the end of Table 2) that are located in areas where fluvial deposits along riverbeds are directly connected with the Rio da Batateira aquifer;

- The Rio da Bateteira/Missão Velha wells produce waters with EC between 200 μS cm^{-1} and 300 μS cm^{-1} (excluding P6 and P10, see comments below) (Table 3);
- The Missão Velha wells have from 300 μS cm^{-1} to 580 μS cm^{-1} (Table 4);
- The Mauriti wells have from 600 μS cm^{-1} to 980 μS cm^{-1} (Table 5).

TABLE 1. The Major Springs in the Cariri Basin, their Coordinates, EC and Discharge (Q)

Locality	Town-ship*	Lat. S	Long. W	EC (μS cm^{-1})	Q† (m^3 h^{-1})	$\delta^{18}O$ (‰)	Origin
Springs on the Slope of the Plateau							
Batateira	Ct	7°15′35″	39°28′17″	28	376		Exu/Arajara
Pendência	MV	7°24′35″	39°12′46″	25	352	−3.4	Exu/Arajara
Bica do Farias	Bb	7°19′50″	39°24′45″	27	348		Exu/Arajara
Sítio Cocos	Bb	7°22′36″	39°17′14″	19	182		Exu/Arajara
Sítio Saco	Po	7°29′38″	39°09′45″	20	182		Exu/Arajara
Bom Jesus	Bb	7°22′39″	39°17′19″	30	180		Exu/Arajara
Sozinho	Ct	7°19′15″	39°24′48″	17	154		Exu/Arajara
Coqueiro	Ct	7°17′02″	39°25′57″	23	140		Exu/Arajara
Boca da Mata	Jd	7°33′20″	39°16′21″	26	132	−2.9	Exu/Arajara
Camelo	Bb	7°22′23″	39°20′33″	15	120		Exu/Arajara
Água Grande	Ct	7°17′15″	39°24′58″	25	113		Exu/Arajara
Santa Rita	Bb	7°21′21″	39°18′48″	15	102		Exu/Arajara
Angélica	Ct	7°12′46″	39°26′33″	69			Arajara
Olho d'água	BS	7°28′05″	39°04′49″	77			Arajara
Recanto	Ex	7°25′33″	39°50′25″	118			Arajara
Solzinho	Jd	7°34′43″	39°16′17″	234		−3.5	Arajara/Santana
Macauba	MV	7°12′46″	39°39′06″	266			Arajara/Santana
Springs in the Cariri Valley							
Rosário	Mi	7°18′20″	39°58′05″	118		−3.4	Mauriti
Ciciaca	NO	7°06′11″	39°38′22″	339		−2.9	Mauriti/basement

*Bb = Barbalha; BS = Brejo Santo; Ct = Crato; Ex = Exu; Jd = Jardim; Mi = Milagres; MV = Missão Velha; NO = Nova Olinda; Po = Porteiras.
†After Mont'Alverne *et al.* (1995)

DISCUSSION

Based on the values given in Tables 1–5 and previous isotope measurements from springs (Santiago *et al.* 1992) and rain (Frischkorn *et al.* 1990) we designed the following conceptual model for groundwaters on the Araripe Plateau and in the Cariri Valley.

Infiltrated rainwater from the top of the Araripe Plateau percolates the Exu sandstone and feeds a group of *ca.* 300 springs. As shown in Table 1, and in a previous publication (Santiago *et al.* 1988), the springs with the highest discharge are situated at an elevation of *ca.* 700 m and have EC <30 μS cm^{-1}. According to its drilling profile, a well in Fazenda Janaguba (elevation 730 m, depth 50 m) produces water from the contact of the formations Exu and Arajara. Its water has an EC of 32 μS cm^{-1} and a tritium concentration of 1.3 TU, which is comparable to values for the first group of springs, which lie between 0.3 TU and 1.3 TU (Santiago *et al.* 1990). Thus, these values verify that springs with EC <30 μS cm^{-1} discharge from the Exu/Arajara contact.

$\delta^{18}O$ for one of these springs (Batateira in Crato) was monitored for 10 months and was found to follow seasonal rainfall variations of ^{18}O with a lag of *ca.* 5 months (Frischkorn *et al.* 1990). The discharge from two springs in Barbalha (Studart *et al.* 1992) was monitored for >2 yr. In this case, we

TABLE 2. Wells that Exploit the Rio da Batateira Aquifer*

No.	Locality	Town-ship†	*P* (m)	Lat. S	Long. W	$\delta^{18}O$ (‰)	EC (μS cm^{-1})	^{14}C (pMC)
P5	Rch. Macacos 2	Jz	150	7°13′37″	39°18′26″	−3.1	168	74.6 ± 0.9
P26	Conj. Mirandão	Ct	102	7°14′11″	39°23′51″	−3.0	198	91.4 ± 0.8
P27	Lagoa Seca 10	Jz	91	7°14′51″	39°19′19″	−3.3	98	80.8 ± 0.5
P28	Lagoa Seca 11	Jz	115	7°14′56″	39°19′22″	−3.3	186	66.6 ± 0.5
P29	Lagoa Seca 16	Jz	129	7°14′34″	39°18′51″	−3.0	182	88.7 ± 0.6
P34	Rch. Macacos 2a	Jz	32	7°13′38″	39°18′22″	−3.2	154	124.8 ± 0.9
P40	Lagoa Seca 17	Jz	180	7°14′23″	39°18′04″	−3.1	162	80.5 ± 0.6
P47	Cafundó 5	Ct	110	7°14′26″	39°24′20″	−3.0	183	98.8 ± 0.8
P54	SENAI	Ct	95	7°13′34″	39°23′49″	−2.9	199	--
P63	Lagoa Seca 15	Jz	130	7°15′43″	39°19′20″	−3.1	157	--
P67	Floresta	Ct	129	7°14′29″	39°24′59″	−3.1	113	--
P69	São Raimundo Novo 2	Ct	100	7°13′47″	39°25′31″	−2.8	169	--
P70	Café da Linha	Ab	60	7°17′54″	39°02′05″	−2.9	79	--
P77	Rosário	Mi	50	7°18′29″	38°57′54″	−3.5	98	--
P79	Sizani	Ct	120	7°13′20″	39°25′20″	−3.1	174	--
P80	Recanto 1	Ct	130	7°14′37″	39°24′56″	−3.1	134	--
P15	São Raimundo 2	Ct	126	7°13′47″	39°25′31″	--	219	111.5 ± 1.1
P20	St. Monte Alegre	Ct	60	7°12′25″	39°24′37″	--	497	121.4 ± 1.1
P22	V. Padre Cícero	Ct	98	7°13′08″	39°21′32″	--	88	108.3 ± 0.8
P41	Batateira - lav.	Ct	32	7°13′25″	39°25′31″	−3.2	312	115.5 ± 1.1
P55	São Raimundo N1	Ct	130	7°13′49″	39°25′37″	−3.1	144	104.2 ± 1.1

*For Tables 2–5: No.= well number; P (m) = well depth; $\delta^{18}O = \delta^{18}O$ (SMOW); EC = electric conductivity; pMC = percentage of modern carbon.

†Ab = Abaiara; Ct = Crato; Jz = Juazeiro do Norte; Mi = Milagres.

TABLE 3. Wells that Exploit the Rio da Batateira and Missão Velha Aquifers

No.	Locality	Town-ship*	*P* (m)	Lat. S	Long. W	$\delta^{18}O$ (‰)	EC (μS cm^{-1})	^{14}C (pMC)
P4	Lagoa Seca, 9	Jz	119	7°14′27″	39°19′22″	−3.3	291	64.2 ± 0.7
P6	Rch. Macacos 8	Jz	191	7°12′36″	39°18′08″	−3.9	522	35.4 ± 0.6
P10	Poço 2	MV	86	7°15′32″	39°17′46″	−3.6	375	30.3 ± 0.4
P19	Sítio S. Pedro	Bb	78	7°17′50″	39°17′12″	−3.2	226	99.2 ± 0.5
P33	Barro Branco	Bb	76	7°18′50″	39°15′22″	−3.4	288	88.0 ± 0.8
P35	Rch. Macacos 3	Jz	140	7°13′35″	39°18′12″	−3.2	243	92.0 ± 0.7
P36	Rch. Macacos 4	Jz	140	7°13′25″	39°18′13″	−3.4	291	78.2 ± 0.5
P38	Rch. Macacos 7	Jz	200	7°12′46″	39°18′20″	−3.2	281	75.1 ± 0.7
P39	Lagoa Seca 14	Jz	82	7°14′38″	39°19′03″	−3.5	299	61.0 ± 0.5
P46	Vila Alta 2	Ct	107	7°13′24″	39°24′43″	−3.2	232	93.7 ± 1.1
P58	Rch. Macacos 1	Jz	120	7°13′48″	39°18′24″	−3.4	258	77.5 ± 0.7
P71	Lagoa Seca 12	Jz	126	7°15′08″	39°19′21″	−3.4	253	72.4 ± 1.1
P72	Lagoa Seca 13	Jz	102	7°15′20″	39°19′23″	−3.5	213	79.1 ± 0.7

*Bb = Barbalha; Ct = Crato; Jz = Juazeiro do Norte; MV = Missão Velha.

found a delay of 6–8 months with relation to monthly rainfall amounts. These results indicate a surprisingly quick hydraulic response, certainly due to percolation in fractures of the Exu sandstone. As "modern" rainfall has 3.2 TU, the 0.3–1.3 TU for springs are, according to a modified exponential model for the horizontal flow at the Exu/Arajara contact, compatible with times of transit between 4 and 26 yr (Silva *et al.* 1992).

TABLE 4. Wells that Exploit the Missão Velha Aquifer

No.	Locality	Town-ship*	*P* (m)	Lat. S	Long. W	$\delta^{18}O$ (‰)	EC ($\mu S\ cm^{-1}$)	^{14}C (pMC)
P9	Alto da Alegria	Bb	113	7°18′27″	39°08′12″	−3.2	349	93.2 ± 0.7
P31	Usina, prof. 200	Bb	200	7°18′08″	39°14′09″	−3.2	363	84.5 ± 0.7
P37	Rch. Macacos 5	Jz	160	7°13′14″	39°18′15″	−3.6	380	48.9 ± 0.4
P48	Abaiara - lav.	Ab	130	7°21′10″	39°02′47″	−3.8	417	44.9 ± 0.6
P50	CAGECE 7	Mi	118	7°18′54″	38°56′20″	−5.1	569	--
P53	Bela Vista	Bb	88	7°19′40″	39°17′46″	−4.3	456	28.1 ± 0.5
P59	Rch. Macacos 6	Jz	200	7°13′02″	39°18′17″	−3.6	438	54.2 ± 1.1
P68	Sítio S. Paulo	Bb	144	7°18′07″	39°17′49″	−3.0	332	--

*Ab = Abaiara, Bb = Barbalha, Jz = Juazeiro do Norte, Mi = Milagres.

TABLE 5. Wells that Exploit the Mauriti Aquifer

No.	Locality	Town-ship*	*P* (m)	Lat. S	Long. W	$\delta^{18}O$ (‰)	EC ($\mu S\ cm^{-1}$)	^{14}C (pMC)
P1	R. M. Ferreira	NO	80	7°05′21″	39°41′32″	−3.6	967	--
P2	Poço 2	NO	128	7°06′32″	39°41′02″	−3.4	752	62.9 ± 0.6
P3	Baixio 3	NO	130	7°06′58″	39°41′19″	−3.8	976	3.6 ± 0.4
P42	SESI	Ct	63	7°13′37″	39°23′46″	−3.1	639	99.1 ± 0.7
P44	Hp. S. Vicente	Bb	150	7°18′39″	39°18′03″	−2.9	602	90.8 ± 0.8
P73	Abaiara 1	Ab	130	7°21′20″	39°02′40″	−3.5	776	59.7 ± 0.7
P74	Jacu	NO	127	7°05′42″	39°41′10″	−3.5	866	--
P76	Pedras Cariri	NO	50	7°05′43″	39°40′35″	−3.0	631	--
P78	Vila Esperança	Ma	80	7°26′33″	38°57′14″	−2.8	670	--

*Ab = Abaiara; Bb = Barbalha; Ct = Crato; Ma = Mauriti; NO = Nova Olinda.

A second group of springs that emerges from the slope of the Plateau, characterized by EC between 69 $\mu S\ cm^{-1}$ and 118 $\mu S\ cm^{-1}$, comprises mostly discharges of groundwater from the Arajara Formation that are not well concentrated but resemble seepage areas. Their discharge is difficult to evaluate. A well at the Colégio Agrícola (agricultural school) in Crato, at an elevation of 630 m and a depth of 45 m, produces, following the drilling profile, water from the Arajara Formation. EC of this well is 71 $\mu S\ cm^{-1}$ and tritium concentration is 0.9 TU, which confirms the attribution of this second group of springs to the Arajara Formation.

At still lower elevation, on the slope of the Plateau, there is another horizon of springs at the Arajara/Santana contact with higher mineralization (with EC *ca.* 250 $\mu S\ cm^{-1}$). Their discharge is much smaller than that of the first group and normally diffuse. Solzinho Spring, which belongs to this group, shows a $\delta^{18}O$ of −3.5‰, which is the lowest value measured for springs. The scattering of $\delta^{18}O$ between −2.9‰ and −3.5‰ demonstrates that, even at an elevation of *ca.* 200 m below the Plateau, the amount effect that marks rainfall is still perceptible without being blurred much by mixing. Even though, due to a very low water table at *ca.* 100 m deep, access to groundwater is difficult on the Plateau, some isolated clayey lenses produce perched aquifers that are being exploited in some places through dug wells. We determined EC for two of them and found 169 $\mu S\ cm^{-1}$ (at Semião) and 526 $\mu S\ cm^{-1}$ (at Romoaldo). The fact that these conductivities are considerably higher than those of the springs far below is still another indication of a vertical flow in fractures in the Exu Aquifer.

Tectonic fracturing is very intense in the Cariri Valley. This causes a varying sequence of formations in the sedimentary basin (Fig. 1C) and produces local mixtures of waters that are difficult to interpret. In our discussion, we adopt the new stratigraphic column proposed by DNPM (Mont'Alverne *et al.*

1995) in our assignments of isotopic characteristics to hydrogeologic structures. This column distinguishes, in the area of interest of the Cariri Valley, the formations, from top to bottom, Rio da Batateira (aquifer), Abaiara (aquitard), Missão Velha (aquifer), Brejo Santo (aquitard) and Mauriti (aquifer).

Phreatic waters from the Rio da Batateira Formation (Table 2) are weakly mineralized (EC <200 μS cm^{-1}). Figures 2A and 3A show pMC between 67 and 125 and $\delta^{18}O$ from −2.8‰ to −3.5‰, with a mean of −3.1‰, which corresponds roughly to the mean value for rainfall in the area. The scattering of $\delta^{18}O$ around the mean reflects seasonal and annual fluctuation in rainfall (amount effect). It is noteworthy that wells in zones of fluvial deposits exhibit special features: EC increases with pMC in a very good correlation (EC = 22.7 pMC − 2295) with a correlation coefficient of $R = 0.94$, different from the "traditional" decrease of EC with increasing pMC as shown by the other groups of wells. This behavior can be explained as a mixing line of very young, yet highly mineralized water from the fluvial deposits with young recharge from the unconfined Rio da Batateira aquifer.

Waters from wells that simultaneously exploit the aquifers Rio Batateira and Missão Velha (Table 3) are characterized by EC from 200 μS cm^{-1} to 300 μS cm^{-1} (with the exceptions of wells P6 and P10; see below). They comprise pMC from 30 to 99 and $\delta^{18}O$ from −3.2‰ to −3.9‰. The following correlations were obtained (Figs. 2B and 3B):

$$EC = -3.21\ \text{pMC} + 524\ (R = -0.83) \quad \text{and} \tag{1}$$

$$\delta^{18}O‰ = 0.008\ \text{pMC} - 3.96\ (R = 0.81)\,. \tag{2}$$

These correlations describe mixtures of young and weakly mineralized waters from the Rio da Batateira with a older and more mineralized water from the Missão Velha Formation. Wells P6 and P10 occupy an extreme position in this group. Even though their drilling profiles integrate them into the Rio da Batateira/Missão Velha wells, their $\delta^{18}O$ and pMC values are the lowest of the group; their conductivities are the highest. As a result, these two wells seem to be "strangers" in an otherwise rather homogeneous group. In fact, mathematical simulation using MODFLOW of the dynamic levels for the battery of wells they are part of, and also the evaluation of pumping tests (Mendonça 1995), confirm that at least P6 is situated exactly upon a leak that, bridging the Abaiara aquitard, directly connects the aquifers Rio da Batateira and Missão Velha. Thus, for wells P6 and P10, pMC of 35.4 and 30.3 (with uncorrected ages of 7840 and 9600 yr, respectively) and $\delta^{18}O$ levels of −3.9‰ and −3.6‰ may be taken as characteristic for this old component of the Missão Velha aquifer.

Wells that produce water from the Missão Velha aquifer (Table 4) are represented in Figures 2C and 3C. EC ranges from 330 μS cm^{-1} to 570 μS cm^{-1}, pMC from 93.2 (corresponding to an uncorrected age of 564 yr) to 28.1 (10,185 yr), and $\delta^{18}O$ from −3.0‰ to −5.1‰. The correlations obtained are

$$EC = -1.50\ \text{pMC} + 489\ (R = -0.87) \quad \text{and} \tag{3}$$

$$\delta^{18}O\ (‰) = 0.016\ \text{pMC} - 4.54\ (R = 0.94)\,. \tag{4}$$

Again, we understand them as mixing of a young component, originating from recharge by rainfall, and an ascending paleo-component. It is noteworthy that P31, P37, P48 and P59 were flowing wells at the time of drilling; now levels are some meters below surface.

The measurement −5.1‰ for $\delta^{18}O$ of P50 is the lowest value for all the wells. It clearly indicates a strong contribution of paleo-waters dating back to a colder and more humid climate than at present in the northeast of Brazil. In previous research (Frichkorn *et al.* 1984; Frischkorn and Santiago 1992; Stute *et al.* 1995) on the deep aquifers in Piaui State we could prove that, at *ca.* 10,000 BP, temperature rose by roughly 5°C in the region, causing $\delta^{18}O$ to rise from *ca.* −6‰ to present day −3‰. Thus, the same paleoclimatic effect should be found in the Cariri. The fact that no values <−5.1‰ have

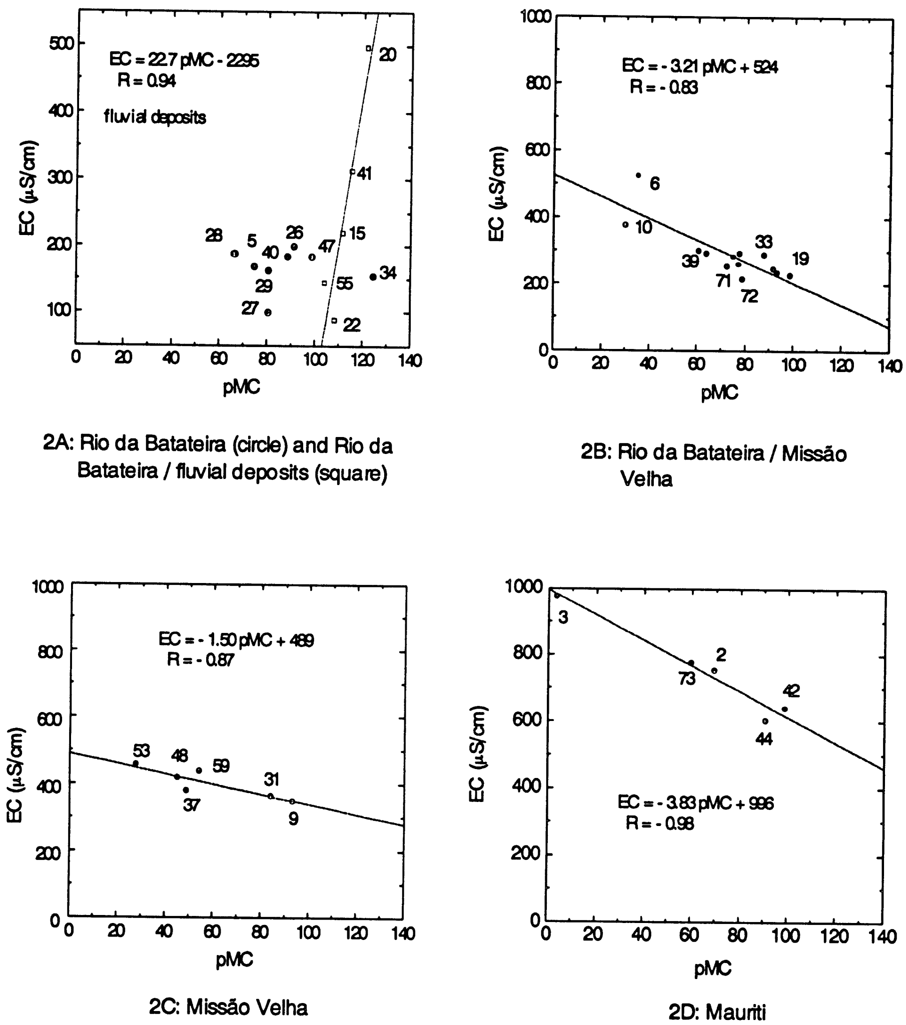

Fig. 2. Electrical conductivity as a function of pMC for wells in the Cariri Valley. The exploited aquifers are listed below each graph.

been found is an indication of mixing with components younger than *ca.* 10,000 yr (unfortunately, we do not have ^{14}C for P50 as it is installed with an air-lift pump). Waters from the Mauriti Formation (Table 5) exhibit EC rates from 600 to 980 μS cm^{-1}, pMC from 99.1 to 3.6 (corresponding to uncorrected ages from modern to 26,800 yr) and $\delta^{18}O$ from −2.8‰ to −3.8‰ with mixing lines:

$$EC = -3.83 \text{ pMC} + 996 \ (R = -0.98) \quad \text{and} \tag{5}$$

$$\delta^{18}O = 0.009 \text{ pMC} - 3.89 \ (R = 0.92)\,. \tag{6}$$

P42, with EC = 639 μS cm^{-1}, pMC = 99.1 and $\delta^{18}O$ = −3.1‰, can stand for the young contribution, originating from infiltration in the recharge area of the Mauriti aquifer. P3, with EC = 976 μS cm^{-1}, pMC = 3.6 and $\delta^{18}O$ = −3.8‰, which exploits the Mauriti aquifer where confined by the aquitard Brejo Santo, may represent the aged component.

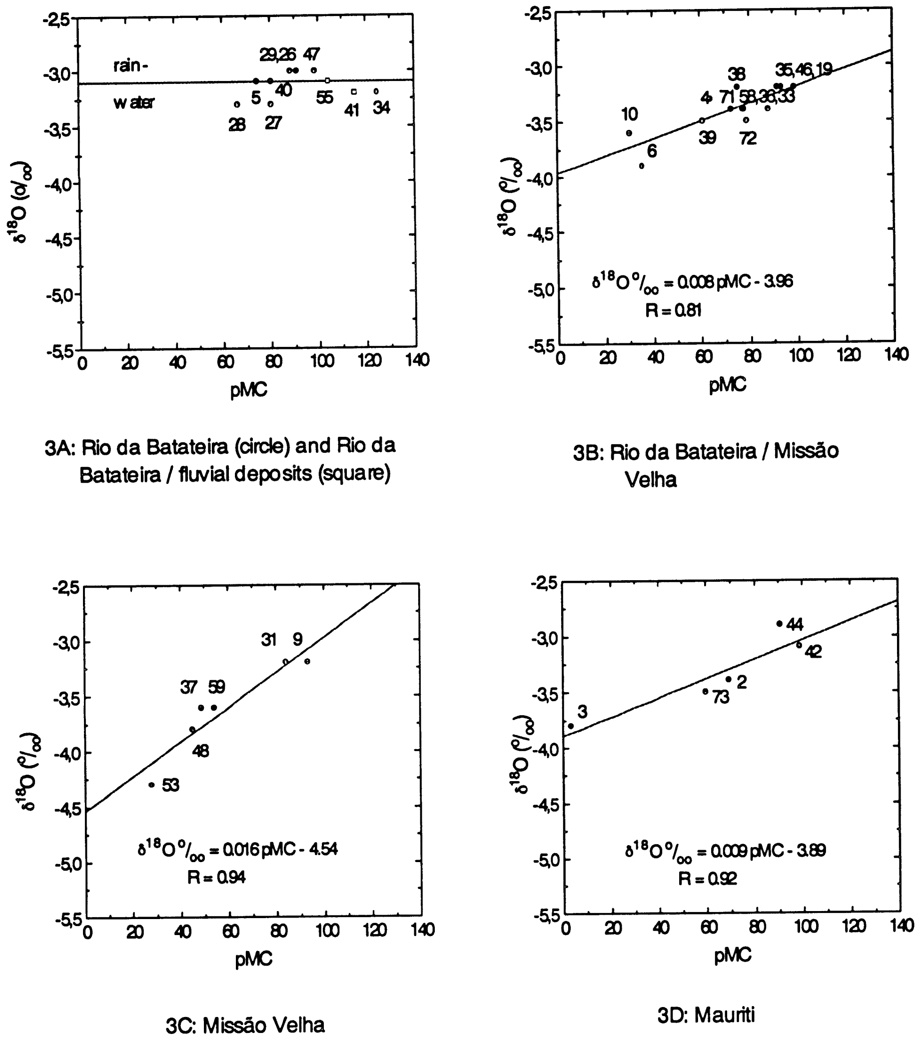

Fig. 3. $\delta^{18}O$ (‰) as a function of pMC for wells in the Cariri Valley. The exploited aquifers are listed below each graph.

Summing up our results, we conclude that the predominant presence of young waters in all aquifers of the Cariri Valley makes them suitable for sustainable exploitation. However, at the same time, our findings reflect a high vulnerability to contamination of these aquifers due to easy infiltration in the sedimentary basin. This is of special importance because of the intense large-scale agricultural activity, mostly from sugar cane plantations, in the basin.

On the other hand, the Cariri Basin constitutes a sedimentary lens engraved in the crystalline basement, with aquifers outcropping on its border and submerging, in the area of this study from north to south, confined by aquitards. Accordingly, one expects the existence of a regional flow pattern for deep groundwaters leading from the margin to the center of the basin. In fact, we detected the presence of a paleo-component of >10,000 yr, marked by a lower atmospheric temperature than at present (as may be seen from the $\delta^{18}O$ values of the paleowaters). This component may have a favorable influence on the exploitation of Cariri Valley aquifers as it can smooth down the influence of drought periods that affect the region.

Acknowledgments

We would like to thank the Municipality of Juazeiro do Norte, the State and Federal Agencies FUNCAP, CAPES, CNPq and FINEP for financial support. We are indebted to Markus Forster/Hydroisotop (Germany) for the ^{18}O measurements. For logistical help we thank the Regional University URCA (especially Helio Germano) and the CAGECE office in Juazeiro do Norte.

References

Frischkorn, H., Santiago, M. F. and Brasil, R. 1990 Aspectos Hídricos do Cariri. *In* Proceedings of the I Simpósio sobre a Bacia do Araripe e Bacias Interiores do Nordeste. Crato, Brazil, Departamento Nacional da Producão Mineral: 99–110.

Frischkorn, H. and Santiago, M. M. F. 1992 The paleoclimate of the Northeast of Brazil according to isotope hydrology. In *Special Papers: Impact of Climatic Variations and Sustainable Development in Semi-Arid Regions.* Fortaleza, Brazil, ICID: 20 p.

Frischkorn, H., Torquato, J. R. and Santiago, M. M. F. 1984 Medidas isotópicas em aquíferos profundos na região Centro-Leste do Piauí. In *Anais do 3º Congresso Brasiliero de Águas Subterrâneas.* Vol. 2. São Paulo, Associacão Brasileiro de Águas Subterrâneas: 42–51.

Gaspary J. 1967 Estudo Geral de Base do Vale do Jaguaribe. Recife/Brazil SUDENE, ASMIC. *Hidroleologia* 7: 250 p.

Ghignone, J. I., Couto, E. A. and Assine, M. L. 1986 Estratigrafia e estrutura das bacias do Araripe, Iguatu e Rio do Peixe. *XXXIV Congresso Brasileiro de Geologia.* Vol. 1. São Paulo, Sociedade Brasileira de Geologia: 271–285.

Kemper, K. E., Gonçalves, J. Y. and Bezerra, F. W. B. 1995 Um sistema local de gerenciamento de água - O caso da fonte da Batateira no Cariri - Ceará - Brasil. *XI Simpósio Brasileiro de Recursos Hídricos.* Vol. 2. São Paulo, Associacão Brasileiro de Recursos Hídricos: 63–68.

Mendonça, L. A. R. 1996 (ms.) Modelagem matemática, química e isotópica de uma bateria de poços na cidade de Juazeiro do Norte - Ceará. Master's thesis, Universidade Federal do Ceará/UFC.

Mont'Alverne, A. A. F., Dantas, J. R. A., Melo Júnior, A. H., Monteiro, E. T., Lima, A. A., Ponte, J. S. A., Ponte, F. C. and Costa, W. C. 1995 *A Bacia Sedimentar do Cariri.* Recife, Brazil, Departamento Nacional da Producão Mineral.

Santiago, M. F., Frischkorn, H., Bezerra A. and Brasil, R. 1988 Medidas hidroquímicas em poços e fontes no Cariri - sul do Ceará. In *Anais do 5º Congresso Brasiliero de Águas Subterrâneas.* São Paulo, Associacão Brasileiro de Águas Subterrâneas: 112–120.

Santiago, M. F., Frischkorn, H. and Serejo, A. N. 1990 Estudo Isotópico das Águas do Cariri. In *Anais do 6º Congresso Brasiliero de Águas Subterrâneas.* São Paulo, Associacão Brasileiro de Águas Subterrâneas: 338–343.

Santiago, M. F., Frischkorn, H., Serejo, A. N., Studart, T. and Mendes Filho, J. 1992 *Impacts of Climatic Variations and Sustainable Development in Semi-Arid Regions.* Fortaleza, Brazil, ICID: 19 p.

Santiago, M. F., Silva, C. M. S. V., Mendes Filho, J. and Frischkorn, H. 1994 Caracterização isotópica da água subterrânea na Bacia Sedimentar do Cariri. *II Congreso Latinoamericano de Hidrologia Isotopica.* Vol. 2. Santiago, Chile, ALHSUD: 731–740.

Silva, C. M. V., Santiago, M. F., Frischkorn, H. and Serejo, A. N. 1992 Contribuição de medidas de trício no conhecimento da hidrologia subterrânea no Cariri. *I Simpósio de Recursos Hídricos do Nordeste.* São Paulo, Associacão Brasileiro de Recursos Hídricos: 287–295.

Studart, T. M. C., Frischkorn, H., Santiago, M. F. and Brasil, R. W. 1992 Medidas de vazões de fontes no Cariri por diluição de um traçador. *I Simpósio de Recursos Hídricos do Nordeste.* São Paulo, Associacão Brasileiro de Recursos Hídricos: 273–282.

Stute, M., Forster, M., Frischkorn, H., Serejo, A., Clark, J. F., Schlosser, P., Broecker, W. S. and Bonani, G. 1995 Cooling of tropical Brazil (5°C) during the last glacial maximum. *Science* 269: 379–383.

[RADIOCARBON, VOL. 39, NO. 1, 1997, P. 61–65]

PENGUIN, A MACINTOSH APPLICATION FOR ENTRY AND PRESENTATION OF RADIOCARBON-DATED SAMPLES

ANTONIO PETRI[1] *and CARLO BARONI*

Dipartimento di Scienze della Terra, Università di Pisa and C.N.R. - Centro di Studio per la Geologia Strutturale e Dinamica dell'Appennino, Via S. Maria 53, I-56126 Pisa, Italy

ABSTRACT. *Penguin* is a Macintosh computer application that facilitates the use of CALIB 3.03, the ^{14}C age calibration program by Stuiver and Reimer (1993). Penguin offers an easy user interface based on the well-known Macintosh standard multiwindow environment to create and edit the CALIB 3.03 calibration files and to export data in text format. *Penguin* and CALIB interact at the file level, *i.e.*, *Penguin* is capable of reading and writing files in CALIB formats. Files containing the data are created in the *Penguin* environment and then saved on disk in the *Penguin* format. *Penguin* allows multiple editing of the calibration parameters and recalibration of the list of samples without the need to insert any modifications manually throughout the list. *Penguin* can also be used to read already calibrated files in order to extract the "cal" ages and display them in a spreadsheet-like window.

INTRODUCTION

Penguin is a Macintosh computer application that facilitates the use of CALIB 3.03, the well-known ^{14}C age calibration program by Stuiver and Reimer (1993).[2] The "*Penguin* project" emerged from our need for flexibility in managing data sets of ^{14}C-dated samples (The name was suggested by the prettiest subject we were dealing with). In particular, we frequently need to update and calibrate sets of ^{14}C dates from marine organisms (Baroni and Orombelli 1991) or from organisms that lived or fed in the sea, such as penguins and seals (Baroni *et al.* 1991; Baroni 1994; Baroni and Orombelli 1994). Nevertheless, the program is also useful for managing and editing sets of calibrated dates of other origin.

Penguin is at an early stage of development and is currently used at the Earth Science Department of the University of Pisa (Italy). Its currently implemented capabilities reflect the needs of the researchers who deal with ^{14}C dates. Features are added or modified each time a new need arises from our work. This means that the look and the functionality of *Penguin* may change in future releases, particularly if users assist us by supplying observations and suggestions for adding capabilities and/or modifying existing ones. Furthermore, some tools for graphical processing are currently being studied and could be added shortly.

Penguin is free software and is available from glsun2.gl.rhbnc.ac.uk via anonymous FTP, in the directory /pub/mac/apps.

PENGUIN CALIBRATION UTILITIES

As is well known, the ^{14}C dates from remains of organisms that lived or fed in the sea are affected by an offset known as the "reservoir effect", induced by the depletion of ^{14}C in the ocean. This depletion is related to regional variations in oceanic and atmospheric circulation and its magnitude has also varied through time (Broecker and Olson 1961; Broecker, Peng and Engh 1980; Östlund and Stuiver 1980; Stuiver and Östlund 1980; Gordon and Harkness 1992). In the Antarctic Ocean, the reservoir effect is particularly elevated, owing to the dilution of circumantarctic water with glacial meltwater and by the upwelling of deep and old oceanic water (Harkness 1979; Omoto 1983;

[1]*Present address:* Department of Geology, Royal Holloway University of London, Egham, Surrey TW20 0EX, United Kingdom
[2]The current version of CALIB is available at http://weber.u.washington.edu/~qil/calib.html.

Stuiver, Pearson and Braziunas 1986). Thus, the apparent ages yielded by Antarctic samples are anomalously old as a consequence of the very low level of ^{14}C concentration in Antarctic water; the error is estimated to be >1000 yr and varies with different organisms and materials (Harkness 1979; Omoto 1983; Stuiver *et al.* 1981; Stuiver, Pearson and Braziunas 1986; Whitehouse, Chinn and Höfle 1988, 1989; Björck *et al.* 1991; Gordon and Harkness 1992; Berkman and Forman 1996). In order to compare the ^{14}C dates obtained from Antarctic samples with ^{14}C ages derived elsewhere, the ^{14}C ages need to be corrected for the reservoir effect and calibrated as accurately as possible.

According to Stuiver, Pearson and Braziunas (1986) and Stuiver and Reimer (1993), the calibration procedure for marine-derived organisms requires the computation of a parameter, ΔR, that is the constant difference in reservoir age of a regional part of the ocean and the world ocean. ΔR values can be determined if samples of known historical age are available (actually, only samples from organisms that died before the era of nuclear tests are suitable for this purpose). Such samples mainly derive from penguins and seals killed at the beginning of the century during the historical Antarctic expeditions (Stuiver *et al.* 1981; Mabin 1985, 1986; Orombelli 1988; Whitehouse, Chinn and Höfle 1988, 1989; Björk *et al.* 1991). Recently, dates from shells of known age have been supplied as well (Berkman and Forman 1996).

Table 1 lists ^{14}C dates of known-age samples; it can be observed that the conventional ages span a wide time interval. Therefore, in order to perform the best possible calibration, different ΔR values should be applied to different sets of ^{14}C dates obtained from different organisms. Namely, ^{14}C dates from penguin remains should be calibrated using a ΔR value derived only from penguin samples of known age (ΔR = 688 ± 55 is the weighted mean of seven values from penguin remains; ΔR = 656 ± 55 is the weighted mean of three values from Adélie penguin remains only).

TABLE 1. Radiocarbon Dates from Samples of Known Age from Antarctica

Sample no.	Location	Material	Historical age (AD)	Conv. age (^{14}C yr BP)	ΔR (^{14}C yr BP)	Reference
Lu31101	Hope Bay	Penguin bones	1903	1280 ± 50	816 ± 50	Bjork *et al.* 1991
4432	Cape Royds	Adélie penguin flesh	1904	925 ± 75	462 ± 75	Geyh and Wirth in Whitehouse, Chinn and Hofle 1988
4433	Cape Adare	Flesh mew of prey	1902	1125 ± 90	660 ± 90	Geyh and Wirth in Whitehouse *et al.* 1988
QL173	Inexpressible Is.	Emperor penguin	1912	1300 ± 50	838 ± 50	Stuiver *et al.* 1981
QL171	Inexpressible Is.	Weddell seal	1912	1390 ± 40	928 ± 40	Stuiver *et al.* 1981
NZ6339A	Inexpressible Is.	Emperor penguin bones	1912	1065 ± 50	603 ± 50	Mabin 1985
NZ6327A	Inexpressible Is.	Weddell seal bones	1912	1760 ± 55	1298 ± 55	Mabin 1985
NZ6842A	Inexpressible Is.	Adélie penguin bones and flesh	1912	1060 ± 45	598 ± 45	Whitehouse *et al.* 1988
NZ6872	Inexpressible Is.	Charcoal from seal blubber stove	1912	1240 ± 45	778 ± 45	Greenfield in Whitehouse *et al.* 1988
GX-12759	Inexpressible Is.	Seal bones	1912	1175 ± 75	713 ± 75	Orombelli 1988
NZ7079A	Cape Evans	Emperor penguin bone collagen	1916	1105 ± 55	642 ± 55	Mabin 1986
NZ7076A	Cape Evans	Emperor penguin flesh and feathers	1916	1220 ± 55	757 ± 55	Mabin 1986
NZ6851A	Cape Evans	Weddell seal bone collagen	1916	1610 ± 80	1147 ± 80	Mabin 1986
GX-18581	68°30'S–67°00'W	*Adamussium colbecki*	1940	1476 ± 39	1001 ± 39	Berkman and Forman 1996
GX-18582	67°52'S–67°17'W	*Adamussium colbecki*	1940	1416 ± 40	941 ± 40	Berkman and Forman 1996
AA 14785	68°47'S–90°35'W	*Neobuccinum eotoni*	1917	1215 ± 57	750 ± 57	Berkman and Forman 1996
GX-19205	78°30'S–164°20'W	*Thracia meridionalis*	1935	1278 ± 62	798 ± 62	Berkman and Forman 1996

With our *Penguin* program it is easy to recalibrate the set of data using both the mean value calculated from all the available samples or different ΔRs obtained from penguin remains only. Furthermore, regional values can be calculated and compared for different sets of data.

Calibration is performed by the computer program CALIB (Stuiver and Reimer 1993); it allows the manual insertion of the data or can take as input a text file that can be created with a word processor. Normally, sample data (code, locality, description) are maintained using common commercial database programs, although the latter are not able either to export data directly in CALIB file format or to import data results (mainly calibrated age ranges) from CALIB output text files; in both cases data must be transferred one at time by retyping or through a tedious copy-and-paste process. Alternatively, sample data can be kept in CALIB input text files and handled with a word processor. However, because such programs are not aware of the format of those files, it is very easy to accidentally modify their structure, making them unreadable by CALIB.

Penguin's main goal is data management, focusing on data exchange with CALIB files in order to speed up the recalibration procedure. *Penguin* allows easy maintenance of sample data files, much like a database application. In our view, the program is particularly suited for the calibration procedure when one of the following conditions applies: 1) new ^{14}C dates are to be added to the set of data; 2) new samples of known age are supplied. In the first case, only the new conventional ages are to be calibrated, using one or more ΔR values. In the latter case, the ΔR values must be recalculated and the existing sets of ^{14}C dates must be recalibrated.

The usefulness of *Penguin* can be explained via an example (see the flow chart in Fig. 1). If we assume that new penguin remains (either bone or flesh) of historical known age have been discovered and dated, the existing ΔR value based on penguin remains must be updated in order to take into account the new *datum* (actually a weighted mean is computed of all the ΔR values derived from each dated sample). Then, this new ΔR value is used to recalibrate all the penguin ^{14}C dates.

If we have our sample data in a *Penguin* file called "MySamples" (Fig. 2), all we have to do is to open this file, assign the new ΔR value to all samples contained in the file and save a copy of the file in CALIB format. At this point we can use CALIB to calibrate all the dates. Calibration results are collected by CALIB in one

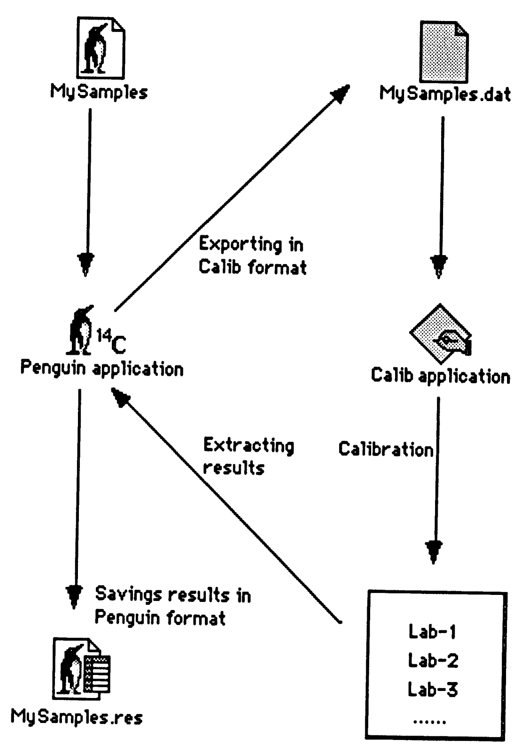

Fig. 1. Flowchart showing the role of *Penguin* in the calibration process. Data are kept in *Penguin* data files and CALIB input files are generated only when ^{14}C dates need to be calibrated. *Penguin* then puts into a unique file the calibration results extracted from each output file created by CALIB.

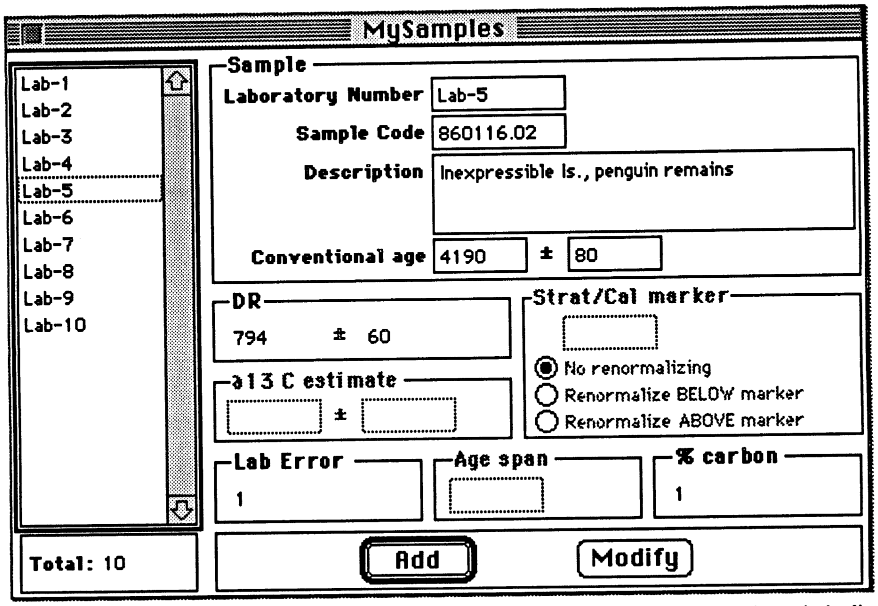

Fig. 2. *Penguin* allows easy editing of sample data files. Sample records are selected through the list on the left side of the window. Text boxes and radio buttons are provided for editing the content of the fields.

file for each sample, so after a calibration session there are as many files as the number of samples contained in the original input file. With *Penguin,* all these files can be parsed in order to extract the calibration results, which can be saved in unique file (Fig. 3). The current release of *Penguin* accepts only the calibrated age ranges from CALIB output files; future releases will allow extraction of all the other information. Furthermore, *Penguin* allows calibration results to be exported in standard text format files (variable-sized records with variable-sized fields separated by a tab character or comma) that can be directly read by database or spreadsheet programs.

Following a basic rule, common sample data should be kept in a *Penguin* file, which can be edited by either adding, deleting or modifying sample records; CALIB input files should be created only

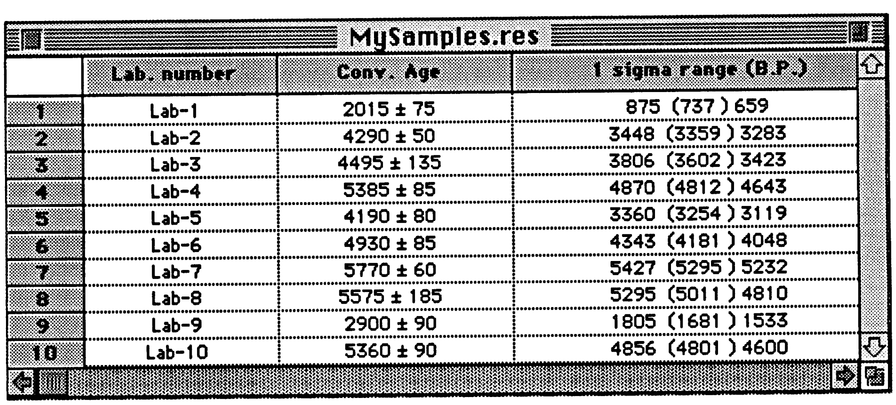
MySamples.res

	Lab. number	Conv. Age	1 sigma range (B.P.)
1	Lab-1	2015 ± 75	875 (737) 659
2	Lab-2	4290 ± 50	3448 (3359) 3283
3	Lab-3	4495 ± 135	3806 (3602) 3423
4	Lab-4	5385 ± 85	4870 (4812) 4643
5	Lab-5	4190 ± 80	3360 (3254) 3119
6	Lab-6	4930 ± 85	4343 (4181) 4048
7	Lab-7	5770 ± 60	5427 (5295) 5232
8	Lab-8	5575 ± 185	5295 (5011) 4810
9	Lab-9	2900 ± 90	1805 (1681) 1533
10	Lab-10	5360 ± 90	4856 (4801) 4600

Fig. 3. Calibration results are displayed in a spreadsheet-like window

for calibration purposes and then deleted when they are no longer needed. Of course, for each set of ^{14}C dates there will be as many *Penguin* calibration result files as the number of times the same set of dates has been calibrated.

ACKNOWLEDGMENTS

This work has been carried out within the framework of the Italian Antarctic Research Programme and was financially supported by ENEA through a joint research program on Antarctic Earth Sciences with the University of Siena.

REFERENCES

Baroni, C. 1994 Notes on Late-Glacial retreat of the Antarctic ice sheet and Holocene environmental changes along the Victoria Land coast. *Memoirs of the National Institute of Polar Research* (Tokyo), Special Issue, 50: 85–87.

Baroni, C., Belluomini, G., Branca, M. E., Improta, S. and Orombelli, G. 1991 Radiocarbon dates from Terra Nova Bay (Northern Victoria Land, Antarctica): Conventional and calibrated ages. *Memorie della Società Geologica Italiana* 46: 81–92.

Baroni, C. and Orombelli, G. 1991 Holocene raised beaches at Terra Nova Bay, Victoria Land, Antarctica. *Quaternary Research* 36: 157–177.

____1994 Abandoned penguin rookeries as Holocene palaeoclimatic indicators in Antarctica. *Geology* 22: 23–26.

Berkman, P. A. and Forman, S. L. 1996 Pre-bomb radiocarbon and the reservoir correction for calcareous marine species in the southern ocean. *Geophysical Research Letters* 23(4): 363–366.

Björk, S., Hjort, C., Ingólfsson, O. and Skog, G. 1991 Radiocarbon dates from the Antarctic peninsula Region. Problems and potential. *Quaternary Proceedings* 1: 55–65.

Broecker, W. S. and Olson, E. A. 1961 Lamont radiocarbon measurements VII. *Radiocarbon* 3: 176–204.

Broecker, W. S., Peng, T. H. and Engh, R. 1980 Modeling the radiocarbon system. *In* Stuiver, M. and Kra, R., eds., Proceedings of the 10th International ^{14}C Conference. *Radiocarbon* 22(3): 565–598.

Gordon, J. E. and Harkness, D. D. 1992 Magnitude and geographic variation of the radiocarbon content in Antarctic marine life: Implications for reservoir corrections in radiocarbon dating. *Quaternary Science Reviews* 11: 697–708.

Harkness, D. D. 1979 Radiocarbon dates from Antarctica. *British Antarctic Survey Bulletin* 47: 43–59.

Mabin, M. C. G. 1985 ^{14}C ages for "Heroic Era" penguin and seal bones from Inexpressible Island, Terra Nova Bay, North Victoria Land. *New Zealand Antarctic Record* 6(2): 24–25.

Mabin, M. C. G. 1986 ^{14}C ages for "Heroic Era" penguin and seal remains from Cape Evans, McMurdo Sound. *New Zealand Antarctic Record* 7(2): 19–20.

Omoto, K. 1983 The problem and significance of radiocarbon geochronology in Antarctica. *In* Oliver, R. L., James, P. R. and Jago, J. B., eds., *Antarctic Earth Science*. Cambridge, Cambridge University Press: 450–452.

Orombelli, G. 1988 Le spiagge emerse oloceniche della Baia Terra Nova (Terra Vittoria, Antartide). *Atti della Accademia Nazionale dei Lincei*, VIII, 81 (1987): 403–416.

Östlund, H.G. and Stuiver, M. 1980 GEOSECS Pacific Radiocarbon. *Radiocarbon* 22(1): 25–53.

Stuiver, M., Denton, G. H., Hughes, T. and Fastook, J. L. 1981 History of the Marine Ice Sheet in West Antarctica during the last glaciation: A working hypothesis. *In* Denton, G. H. and Hughes, T., eds., *The Last Great Ice Sheets*. New York, John Wiley & Sons: 319–369.

Stuiver, M. and Östlund, H. G. 1980 GEOSECS Atlantic Radiocarbon. *Radiocarbon* 22(1): 1–24.

Stuiver, M., Pearson, G. W. and Braziunas, T. 1986 Radiocarbon age calibration of marine samples back to 9000 cal yr BP. *In* Stuiver, M. and Kra, R., eds., Calibration Issue. *Radiocarbon* 28(2B): 980–1021.

Stuiver, M. and Reimer, P. J. 1993 Extended ^{14}C data base and revised CALIB 3.0 ^{14}C age calibration program. *In* Stuiver, M., Long, A. and Kra, R. S., eds., Calibration 1993. *Radiocarbon* 35(1): 215–230.

Whitehouse, I. E., Chinn, T. J. and Höfle, H. C. 1988 Radiocarbon contaminated penguin bones from Terra Nova Bay, Antarctica. *New Zealand Antarctic Record* 8(3): 11–23.

____1989 Radiocarbon dates from raised beaches, Terra Nova Bay, Antarctica. *Geologisches Jahrbuch* E38: 331–334.

[RADIOCARBON, VOL. 39, NO. 1, 1997, P. 67–72]

INGEIS RADIOCARBON LABORATORY DATES III

ROBERTO CORDERO, N. G. GUIDA and J. L. NOGUEIRA

INGEIS, Pabellón INGEIS, Ciudad Universitaria, 1428 Buenos Aires, Argentina

INTRODUCTION

The following list presents results of dating of 55 paleoenvironmental and archaeological samples from Argentina, processed between 1984 and 1986 by M. A. Albero and F. Angiolini. Procedures for sample pretreatment, counting, statistical analysis and age calculation were essentially the same as previously described by Albero and Angiolini (1985). Results are reported as conventional ^{14}C dates in years before AD 1950. They are corrected for isotopic fractionation.

ACKNOWLEDGMENTS

We thank the Consejo Nacional de Investigaciones Científicas y Técnicas for financial support and E. Linares for his collaboration. We also wish to thank the Stable Isotope Laboratory staff for $\delta^{13}C$ analysis and Estela Ducós for her help in the translation.

PALEOENVIRONMENTAL SAMPLES

La Poma Series

Peat samples from Río Grande holocenic terraces of La Poma, Humahuaca, Jujuy (23°17′S, 65°42′W), 3600 m asl. Collected and submitted 1983 by J. Fernández.

AC-691 — **3280 ± 90**
Depth 4.30 m — $\delta^{13}C = -25.9 \pm 0.2‰$

AC-692 — **3460 ± 120**
Depth 4.50 m — $\delta^{13}C = -26.0 \pm 0.2‰$

Comment (J.F.): Dates related to leaf-shaped stemless points. The paleoenvironmental interpretation and chronology have been published in Coleman (1973) and Fernández (1973).

Guayatayoc Series

Peat samples from Guayatayoc stream, Guayatayoc, Rinconada Jujuy (22°18′S, 66°02′W), 3500 m asl. Collected and submitted 1983 by J. Fernández.

AC-0733 — **9170 ± 170**
Depth 1.82 m — $\delta^{13}C = -27.4 \pm 0.2‰$

AC-0734 — **10,390 ± 190**
Depth 1.97 m — $\delta^{13}C = -26.5 \pm 0.2‰$

Comment (J.F.): Data belonging to this same profile were published in Albero and Angiolini (1985: 333). Human occupation, *ca.* 2800 yr BP, is indicated by quartzitic artifacts.

Leuto Caballo Series

Peat, marl and other carbonatic sediments from terraces of the Bordo Leuto Caballo stream (37°05'S, 70°15'W),1670 m asl, Chos Malal, Neuquén. Collected and submitted 1983 by J. Fernández. All samples belong to peat layers.

AC-0980	**12,280 ± 160**
Depth 9.67 m	$\delta^{13}C = -25.0 \pm 0.2‰$
AC-0981	**11,940 ± 160**
Depth 8.57 m	$\delta^{13}C = -27.9 \pm 0.2‰$
AC-0979	**11,300 ± 160**
Depth 7.67 m	$\delta^{13}C = -25.0 \pm 0.2‰$
AC-0983	**11,070 ± 140**
Depth 7.52 m	$\delta^{13}C = -25.0 \pm 0.2‰$
AC-1048	**10,180 ± 130**
Depth 7.32 m	$\delta^{13}C = -7.0 \pm 0.2‰$

Comment (J.F.): Dates are related to a Late Pleistocenic marshy environment with megafaunal remains (*Megatherium, Hippidion* and *Paleolama*); see Panarello and Fernández (1992).

Barro Negro Series

Peat, marl and collagen of several profiles from Barro Negro (23°S, 65°37'W), 3.820 m asl, Humahuaca, Jujuy. Collected and submitted 1980–1986 by J. Fernández. All samples belong to peat layers.

A) Quebrada Linda Profile (Site A)

AC-0748	**510 ± 70**
Depth 0.20 m	$\delta^{13}C = -25.3 \pm 0.2‰$
AC-0740	**940 ± 80**
Depth 1.42 m	$\delta^{13}C = -27.6 \pm 0.2‰$
AC-0738	**1270 ± 80**
Depth 2.10 m	$\delta^{13}C = -25.4 \pm 0.2‰$
AC-0739	**1690 ± 80**
Depth 2.80 m	$\delta^{13}C = -27.6 \pm 0.2‰$
AC-0735	**12,530 ± 160**
Depth 8.40 m	$\delta^{13}C = -26.8 \pm 0.2‰$

B) Quebrada de Las Piedras Profile

AC-0747	**1000 ± 80**
Depth 1.17 m	$\delta^{13}C = -24.0 \pm 0.2‰$
AC-0673	**1140 ± 80**
Depth 1.60 m	$\delta^{13}C = -23.7 \pm 0.2‰$
AC-0682	**1680 ± 120**
Depth 1.70 m	$\delta^{13}C = -25.0 \pm 0.2‰$

AC-0680	**2890 ± 110**
Depth 1.90 m	$\delta^{13}C = -24.3 \pm 0.2‰$
AC-0746	**3470 ± 90**
Depth 2.12 m	$\delta^{13}C = -27.5 \pm 0.2‰$
AC-0745	**10,200 ± 140**
Basal depth 5.82 m	$\delta^{13}C = -25.0 \pm 0.2‰$
AC-0744	**12,300 ± 170**
Basal depth 6.77 m	$\delta^{13}C = -28.7 \pm 0.2‰$

Comment: Marl and collagen samples were found in basal peat layer

AC-0974	**9870 ± 220**
Marl 2. depth 5.90 m	$\delta^{13}C = -4.0 \pm 0.2‰$
AC-0975	**13,400 ± 400**
Marl 4. depth 6.20 m	
AC-0976	**11,600 ± 160**
Marl 5. depth 6.80 m	$\delta^{13}C = -3.8 \pm 0.2‰$
AC-0969 I	**9120 ± 130**
Collagen from *Hippidion* bone.	$\delta^{13}C = -18.0 \pm 0.2‰$
AC-0969 II	**11,500 ± 400**
Collagen from *Hippidion* bone.	$\delta^{13}C = -18.0 \pm 0.2‰$

C) Zanjón Largo Profile

AC-0742	**9050 ± 140**
Peaty silt with *Lymnaea*, depth 4.56 m	$\delta^{13}C = -24.8 \pm 0.2‰$
AC-0743	**9200 ± 140**
Peaty silt with fragmented camel bones and lithic objects, depth 5.08 m	$\delta^{13}C = -24.8 \pm 0.2‰$

Comment (J.F.): Important superior Pleistocenic and Holocenic chronostratigraphic record with archaeological contents, fossil animal remains and paleoenvironmental indicators. Published in Alberdi *et al.* (1986); Fernández *et al.* (1991); Fernández (1983–1985).

Archaeological samples

Haichol Series

Charcoal samples from Haichol cave (38°35′S, 70°40′W) 1050 m asl. Pehuenches, Neuquén. Collected and submitted 1979–1981 by J. Fernández.

AC-0896	**2350 ± 150**
Grid 13B2. depth 0.40–0.50 m	$\delta^{13}C = -25.0 \pm 0.2‰$
AC-0897	**1290 ± 110**
Grid 9B1, depth 0.50–0.60 m	$\delta^{13}C = -22.8 \pm 0.2‰$
AC-0898	**1440 ± 90**
Grid 14B1, depth 0.50–0.60 m	$\delta^{13}C = -25.0 \pm 0.2‰$

AC-0899 **2290 ± 120**
Grid 16B2, depth 0.50–0.60 m *$\delta^{13}C$ = –22.6 ± 0.2‰*

AC-0900 **2130 ± 110**
Grid 11B2, depth 0.60–0.70 m *$\delta^{13}C$ = –22.9 ±0.2‰*

AC-0901 **2440 ± 100**
Grid 17B2, 0.80–0.90 m *$\delta^{13}C$ = –21.9 ±0.2‰*

Comment (J.F.): Dates belonging to Late Preceramic occupations (2440–2130 yr BP) and Early Pottery occupations (1830–1250 yr BP). Published in Fernández (1988–1990).

Vizcayachoc Peat

Peat from lower part of Vizcachayoc peat bog, north of Miyuyoc (22°55′S, 65°20′W) 4000 m asl, Humahuaca, Jujuy. Collected and submitted 1983 by J. Fernández.

AC-0982 **9540 ± 170**
$\delta^{13}C$ = –21.2 ± 0.2‰

Comment (J.F.): Lower part of peat bed 7 m width, on western slope of Cordillera Oriental.

Pluma De Pato

Eggshell of *Pterocnemia pennata* (choique) from Pluma del Pato, Añelo, Neuquén (38°10′S,69 5′W) 250 m asl. Collected and submitted 1979 by J. Fernández.

AC-1049 **1700 ± 90**
$\delta^{13}C$ = –8.0 ± 0.2‰

Comment (J.F.): Associated with ceramics and triangular stemless projectile points with concave base, made of obsidian.

Ojo De Agua

Interbedded wood at 2.10 m depth in a small fluvial terrace in Ojo de Agua, near Susques (23°23′S, 66°22′W, 3700 m asl. Collected and submitted 1983 by J. Fernández.

AC-1053 **870 ± 85**
Wood *$\delta^{13}C$ = –22.6 ± 0.2‰*
Calcium carbonate biostromal accretion from Pastos Chicos (23°45′S, 66°23′W) 3900 m asl. Collected and submitted 1983 by J. Fernández.

AC-1056 **16,250 ± 290**
$\delta^{13}C$ = +8.8 ± 0.2‰

Comment (J.F.): Stromatolite (oncolite) from ancient Pastos Chicos stream flood terrace.

Anillaco Series

Charcoal samples from Faldeos del Anillaco, La Rioja (28°46′S, 66°57′W.) 1500 m asl. Collected and submitted 1984 by R. Raffino.

AC-919 **1160 ± 120**
Depth 0.60 m

AC-920 **1200 ± 120**
Depth 0.70 m

AC-921 **2080 ± 120**
Depth 0.80 m

AC-922 **1330 ± 120**
Depth 0.90 m

AC-923 **1330 ± 120**
Depth 1.00 m $\delta^{13}C = -22.9‰$

AC-924 **1150 ± 140**
Depth 1.10 m $\delta^{13}C = -21.0‰$

AC-925 **1440 ± 120**
Depth 1.20 m $\delta^{13}C = -23.8‰$

AC-926 **1270 ± 120**
Depth 1.30 m

La Huerta Series

Bone and charcoal samples from La Huerta, Jujuy, (23°20′S, 65°20′W) 2700 m asl. Collected and submitted 1985 by R. Raffino and published by Raffino *et al.*(1993).

AC-960 **480 ± 100**
Bone collagen, between 0.22 and 0.32 m $\delta^{13}C = -16.5‰$

AC-1069 **540 ± 90**
Charcoal, depth 0.12 m

Valle De La Ciénaga Series

Charcoal samples from La Ciénaga valley, Tucumán (26°49′S, 65°39′W) 2700 m asl. Collected and submitted 1984 by B. Cremonte.

AC- 720 **1560 ± 80**
Depth 1.40 m $\delta^{13}C$ = *est. 0*

AC-721 **1240 ± 80**
Depth 0.80 m $\delta^{13}C = -24.80‰$

Dates related to large settlements of early potter and agricultural societies from the northwest of Argentina, especially with those of Tafí valley. Published by Cremonte (1988).

Puesto El Rodeo Series

Vegetal remains and charcoal samples from La Magdalena estancia, Río Pinturas area, Santa Cruz, (46°53′S, 70°27′W) 240 m asl. Collected and submitted 1985 by C. Gradin and A. Aguerre.

AC-943 **1380 ± 90**
Depth 0.47 m $\delta^{13}C = -22.1‰$

AC-1075 **4860 ± 90**
Depth 0.90 m

Comment: Dates correspond to vegetal remains found over a bedded burial place containing three skeletons. The first date is related to the Rio Pinturas IV cultural level and the second one to the Rio Pinturas IIb–III cultural level.

Puesto Giles Series

Charcoal samples from Puesto Giles Site, Casa de Piedra, La Pampa (38°11'S, 67°13'W) 250 m asl. Collected and submitted 1983 by C. Gradin and A. Aguerre.

AC-728 **700 ± 100**
Depth 0.53 m $\delta^{13}C = -21.3‰$

AC-731 **320 ± 120**
Depth 0.40 m $\delta^{13}C = -21.7‰$

Comment: Dates related to a late human occupation of hunter-gatherers who used ceramics (under investigation).

El Cuy Series

Charcoal sample from El Cuy, Cañadón Santa Victoria, Río Negro (40°S, 68°W) 400 asl. Collected and submitted 1986 by C. Gradin and A. Aguerre.

AC-1074 **420 ± 110**
Depth between 0.05-0.20 m $\delta^{13}C = -21.2‰$

Comment: Date related to tool remains made of bone and a stemmed point, with small patagoniense-type fins. Investigation was stopped at prospecting stage.

References

Alberdi, M. T., Fernandez, J., Menegaz, A. N. and Prado, J. L. 1986 *Hippidion owen* 1869 (Mammalia, Perissodactyla) en sedimentos del Pleistoceno tardío de la localidad de Barro Negro (Jujuy, Argentina). *Estudios Geológicos* 42: 487–493.

Albero, M. C., and Angiolini, F. 1985 INGEIS Radiocarbon Laboratory dates II. *Radiocarbon* 27(2B): 314–337.

Coleman, D. 1973. Illinois State Geological Survey radiocarbon dates IV. *Radiocarbon* 15(1): 314–337.

Cremonte, M. B. 1988 Comentario acerca de fechados radiocarbónicos del sitio El Pedregal (Qda. La Ciénaga, Tucumán, Argentina). *Revista Chungará* 20: 57–59.

Fernandez, J. 1973 Primeros fechados radicarbónicos de formaciones holocenas de la Puna, portadoras de materiales arqueológicos. *Actas del Quinto Congreso Geológico Argentino*, Vol. 3. Buenos Aires, Argentina: 223–226.

____1983–1985 Cronología y paleoambientes del intervalo 12.550–520 años A.P. (Pleistoceno-Holoceno) de la Puna jujeña. *Anales de Arqueología y Etnología* 38–40: 29–42.

____1988–1989 Ocupaciones alfareras (2.860 ± 160 años A.P.) en la Cueva de Cristóbal, Puna de Jujuy, Argentina. *Relaciones de la Sociedad Argentina de Antropología* 17(2): 139–182.

____1988–1990. La cueva de Haichol. Arqueología de los pinares cordilleranos del Neuquén. *Anales de Arqueología y Etnología* 43–45: 1–738.

Fernandez, J., Markgraf, V., Panarello, H. O., Albero, M., Angiolini, F. E., Valencio, S. and Arriaga, M. 1991 Late Pleistocene / Early Holocene environments and climates, fauna and human occupation in the Argentine altiplano. *Geoarchaeology* 6(3): 251–272.

Panarello, H. O., and Fernandez, J. (ms.) 1992 First paleotemperature record in arid northwest Patagonia (Neuquén, Argentina) during the late Pleistocene-Holocene transition (12.300–10180 yr B.P.) derived from pallustrine shells (*Lymnnaea*) and marl ^{18}O analyses. Report submited to the International Atomic Energy Agency. Vienna. Austria.

Raffino, R. A. 1993 *Inka. Arqueología, Historia y Urbanismo del Altiplano Andino*. Buenos Aires, Ed. Corregidor: 318 p.

[RADIOCARBON, VOL. 39, NO. 1, 1997, P. 73–77]

UNIVERSITY OF GRANADA RADIOCARBON DATES VII

CECILIO GONZÁLEZ-GÓMEZ

Consejo Superior de Investigaciones Científicas and Departamento de Química Inorgánica, Radioquímica, Facultad de Ciencias, Universidad de Granada, E-18071 Granada, Spain

and

ELENA VILLAFRANCA-SÁNCHEZ

Centro de Instrumentación Científica, Servicios Técnicos de Apoyo a la Investigación, Universidad de Granada, E-18071 Granada, Spain

INTRODUCTION

This paper includes determinations of archaeological, geological and palaeobotanical samples from Spain and Portugal, measured at the University of Granada Radiocarbon Dating Laboratory, from 1990 to 1991. Pretreatment of charcoal and wood samples is a standard acid-basic procedure using 8% HCl and 2% NaOH at boiling temperature. The collagen of bone samples is obtained by the Longin (1971) method. The method of dating is benzene synthesis and liquid scintillation counting.

As previously reported (González-Gómez 1992), the sample size and the scintillator were 7 ml low K-40 Packard counting picovials with 5 ml synthesized benzene and 83.5 mg Butyl-PBD directly dissolved in the benzene (16.7 g/liter) as a scintillator; smaller samples were expanded to 5 ml with inactive benzene. ^{14}C activity was measured in a Packard Tri-Carb® Mod 4640 liquid scintillation spectrometer. Efficiency was ~65% using the part of the spectrum above the end point of tritium, with a background of ~7 cpm. At least one modern reference standard and two background vials were measured together with each series of measurements. All results are corrected for fractionation according to the quoted $\delta^{13}C$ (w.r.t. PDB) values.

In order to prevent any loss of benzene during counting and storage, we sealed the vials hermetically using metallic caps. The joint was made of a sheet composed of 3 mm silicone + 0.05 mm Teflon™. As a second barrier we placed a silicone O-ring, 10 mm in inner diameter and 2 mm thick, around the neck of the vial. The weight of vials, checked one year after filling, remained constant (González-Gómez 1992).

Dates reported here are based on 0.95 of the activity of NBS oxalic acid modern standard, on the Libby ^{14}C half-life of 5568 yr, and are expressed in radiocarbon years relative to AD 1950, as suggested by Stuiver and Polach (1977). Samples were measured for 100 min repeated 40–45 times, as well as background and standard vials. The standard deviation quoted includes only 1 σ of the counting statistics of background, sample and modern standard counts. Calculations and data were processed using a PC running a general program for radiocarbon dating laboratories written by González-Gómez (1995). Calibrated ages for a 2 σ interval were obtained by the method of Pearson *et al.* (1986), running the computer programs CALIB (Stuiver and Reimer 1986) and CALI (González-Gómez 1988) and using the bidecadal curve for samples of atmospheric origin. Sample descriptions and comments are essentially based on information provided by submitters.

ACKNOWLEDGMENT

We thank the Departamento de Química Analítica, Facultad de Química, Universidad de Barcelona, for the $\delta^{13}C$ determinations.

ARCHAEOLOGICAL SAMPLES

SPAIN

Acinipo. Ronda La Vieja Series

Charcoal samples from Acinipo, Ronda la Vieja (36°45′N, 5°10′W), Ronda, Málaga province, were collected from 1986 to 1988 by O. Garrido and M. Carrilero and submitted in 1990 by P. Aguayo, Departamento de Prehistoria y Arqueología, Universidad de Granada, to date the Bronze Age and particularly the building systems of the habitats in the site.

UGRA-360. Ac'88 - 41568 **3720 ± 70**
Charcoal from depth 6.92 m; 2350–1930 cal BC. $\delta^{13}C = -26.2‰$

UGRA-374. Ac'86 - 40710 **3640 ± 70**
Charcoal from depth 6.87 m; 2200–1786 cal BC. $\delta^{13}C = -24.8‰$

UGRA-375. Ac'86 - 40718 **3640 ± 50**
Charcoal from depth 6.40 m; 2180–1890 cal BC. $\delta^{13}C = -24.5‰$

General Comment: Expected ages were ~3710 ± 250 BP.

Cerro De Los Encaños Series

Charcoal samples from Cerro de los Encaños (40°03′N, 2°27′W), Villar del Horno, Pajaroncillo, Cuenca province, were collected and submitted 1990 by A. Gómez-Ruiz, Granada, to date the violent destruction and abandonment of an Iron Age village.

UGRA-363. VILLAR I **2475 ± 50**
Sample from depth 1.6 m; 800–400 cal BC. $\delta^{13}C = -25.1‰$

Comment: This sample corresponds to a temporary abandonment of the village, in the first Iron Age; expected age was ~2460 ± 100 BP.

UGRA-367. VILLAR II **1940 ± 50**
Sample from depth 1.2 m; 60 cal BC–cal AD 140. $\delta^{13}C = -23.5‰$

Comment: This sample corresponds to the definitive abandonment of the village, in the second Iron Age.

Los Barruecos Series

Charcoal samples from Los Barruecos (39°25′N, 6°30′W), Malpartida de Cáceres, Cáceres province, were collected and submitted 1987 by M. I. Sauceda-Pizaro, Area de Prehistoria y Arqueología, Facultad de Filosofía y Letras, Universidad de Extremadura, Cáceres, to date not only the site but also the later prehistoric sequence in the Extremadura region.

UGRA-352. Nº 1 **4000 ± 70**
Sample from depth 65 cm; 2865–2340 cal BC. $\delta^{13}C = -24.5‰$

UGRA-354. Nº 3 **3710 ± 80**
Sample from depth 1.0 m; 2451–1890 cal BC. $\delta^{13}C = -24.7‰$

UGRA-350. Museo de El Puerto de Santa María. IMAGEN. **870 ± 60**
$\delta^{13}C$ = −25.0‰

Wood sample from the Museum of the town of El Puerto de Santa María, Cádiz province, submitted 1987 by J. de Lucas-Almeida. The sample dated an image of which the original polychromy had disappeared; cal AD 1020–1270.

Comment: Expected age was ~760 BP.

UGRA-349. El Pla del Riu de les Marcetes PR **5040 ± 100**
$\delta^{13}C$ = −19.7‰

Bones from El Pla del Riu de les Marcetes (41°23′N, 1°50′E), Manresa, Barcelona province. Sample collected and submitted 1986 by J. Castany-Llusa, Instituto de Prehistoria y Arqueología, Universidad de Barcelona, to date a Neolithic grave. Ceramics and flint objects were found in the burial.

Comment: Sample from depth 1.2 m; expected age was ~5210 ± 250 BP; 4038–3640 cal BC.

UGRA-351 Puerto Guetaria PG **900 ± 50**
$\delta^{13}C$ = −27.6‰

Wood from Puerto Guetaria (43°18′N, 2°12′W), Guetaria, Guipuzcoa province. Sample collected and submitted 1988 by A. M. Benito, Sociedad de Ciencias Aranzadi, Museo San Telmo, San Sebastián. The sample was in a hole in a stone three-cornered anchor submerged at the entrance of the Guetaria port.

Comment: Sample from depth 9 m (under the sea level); cal AD 1020–1250.

Ronda City Area Series

Samples from Ronda city area (36°45′N, 5°10′W), Ronda, Málaga province, were collected from 1985 to 1989 by B. Padial, J. Castilla and P. Aguayo and submitted from 1990 to 1992 by P. Aguayo, Departamento de Prehistoria y Arqueología, Universidad de Granada, to date several periods in the city as detailed below.

UGRA-376. Ro'89 - 7556 **2400 ± 50**
765–390 cal BC. Expected age was ~2310 ± 150 BP. *$\delta^{13}C$ = −25.4‰*

Comment: Charcoal from depth 3.2 m, to date the use of a kiln and its pottery production.

UGRA-423. RO-89-AA-6695 **955 ± 40**
cal AD 1001–1168. *$\delta^{13}C$ = −25.0‰*

Comment: Charcoal from depth 3.5–3.6 m, to date the Iberic levels of establishment from Prehistory to the present time.

UGRA-427. RO-89-AA-6695 **985 ± 40**
cal AD 981–1159. *$\delta^{13}C$ = −25.0‰*

Comment: This is a repetition of the previous sample UGRA-423, in order to confirm the result.

UGRA-424. RO-87-AA-6136 **415 ± 45**
cal AD 1419–1628. *$\delta^{13}C$ = −25.0‰*

Comment: Charcoal from depth 3.1–3.2 m, to date the same as UGRA-423.

UGRA-425. RO-89-AA-6671 **930 ± 40**
cal AD 1015–1213. $\delta^{13}C = -25.0‰$

Comment: Charcoal from depth 3.4 m, to date the same as UGRA-423 and UGRA-425.

UGRA-426. RO-89-AA-C/7 **2495 ± 50**
800–410 cal BC. Expected age was ~2700 ± 250 BP. $\delta^{13}C = -25.0‰$

Comment: Wheat seeds sample from depth 4.5 m, to date Final Bronze Age levels in the site.

UGRA-432. RO-85 GC 3090 **2730 ± 70**
1040–800 cal BC. $\delta^{13}C = -25.0‰$

Comment: Charcoal sample, to date levels of superimposed villages.

Las Viñas Series

Shell samples from Las Viñas (36°39′N, 6°10′W), El Puerto de Santa María, Cádiz province, were collected and submitted 1987 by F. Giles-Pacheco, Municipal Museum of El Puerto de Santa María.

UGRA-369. Silo nº 50 **4800 ± 90**
3350–2890 cal BC. $\delta^{13}C = +0.15‰$

Comment: Shells from depth 1.6 m, to date the geographic area of western Andalusia.

UGRA-370. Silo nº 16 **4950 ± 60**
cal AD 1001–1168. $\delta^{13}C = -1.00‰$

Comment: Shells from depth 1.2–1.5 m. This is the first dating of the site context; it can be related to nearby Chalcolithic sites with similar pottery.

PORTUGAL

UGRA-355 Mamoa 1 de Chã de Carvalhal Amostra nº 2 **5860 ± 60**
$\delta^{13}C = -25.7‰$

Charcoal from Mamoa 1 de Chã de Carvalhal (41°08′N, 8°05′W), Serra da Aboboreira, Baião, Distrito Porto, Douro Litoral province. Sample collected 1986 and submitted 1988 by D. de Jesus da Cruz, Instituto de Arqueologia, Faculdade de Letras, Universidade de Coimbra. The sample is from a megalithic necropolis with more than 40 tumulis. To date the Megalithic tomb episode in the region.

Comment: Sample from depth 1.29 m; 4900–4586 cal BC.

GEOLOGICAL SAMPLES

SPAIN

Rambla Guzmaina Series

Wood samples from Rambla Guzmaina (37°24′N, 1°58′W), Huercal Overa, Almería province, collected 1990 by A. Martín-Penela and submitted 1990 by L. García-Rossell, Instituto Andaluz de Geología Mediterránea, Facultad de Ciencias, Universidad de Granada, to study an episode of recent sedimentation in the Almanzora River basin.

UGRA-371. G-A-I Sup. **200 ± 60**
Sample from depth 1.3 m; cal AD 1522–1955. $\delta^{13}C = -25.3‰$

UGRA-372. G-A-I Inf. **> Modern**
Sample from depth 2.3 m. $\delta^{13}C = -24.9‰$

UGRA-373. G-A-II **> Modern**
Sample from depth 30 cm. $\delta^{13}C = -25.0‰$

PALAEOBOTANICAL SAMPLES

SPAIN

Lobeiras Series

Samples from Lobeiras (43°25′N, 7°31′W), Vivero, Lugo province, collected and submitted 1989 by M. P. Saa-Otero, Colegio Universitario de Orense, Las Lagunas, Orense province, to establish the vegetation existing in this zone during the Quaternary.

UGRA-347. LOB-1 **2080 ± 60**
Peat sample from depth 51 cm; 354 cal BC–cal AD 52. $\delta^{13}C = -28.1‰$

UGRA-348. LOB-2 **9800 ± 120**
Wood sample from depth 1.2 m. $\delta^{13}C = -26.3‰$

UGRA-324. Pico del Lobo. PLB II C' **1830 ± 110**
$\delta^{13}C = -28.1‰$

Peat from Pico del Lobo (40°59′N, 3°58′W), La Pinilla, Segovia province; sample was collected and submitted 1989 by M. J. Gil-García, Departamento de Geología, Universidad de Alcalá de Henares, Madrid province, to establish the vegetation history of this zone, cal AD 670–1020.

Puerto De Canencia Series

Peat samples from Puerto de Canancia (40°52′N, 3°47′W), Canencia de la Sierra, Madrid province, were collected 1988–1990 and submitted 1990 by M. J. Gil-García, Departamento de Geología, Universidad de Alcalá de Henares, Madrid province, to establish the vegetation history of this zone and confirm the pollen data.

UGRA-368. PCO **1170 ± 50**
Sample from depth 80–90 cm; cal AD 714–980. $\delta^{13}C = -27.9‰$

UGRA-411. PCO 2 **2580 ± 80**
Sample from depth 1.20–1.45 m; 900–421 cal BC. $\delta^{13}C = -27.9‰$

REFERENCES

González-Gómez, C. 1988 CALI, a computer program for calibration of radiocarbon dates. Unpublished software.

____1992 University of Granada radiocarbon dates VI. *Radiocarbon* 34(1): 133–139.

____1995 A general computer program for radiocarbon dating laboratories. *In* Cook, G. T., Harkness, D. D., Miller, B. F. and Scott, E. M., eds., Proceedings of the 15th International ^{14}C Conference. *Radiocarbon* 37(2): 789–790.

Longin, R. 1971 New method of collagen extraction for radiocarbon dating. *Nature* 230: 241–242.

Pearson, G. W., Pilcher, J. R., Baillie, M. G. L., Corbet, D. M. and Qua, F. 1986 High-precision ^{14}C measurements of Irish oaks to show the natural ^{14}C variations from AD 1840 to 5210 BC. *In* Stuiver, M. and Kra, R. S., eds., Proceedings of the 12th International ^{14}C Conference. *Radiocarbon* 28(2B): 911–934.

Stuiver, M. and Polach, H. 1977 Reporting of ^{14}C data. *In* Stuiver, M. and Kra, R., eds., Calibration Issue. *Radiocarbon* 19(3): 355–363.

Stuiver, M. and Reimer, P. J. 1986 A computer program for radiocarbon age calibration. *Radiocarbon* 28(2B): 1022–1030.

[RADIOCARBON, VOL. 39, NO. 1, 1997, P. 79–87]

RESEARCH CENTER OF RADIOISOTOPES AT UNIVERSITY OF OSAKA PREFECTURE RADIOCARBON DATES I

SETSUKO SHIBATA, EIKO KAWANO and TAKESHIGE NAKABAYASHI

Research Center of Radioisotopes, Research Institute for Advanced Science and Technology, University of Osaka Prefecture, 1-2, Gakuen-cho, Sakai, Osaka, Japan

INTRODUCTION

The radiocarbon dating laboratory has been in operation since 1984 at the Radiation Center of Osaka Prefecture (OR), predecessor of the Research Center of Radioisotopes, University of Osaka Prefecture. We use liquid scintillation counting (LSC), following sample conversion to methanol through combustion and $LiAlH_4$ reduction. This method was developed by Yamada *et al.* (Yamada, Higashimura and Shidei 1966; Yamada and Kobashigawa 1986). In cooperation with Yamada, we somewhat modified their procedure: 1) sample charcoal is burned at 700°C in the presence of CuO needles and Sulfix grains to remove sulfur and halogen compounds produced during the combustion; 2) the combustion is carried out by using N_2-O_2 mixed gas of minimized O_2 content and stopped when a small amount of the charcoal still remains unchanged, because precise investigation of methanol preparation revealed that O_2 gas stimulates byproduct formation during $LiAlH_4$ reduction (Shibata *et al.* 1985; Shibata *et al.* 1993). Usually, methanol is prepared directly from sample charcoal in a reaction apparatus ("direct method"). When the sample quantity is insufficient, generated CO_2 is isolated as $CaCO_3$ and diluted with inactive commercial $CaCO_3$ if necessary (< 40 g of $CaCO_3$ yield). Then $CaCO_3$ is hydrolyzed with HCl to CO_2 for methanol preparation in the usual way ("separate method"). We use standard oxalic acid SRM 4990C (HOxII) for determination of modern ^{14}C (Stuiver 1983). The acid is oxidized to CO_2 using the wet method of Valastro, Land and Valera (1977) followed by methanol preparation in the same manner as for unknown samples.

Methanol obtained is purified and checked via gas chromatographic analysis prior to ^{14}C measurement. Six grams of methanol (7 g, later) are dissolved into 11 g (4 g, later) of homemade xylene cocktail for LSC, using a Packard TRI-CARB® 460CD). The counting efficiency is measured using a series of quenched standards close in composition to sample cocktails, while counting conditions are continually checked by measuring methanol prepared from contemporary rice grains as a secondary standard. Sample and background cocktails are alternatively measured for 100 min to attain desired statistical errors. We measure ^{14}C in HOxII for every batch of samples. The averaged value is 18.209 ± 0.105 dpm/gC (one standard deviation, 1 σ) for all measurements so far (11 times).

Smokeless coal was used for a blank test of methanol preparation and gave a ^{14}C date of >35,000 yr BP under routine conditions. As a control on our procedures, we ^{14}C-dated several samples that had been dated by other laboratories. Our results were quite consistent with ^{14}C dates of other laboratories (Shibata *et al.* 1990).

Samples dated were wood, charcoal and peat. The quoted errors (at the 1 σ confidence level) include the standard deviations of count rates for unknown, background and modern samples. We report dates according to the guidelines of Stuiver and Polach (1977), *i.e.*, in yr BP, based on the conventional Libby half-life for ^{14}C of 5568 yr. Correction for isotopic fractionation was not made. Calendar years shown in parentheses were age ranges (2 σ) calculated by use of Method B (Probabilities) in the CALIB calibration program, Version. 3.3 (Stuiver and Reimer 1993).

ARCHAEOLOGICAL SAMPLES

JAPAN

Kankoji Series

Kankoji site, Kanan-cho, Minamikawachi dist, Osaka pref (34°2′N, 135°37′E), 102 m asl, is a typical upland village of Late Yayoi Age. Site was investigated by Educ Bd, Osaka pref. Collected and submitted 1985 by H. Otani, Educ Bd, Osaka Pref.

OR-5. KNJ-No. 1 **1680 ± 85**

Charcoal from hearth in rounded square ancient dwelling (sides 3.7 by 3.6 m) No 1, located at the central part of Kankoji site (cal AD 147 to 591).

Comment (H.O.): Estimated as Late Yayoi Age. Result reasonable.

OR-9. KNJ-No. 2 **29,260 ± 3860**

Wood from dark-gray clay layer, *ca.* 3 m deep, at northwest corner of Kanroji pond located at northeast edge of Kankoji site.

Comment: Separate method with $CaCO_3$ dilution was used.

OR-6. KNJ-No. 3 **32,000 ± 1810**

Wood from dark green-gray sandy clay layer, just under portion of OR-9.

OR-7. KNJ-No. 4 **>37800**

Wood from black-gray clay layer, *ca.* 4 m deep, at same place as OR-9.

Shinpukuji Series

Shinpukuji site, Mihara-cho, Minamikawachi dist, Osaka pref (34°32′N, 135°33′E) includes remains of temple bell foundry, kilns and structures from Nara to Middle Age. Site was investigated 1984 to 1985 by joint Educ Bd, Osaka pref and Osaka ctr of Cultural Properties. Samples collected at kiln remain, 41 m asl, and submitted 1985 by A. Yamamoto, Osaka ctr of Cultural Properties.

OR-13. Sample No. 1 **1550 ± 85**

Mixture of smashed charcoal and mud from tile-kiln No 2 (cal AD 344 to 658).

OR-23. **1190 ± 55**

Same sample as OR-13. Dated to confirm or correct date for OR-13, above (cal AD 706 to 979).

OR-17. Sample No. 2 **1380 ± 190**

Mixture of smashed charcoal and mud from tile-kiln No 5 (cal AD 254 to 1024).

OR-15. Sample No. 5 **1540 ± 60**

Mixture of smashed charcoal and mud from surroundings of tile-kilns No 2 and No 5 (cal AD 418 to 637).

OR-16. Sample No. 6 **1570 ± 80**

Mixture of smashed charcoal and mud from same place as OR-15 (cal AD 270 to 649).

OR-14. Sample No. 10 **1410 ± 65**

Mixture of smashed charcoal and mud from same place as OR-15 (cal AD 535 to 778).

OR-11. Sample No. 7 **1230 ± 55**

Charcoal from charcoal-kiln No 1 (cal AD 676 to 954).

OR-12. Sample No. 9 **1450 ± 55**

Charcoal from charcoal-kiln No 1 (cal AD 452 to 682).

Comment: Separate method was used for all samples in this series. Samples OR-13, -16 and -17 were diluted with inactive $CaCO_3$. Tile kilns No 2 and No 5 est. as Nara Age (AY) and ^{14}C dates reasonable. Age of charcoal kiln No 1 was either AD 8 or 13 (AY). ^{14}C dates matched AD 8. Archaeological magnetic date for charcoal kiln No 1 (either AD 730 or 600, H. Shibuya) was quite consistent with our results.

Joyama Series

Joyama site, Hirano Ward, Osaka city, Osaka pref (34°36′N, 135°35′E), 10 m asl, includes many remains from Jomon to Modem Age. Site was investigated 1983 to 1985 by joint Educ Bd, Osaka Pref and Osaka Ctr of Cultural Properties. Samples were in Trench D, at 3 m depth. Collected 1984 to 1985 and submitted 1985 by S. Kanbayashi, Osaka ctr of Cultural Properties.

OR-18. SB0901W-11 **2190 ± 60**

Fragments of burnt wood from rectangular ancient dwelling 5.7 m by 4.3 m, SB0901. Associated with earthenware of Yayoi Age (cal 380 to 68 BC).

OR-19. SB1001W-4 **2200 ± 80**

Fragments of burnt board from ancient dwelling (*ca.* 7 m in diam), SB1001. Associated with earthenware of Yayoi Age (cal 393 to 50 BC).

OR-19′. **2080 ± 60**

Same sample as OR-19. Re-dated at submitter's request to confirm or correct date for OR-19, above (cal 345 BC to AD 71).

OR-20. SB1001W-41 **1970 ± 50**

Fragments of burnt wood from same dwelling as OR-19 (cal 66 BC to AD 194).

OR-21. SB1004W-38 **2150 ± 65**

Burnt stick wood from ancient dwelling (8.1–6.0 m in diam), SB1004. Associated with earthenware of Yayoi Age and a spindle wheel (cal 372 BC to 10).

OR-22. SB1004W-14 **2090 ± 75**

Burnt board wood from same dwelling as OR-21 (cal 357 BC to AD 72).

Comment: Burnt materials such as grounds and woods were scattered throughout these ancient dwellings. These were estimated as fire-destroyed dwellings in Late Yayoi Age: dwelling SB0901 est. as middle part and dwellings SB1001 and SB1004 estimated as early part of Late Yayoi Age (SK). Sample for OR-22 was also dated by Kyoto Sangyo Univ (KSU). Result (1970 ± 20 BP, cal 150 BC to AD 205) agreed with our datum at 2 σ confidence level.

Tai Series

Tai site, Mihara-cho, Minamikawachi dist Osaka pref (34°32′3″N, 135°35′42″E) is located at midpoint of terrace, *ca.* 39 m asl. Investigated 1986 by Osaka ctr of Cultural Properties. Collected and submitted 1986 by K. Kuninori.

OR-24. Driftwood 1 **31,110 ± 1640**

Driftwood from bluish-green clay layer 12, Trench 1A, at 2 m depth.

OR-25. Driftwood 2 **30,470 ± 1520**

Driftwood from just under portion of OR-24.

Kosaka Series

Kosaka site, Hirai, Sakai city, Osaka pref (34°30′55″N, 135°29′33″E), at valley in northern extremity of Senboku Hill, 22–25 m asl, includes many remains from Jomon to Modern Age. Site was investigated 1985 to 1990 by joint Educ Bd, Osaka Pref and Osaka Ctr of Cultural Properties. Samples collected at H, F and I dists.

H dist group

H dist is located at bed of Hara Reservoir. Collected and submitted 1988 by K. Kuninori.

OR-58. Tree sample A **2630 ± 65**

Piece of tree from layer 12, Trench 1H, at 1.5 m depth (cal 919 BC to 530).

OR-59. Tree sample B **2770 ± 75**

Piece of tree sample same as OR-58 (cal 114 to 802 BC).

OR-60. Tree sample C **2790 ± 60**

Piece of tree sample same as OR-58 (cal 1113 to 813 BC).

OR-61. Tree sample D **2710 ± 80**

Piece of tree sample same as OR-58 (cal BC 1113 to 600).

OR-62. Peat No. 1 **3600 ± 75**

Peat from dark brown peat layer 13, Trench 1 H, just under portion of tree sample, above (cal 2140 to 1742 BC).

OR-63. Peat No. 2 **3500 ± 80**

Peat from same portion as OR-62 (cal 2031 to 1613 BC).

Comment: Final Jomon Age remains were found at just upper portion of tree sample for OR-58, -59, -60 and -61. Samples were est. as before Final Jomon Age (KK). ^{14}C dates for tree sample corresponded to Late Jomon Age.

F dist group

Collected and submitted 1988 by K. Akaki, Senboku branch office, Osaka ctr of Cultural Properties.

OR-69. Water pipe 1 **1280 ± 55**

Fragment of water pipe, 42 cm in diam 5.3 m long and 5–12 cm thick, from drain in layer 4 Trench 1 OF (cal AD 664 to 878).

OR-67. Driftwood 2 **1260 ± 50**

Driftwood from same place as OR-69 (cal AD 672 to 883).

OR-68. Driftwood 3 **1270 ± 55**

Driftwood from drain in layer 4 or 5, Trench 12F (cal AD 666 to 883).

Comment: Samples for OR-69 and -67 est. as Nara Age (KA) and sample for OR-68 estimated as before Kofun Age (KA). ^{14}C dates for these three samples corresponded to Nara Age. Portion including these samples was classified to old river 4 of Nara Age.

OR-64. Driftwood 8 **2460 ± 65**

Driftwood from drain 3 in layer 4, Trench 16F (cal 768 to 405 BC).

OR-70. Driftwood 10 **2560 ± 60**

Driftwood from valley-sand layer in Layer 4, Trench 16F (cal 820 to 424 BC).

OR-73. Decayed plant 11 **2490 ± 65**
Decayed plant from valley-humus layer in layer 4, Trench 16F (cal 783 to 415 BC).

OR-82. Root 12 **3630 ± 65**
Root, Trench 16F (cal 2182 to 1775 BC).

Comment: Sample for OR-64 est. as Kofun Age and samples for OR-70 and -73 est. as before Kofun Age (KA). ^{14}C dates for these samples corresponded to Late Jomon Age. They were assigned to period before Final Jomon Age.

OR-72. Board 7 **1510 ± 110**
Board from base of layer 6, Trench 8F (cal AD 264 to 766).

OR-65. Root 6 **2570 ± 50**
Root from same place as OR-72 (cal 818 to 526 BC).

OR-71. Root 5 **2640 ± 60**
Root from base of layer 6, Trench 9F. Associated with earthenware of Final Jomon Age (cal 917 to 546 BC).

Comment: Samples for OR-72, -65 and -71 est. as Final Jomon Age (KA). ^{14}C date for OR-72 was younger than Yayoi Age. Portion including sample for OR-72 was classified to Kofun Age river 6 Samples for OR-65 and -71 were assigned to periods before and just Final Jomon Age, respectively.

OR-66. Root 4 **3320 ± 65**
Root from base of layer 6, Trench 11 F (cal 1738 to 1447 BC).

OR-74. Carbonized root 9 **3790 ± 75**
Carbonized root from base of layer 6, Trench 12F (cal 2455 to 1984 BC).

I dist group

I dist is at flood plain located at left bank of Toki River. Samples collected at Trench 51 and submitted 1988 by K. Akaki.

OR-75. 1 **2350 ± 45**
Peat from the highest peat layer in old river route (cal 534 to 210 BC).

OR-76. 2 **3390 ± 70**
Peat from the second peat layer at same place as OR-75 (cal 1877 to 1517 BC).

OR-77. 3 **3800 ± 70**
Peat from the third peat layer at same place as OR-75 (cal 2455 to 2034 BC).

OR-78. 4 **4490 ± 70**
Peat from the fourth peat layer at same place as OR-75 (cal 3356 to 2926 BC).

OR-79. 6 **2500 ± 65**
Peat from peat layer in another portion of the old river route, above (cal 791 to 417 BC).

OR-80. 7 **2600 ± 75**
Piece of tree from peat layer in wetland behind the old river, above (cal 903 to 425 BC).

OR-81. 8 **2570 ± 75**
Peat from peat layer including tree sample for OR-80 (cal 834 to 418 BC).

OR-83. 5 **8990 ± 230**
Peat from peat layer in natural levee of the old river route, above (cal 8522 to 7534 BC).

Comment: Sample for OR-83 est. as before 500 BC and others est. as between 500 BC and AD 800 (KA). ^{14}C date for OR-83 corresponded to Initial Jomon Age. ^{14}C dates for OR-75, -76, -77, -78 and -79 were dispersed during Middle to Final Jomon Age. These samples showed more and more low ^{14}C activity along with their depth, helping to determine start chronology at the area. The old river was named as Jomon River 28. Samples for OR-80 and -81 were classified as Final Jomon to early part of Yayoi Age.

SYRIA

OR-36. **1060 ± 55**
Chip of wood from ancient sunken ship found at bottom, 32 m deep, 2 km off coast of Tartous, Syria (34°54′N, 35°51′E). Excavation was made (1985 to 1987) for research into maritime trade history in the Mediterranean jointly by the Directorate of Antiquities and Museums of the Syrian Arab Republic and the Syrian Coastal Archaeological Excavation Operation Committee of Japan. More than 5000 amphorae were found in the sunken ship (cal AD 879 to 1157).

Comment: Initially, amphorae est. as Greco-Roman period. ^{14}C date for OR-36 corresponded to period from 9th to 12th century. Age of the sunken ship was eventually determined to be the first half of 13th century AD on the basis of heat luminescence date and ^{14}C dates by Nagoya University (Tandetron Accelerator Mass Spectrometry), in addition to our result.

GEOLOGICAL SAMPLES

JAPAN

Buried Forest of Japan Cedar Series

Japanese cedars (*Cryptomeria japonica* D. DON) buried under rice field, 50–80 cm deep, Mikatacho, Fukui pref (35°31′50″N, 135°53′22″E), 20 m asl, were investigated and submitted 1986 by H. Takahara, Osaka Agric Res Center (Kyoto pref Univ. For, since 1989).

OR-26. KR-W-1 **3390 ± 55**
Chip of buried Japanese cedar, 35 cm in diam. There was a feeding-trace due to insects.

OR-28. KR-W-2 **3130 ± 70**
Chip of buried Japanese cedar, 30 cm in diam and 6 m long. There were three feeding-traces due to insects.

Comment (HT): Feeding traces were recognized as larval tunnels of sugi bark borers, *Semanotus japonicus* Lacordaire (Coleoptera: Cerambycidae). Samples yielded first date when sugi bark borers had been inhabitant in Japan (Takahara, Ito and Takeoka 1988).

Kigo and Yakumogahara Moors Series

Samples from Kigo moor, Miyazu city, Kyoto pref (35°40′N, 135°11′E), alt 550 m, and from Yakumogahara moor, Shiga district, Shiga pref (35°15′15″N, 135°54′46″E), alt 910 m, were investigated and submitted 1987 by H. Takahara.

OR-54. KG-46-58 **910 ± 100**
Peat from Kigo moor, at 46–58 cm depth.

OR-27. **14,760 ± 220**
Peat from Kigo moor, at 520–530 cm depth.

OR-55. YK-B-47-55 **1050 ± 90**
Peat from Yakumogahara moor, at 47–55 cm depth.

Comment: Separate method with $CaCO_3$ dilution was used for OR-54 and -55. Pollen analysis revealed that just upper portion of OR-54 or -55 corresponded to increasing period of pine tree forest at each region (HT). These ^{14}C dates helped determine beginning of natural forest destruction due to human activities, because pine tree forest tends to increase in parallel with destruction of the natural forest (HT). OR-27 est. age from 10,000 to 15,000 years BP and ^{14}C date was as expected.

Koseinuma Moor Series

Koseinuma moor, Yabu district, Hyogo pref. (35°21′N, 134°31′09″E), alt 1470 m, is located in Japanese cedar forest near top of Mt. Hyonosen. Collected 1989 to 1991 and submitted by H. Takahara.

OR-107. KS-23-33 **780 ± 75**
Peat from peat layer, 23–33 cm deep.

OR-108. KS-50-60 **1600 ± 75**
Peat from same peat layer as OR-107, 50–60 cm deep.

OR-109. KS-85-95 **2380 ± 60**
Peat from same peat layer as OR-107, 85–95 cm deep.

OR-97. KS89-II **3450 ± 90**
Peat from clayey peat layer at same place as OR-107, 108–118 cm deep.

Comment: Separate method with $CaCO_3$ dilution was used for OR-107, -108 and -97. Samples were measured to date changes in natural forests of Japanese cedar or pine tree at Mt. Hyonosen. ^{14}C activity for these peat samples decreased linearly along with their depth, implying constant speed of deposition at the area.

OR-110. IH-520-530 **8820 ± 360**
Peat, 520–530 cm deep, from Ikenotaira moor, Ichishi dist, Mie pref (34°31′27″N, 136°10′43″E), alt 600 m. Collected and submitted 1990 by H. Takahara.

Comment: Akahoya ash (*ca.* 6400 BP) was found at 264–271 cm depth and sample estimated as deposited during last glacial period (HT).

OR-94. **230 ± 45**
Peat, 1170–1200 cm deep, from Ukishimanomori moor, Shingu city, Wakayama pref (33°43′N, 135°59′E). Collected and submitted 1989 by M. Takeoka, Kyoto pref Univ.

Comment: Akahoya ash was found at 2000 cm depth and sample est. as 3000 to 4000 BP, whereas ^{14}C date was nearly modern (MT). Separate method with inactive $CaCO_3$ dilution was used.

OR-95. KR-89-2 **6530 ± 95**
Peat, at 134–143 cm depth, from Karakemi moor, Kita-azumi dist, Nagano pref (36°29′10″N, 137°53′35″E), alt 945 m, located in cold temperate zone of Shinshu area. Collected and submitted 1989 by M. Takeoka.

Comment: Sample was measured to date natural forest changes at inland area of Central Japan (TM). Separate method was used.

OR-96. OG-89-3 **16,110 ± 250**

Peat, at 180–190 cm depth, from Ohoawara moor, Ina dist, Nagano pref (35°52′58″N, 138°10′53″E), alt 1815 m. Collected and submitted 1989 by M. Takeoka.

Comment: Sample was measured to date coniferous tree forest changes at subalpine zone in Central Japan (TM). Separate method was used.

OR-100. TIK-436.6-446.6 **2530 ± 50**

Peat, at 436.6–446.6 cm depth, from Ikenotaira moor, Higashi-tonami dist, Toyama pref (36°25′N, 136°52′30″E). Collected and submitted 1989 by M. Takeoka.

OR-101. NA-350-360 **1670 ± 150**

Peat, at 350–360 cm depth, from Nawagaike moor, Tonami dist, Toyama pref (36°28′30″N, 136°56′E), alt 810 m. Collected and submitted 1990 by M. Takeoka.

Comment: Methanol yield was unexpectedly low due to bad sample contamination with soil. ^{14}C date was obtained by using corrected ^{14}C activities of crude methanol (97% purity).

Kaminokodaira Series

Kaminokodaira, Nakashinkawa dist, Toyama pref (36°34′6″N, 137°30′31″E). Collected and submitted 1990 by M. Takeoka.

OR-103. KA-I-35-41 **6580 ± 65**

Peat, at 35–41 cm depth, alt 1410 m.

OR-104. KA-II-60-66 **1240 ± 40**

Peat, at 60–66 cm depth, alt 1425 m.

OR-102. KA-II-90-94 **10,960 ± 300**

Peat, at 90–94 cm depth, from same place as OR-104.

Comment: ^{14}C date for OR-102 was determined by using corrected ^{14}C activity of crude methanol (98% purity) because of unexpectedly low yield of methanol due to bad sample contamination with soil. Separate method was used for OR-103 and -104.

Borneo

South Kalimantan Series

Peat from swamp in South Kalimantan, Bomeo (3°7′S, 114°30′E). Collected and submitted 1986 by H. Furukawa, Center for Southeast Asian Studies, Kyoto University.

OR-39. BM41 **1420 ± 70**

Peat, 25–75 cm deep.

OR-40. BM41 **2000 ± 50**

Peat, 150–194 cm deep.

Sumatra

Pulan Kijang Series

Samples from swamp in Jambi (0°45′S,103°15′E). Collected and submitted 1986 by H. Furukawa.

OR-41. Pulan Kijang 4 **760 ± 65**

Peat, 30–50 cm deep.

OR-42. Pulan Kijang 4 **1040 ± 50**
Peat, 100–120 cm deep.

OR-43. Pulan Kijang 4 **1550 ± 60**
Peat, 180–200 cm deep.

Dendang Series

Samples from swamp in Jambi (1°10′S, 103°50′E). Collected and submitted 1986 by H. Furukawa.

OR-44. Dendang Unit II **1120 ± 55**
Peat, 30–50 cm deep.

OR-45. Dendang Unit II **1440 ± 55**
Peat, 100–120 cm deep.

OR-46. SK19 (Pelita) **220 ± 40**
Peat, 30–50 cm deep, from swamp in Jambi (1°06′S, 104°04′E). Collected and submitted 1986 by H. Furukawa.

References

Shibata, S., Kawano, E., Nakabayashi, T., Kawamura, S. and Yamada, O. 1985 Estimation of low level carbon-14 in environment: Methanol synthesis from rice grains and liquid scintillation counting. *Annual Report of the Radiation Center of Osaka* 26: 115–121.

Shibata, S., Kawano, E., Nakabayashi, T., Kawamura, S. and Yamada, O. 1990 Radiocarbon dating by Methanol-LSC method. *Annual Report of the Radiation Center of Osaka* 30: 83–90.

Shibata, S., Kawano, E., Nakabayashi, T. and Yamada, O. 1993 Additional study of the direct Methanol-LSC method for low-level ^{14}C measurement. *Applied Radiation and Isotopes* 44: 1491–1493.

Stuiver, M. and Polach, H. A. 1977 Discussion: Reporting of ^{14}C data. *Radiocarbon* 19(3): 355–363.

Stuiver, M. 1983 International agreements and the use of the new oxalic acid standard. *In* Stuiver, M. and Kra. R. S., eds. Proceedings of the 11th International ^{14}C Conference. *Radiocarbon* 25(2): 793–795.

Stuiver, M. and Reimer, P. J. 1993 Extended ^{14}C data base and revised Calib. 3.0. ^{14}C age calibration program. *In* Stuiver, M., Long, A. and Kra, R. S., eds., Calibration Issue. *Radiocarbon* 35(1) 215–230.

Takahara, H., Ito, T. and Takeoka, M. 1988 Woods invaded by the sugi bark borer, *Semanotus japonicus* Lacordaire (Coleoptera: Cerambycidae), about 3000 years ago, and the forest vegetation at that time. *Journal of the Japanese Forestry Society* 70: 143–150.

Valastro, S., Jr., Land, L. S. and Varela, A. G. 1977 An improved procedure for wet oxidation of the ^{14}C NBS oxalic acid standard. *Radiocarbon* 19: 375–382.

Yamada, O., Higashimura, T. and Shidei, T. 1966 ^{14}C-dating by liquid scintillation counting. *Radioisotopes* 15(2): 73–76.

Yamada, O. and Kobashigawa, A. 1986 KSU Radiocarbon dates 1. *Radiocarbon* 28(3): 1077–1101.

[RADIOCARBON, VOL. 39, NO. 1, 1997, P. 89–113]

KSU RADIOCARBON DATES II

OSAMU YAMADA

Faculty of Science, Kyoto Sangyo University, Kyoto 603, Japan

INTRODUCTION

This date list mainly reports on samples processed from 1982 to 1991. Each sample is converted to methanol. Radiocarbon is measured in a Teflon™ vial containing a mixture of 40 g of methanol and 50 cc of xylene, 1% Butyl PBD and 0.1% PBBO using low-background scintillation counters Aloka LSC-800, LB-I and LB-III. The background of LB-III is *ca.* 8 cpm and counting efficiency is *ca.* 70%. The recent ^{14}C standard used is 95% of NBS oxalic acid; 5568 yr is used as the half-life of ^{14}C.

For further detail on our measurement methods, see Yamada and Kobashigawa (1986).

GEOLOGIC SAMPLES

JAPAN

Hokkaido

Hokkaido University Environmental Science (HE) Series

Samples were submitted 1984 to 1986 by H. Yamamoto of the Laboratory of Fundamental Research, the Graduate School of Environmental Science, Hokkaido University.

KSU-905. HE-1 Mizukami 1 **12,300 ± 430**
Charcoal from Mizukami, Koshimizu-cho, Abashirigun (43°47′34″N, 144°29′52. 8″E). Collected 1984 by T. Sone.

Comment (T.S.): Expected age: *ca.* 10,000 BP.

KSU-1248. HE-37 Mizukami 2 **26,100 +2000/−1600**
Charcoal, 1100 cm depth, in Higashi-Kayano scoria, Koshimizu-cho (43°47′34.1″N, 144°29′ 52.8″E, 70 m asl). Collected 1984 by T. Sone.

Comment (T.S.): Expected age: *ca.* 20,000 BP.

KSU-906. HE-2 Kayano **28,200 +1700/−1400**
Charcoal, 210 cm depth, from Kayano, Koshimizu-cho (43°50′44.5″N, 144°30′16.8″E). Collected 1984 by T. Sone.

Comment (T.S.): Expected age: *ca.* 40,000 BP.

KSU-907. HE-3 Kamishari **30,300 +1400/−1200**
Charcoal in Kamishari pumice flow-I, 260 cm depth, from Kamishari, Kiyosato-cho (43°50′ 44.6″N, 144°34′6.8″E). Collected 1984 by T. Sone.

Comment (T.S.): Expected age: *ca.* 32,000 BP.

KSU-908. HE-4 Nakafurano **5220 ± 90**
Peat, 230 cm depth, from Nakafurano-cho, Sorachi-gun (43°22′5.4″N, 142°26′42.4″E). Collected 1984 by H. Daimaru.

Comment (H.D.): Expected age: 4000–5000 BP.

KSU-909. HE-5 Shintoku 1 **2140 ± 70**
Peat from Shintoku-cho, Kamikawa-gun (43°5′52″N, 142°44′10″E, 420 m asl). Collected 1984 by K. Yamamoto.

Comment (K.Y.): Expected age: 2000–5000 BP.

KSU-910. HE-6 Shintoku 2 **1480 ± 110**
Peat from Shintoku-cho (43°9′49″N, 142°48′33″E, 405 m asl). Collected 1984 by K. Yamamoto.

Comment (K.Y.): Expected age: 2000–5000 BP.

KSU-911. HE-7 Shintoku 3 **2140 ± 35**
Peat from Shintoku-cho (43°6′2″N, 142°46′30″E, 440 m asl). Collected 1984 by K. Yamamoto.

Comment (K.Y.): Expected age: 5000–6000 BP.

KSU-913. HE-9 Shintoku 4 **4620 ± 40**
Peat from Shintoku-cho (43°31′26.8″N, 142°49′6.8″E, 1635 m asl). Collected 1984 by N. Takahashi.

KSU-912. HE-8 Kamikawa **140 ± 50**
Peat from Kamikawa-cho, Kamikawa-gun (43°32′14.8″N, 142°57′32.8″E, 1424 m asl). Collected 1983 by N. Takahashi.

KSU-914. HE-10 Biei 1 **3800 ± 40**
Peat, 130 cm depth, from Biei-cho, Kamikawa-gun (43°36′3.2″N, 142°53′17″E, 1735 m asl). Collected 1984 by N. Takahashi.

KSU-915. HE-11 Biei 2 **7540 ± 70**
Peat from same site as KSU-914. Collected 1984 by N. Takahashi.

KSU-1036. HE-12 Konan 12,400 ± 80
Peat, 190 cm depth, from Konan, Kiyosato-cho, Shari-gun (43°48′7.7″N, 144°38′1.3″E, 147 m asl). Collected 1984 by T. Sone.

Comment (T.S.): Expected age: *ca.* 12,000 BP.

KSU-1090. HE-21 Sapporo 1 **3370 ± 25**
Wood, 820 cm depth, from Sapporo City (43°4′27.6″N, 141°21′34.8″E, 14 m asl). Collected 1985 by H. Daimaru.

KSU-1091. HE-22 Sapporo 2 **5930 ± 60**
Wood from same site as KSU-1090.

KSU-1092. HE-23 Saporo 3 **9840 ± 60**
Wood, 140 cm depth, from same site as KSU-1090.

KSU-1105. HE-25 Shintokugawa **5910 ± 60**
Peat from Shintokugawa-cho, Kabato-gun (43°34′58.3″N, 141°44′3.7″E, 100 m asl). Collected 1985 by K. Yamamoto.

Comment (K.Y.): Expected age: 1500–12,000 BP.

KSU-1106. HE-26 Hokuryu **21,100 ± 600**
Peat from Hokuryu-cho, Uryu-gun (43°42′46.6″N, 141°52′39.1″E, 70 m asl). Collected 1985 by K. Yamamoto.

Comment (K.Y.): Expected age: 20,000–30,000 BP.

KSU-1107. HE-27 Kamoi **11,800 ± 800**
Ash under Toyozumi pumice fall, 295 cm depth, from Kamoi, Kiyosato-cho, Abashiri-gun (43°48′27.2″N, 144°33′37.6″E, 42 m asl). Collected 1985 by T. Sone.

Comment (T.S.): Expected age: *ca.* 12,000 BP. *Comment:* gained *ca.* 1 g carbon from 2 kg ash.

KSU-1108. HE-28 Izumikawa 1 **4120 ± 40**
Humus from between Masyudake-e and Masyudake-f ash fall, 125 cm depth, at Izumikawa, Bekkai-cho (43°24′37.2″N, 144°41′15.6″E, 140 m asl). Collected 1985 by T. Sone.

Comment (T.S.): dated to 4150 BP by hydrated layer of obsidian.

KSU-1109. HE-29 Izumikawa 2 **3100 ± 30**
Humus from between Komagatake-lava flow and Masyudake-e ash fall, 105 cm depth. Same site as KSU-1108.

Comment (T.S.): Expected age: 3000 BP.

KSU-1110. HE-30 Kitaoka **25,200 +1300/−1000**
Charcoal under Yoteizan. Ps.-1 pumice fall, 250 cm depth, from Kitaoka, Kyogoku (42°53′27.6″N, 140°51′42.6″E, 300 m asl). Collected 1985 by T. Sone.

Comment (T.S.): Expected age: 12,000–15,000 BP.

KSU-1242. HE-31 Uryunuma 1 **4050 ± 60**
Peat from Uryunuma marshland, 225–240 cm depth, Uryu-cho (43°41′21″N, 141°36′34″E). Collected 1985 by T. Miyagi, Tohoku Gakuin University.

KSU-1243. HE-32 Uryunuma 2 **6220 ± 50**
Peat, 65–70 cm depth, from same site as KSU-1242.

KSU-1244. HE-33 Uryunuma 3 **9580 ± 80**
Peat, 105–110 cm depth, from same site as KSU-1242.

KSU-1245. HE-34 Uryunuma 4 **9910 ± 70**
Peat, 112–118 cm depth, from same site as KSU-1242.

KSU-1246. HE-35 Horokayantou-numa 1 **760 ± 90**
Peat, 80 cm depth, from Horokayantou-numa, Taiki-cho, Hiroo-gun (42°31′42.9″N, 143°27′16.7″E, 8 m asl). Collected 1985 by K. Kanzawa.

KSU-1247. HE-36 Horokayantou-numa 2 **2560 ± 60**
Peat, 170 cm depth, from same site as KSU-1246.

KSU-1249. HE-38 Kami-nishishunbetsu **10,800 ± 230**
Charcoal underlying Masyu-1 pumice fall, 200 cm depth, from Kami-nishishunbetsu, Bekkai-cho, Notsuke-gun (43°25′24.5″N, 144°47′15.6″E). Collected 1985 by T. Sone.

Comment (T.S.): Expected age: 10,000–13,000 BP.

KSU-916. Uryunuma **9500 ± 140**
Peat, 310–325 cm depth, from Uryunuma marshland, Uryu-cho (43°41′21″N, 141°36′34″E). Collected and submitted 1984 by T. Miyagi.

Comment (T.M.): Result agrees with expected age based on pollen analysis.

Kitahara Series

Peat from Kitahara basin, Wassamu-cho (44°2′1″N, 142°22′2″E). Collected and submitted 1984 by T. Miyagi.

KSU-917. 375–390 cm depth	**6800 ± 80**
KSU-918. 600 cm depth	**31,500 +810/−740**

Comment (T.M.): Result agrees with expected age based on pollen analysis.

KSU-1051. Hassamu **60,300 +15,000/−4900**

Peat, 27.0–27.1 m depth, from Shinkotoni-cho, Kita-ku, Sapporo City (43°5′N, 141°18′E, 3.5 m asl). Collected and submitted 1985 by Y. Igarashi, Hokkaido University.

Comment (Y.I.): Expected age: 20,000–30,000 BP.

Nakahurano Series

Peat from Nakahurano-cho, Sorachi-gun (43°20′12″N, 142°25′30″E, 99.5 m above sea level). Collected and submitted by Y. Igarashi.

Comment (Y. I.): Expected period: from last Ice age to early Holocene.

KSU-1417. 5.0–5.2 m depth	**8120 ± 140**
KSU-1418. 7.05–7.08 m depth	**10,200 + 470**
KSU-1078. 8.05–8.10 m depth	**12,400 ± 120**
KSU-1419. 12.05–12.20 m depth	**28,500 +810/−740**
KSU-1079. 16.28–16.35 m depth	**32,400 +1400/−1200**
KSU-1080. 20.0–20.05 m depth	**47,100**

Karumai Series

Peat upper Akan ash fall-1, from Karumai, Atsuma-cho, Yufutsu-gun (42°39′47″N, 141°54′0″E). Collected 1985 by N. Wada, Geological Survey of Hokkaido, submitted 1985 by Y. Igarashi.

KSU-1081. Karumai-1	**26,800 +1900/−1500**
KSU-1082. Karumai-2	**38,800 +1200/−900**
KSU-1083. Hongo	**58,700**

Wood, upper Akan ash fall-2, Hongo, Atsuma-cho (42°44′0″N, 141°51′51″E). Collected 1985 by N. Wada, submitted by Y. Igarashi.

KSU-1084. Abira **56,100 +9000/−4100**

Peat in Shikotsu pumice fall-6 and Shikotsu pumice fall-7, from Nakaabira, Oiwake-cho, Yufutsu-gun (42°50′6″N, 141°50′0″E). Collected 1985 N. Wada and submitted 1985 Y. Igarashi.

Comment (Y.I.): Samples from upper Shikotu pumice fall-1 were dated to 32,200 +4700/−3100, Gak-519, and 32,200 ± 2000, Gak-714 (Kigoshi 1967: 48).

Nemuro Series

Peat from Habomai-cho, Nemuro City (43°21′20″N, 145°45′5″E, 30 m asl). Collected and submitted 1985 by Y. Igarashi.

KSU-1189. 68–73 cm depth	**2030 ± 40**
KSU-1190. 155–160 cm depth	**10,000 ± 140**

Fujino Series

Samples from Fujino, Minami-ku, Sapporo City (42°57.8′N, 141°19′E, 170 cm asl). Collected and submitted 1984 by J. Ishii, Tokai University.

KSU-1000. Fujino A **40,700 +1400/−1200**
Charcoal in Shikotsu pumice flow deposit.

KSU-1001. Fujino B **40,800 +1400/−1200**
Carbonized root in same layer as KSU-1000.

KSU-1002. Fujino C **36,500 +2000/−1600**
Charcoal in peat layer.

KSU-1003. Fujino D **39,500 +1400/−1200**
Peat from same horizon as KSU-1002.

Komoro Series

Radiocarbon dates of these samples show the history of activity in Asama Volcano and landslides in Nagano prefecture. The traces of an old large landslide were found by A. Nakagawa and K. Higuchi, 1986 on the landslides in Komoro district (Annuals of the Disaster Prevention Research Institute, Kyoto University, No. 29B-1, April 1986.) Samples were collected in these tracks. Collected and submitted 1984-1991 by K. Higuchi, Komoro High School. Some pieces of Early Jomon pottery were found under the layer (KSU-1260, KSU-1262, KSU-1264, KSU-1302, KSU-1303, KSU-1493, KSU-1496, KSU-1497, KSU-1498, KSU-1516) (T. Hayata 1992). This pottery is the oldest yet found in Japan (N. Kondou, H. Kobayashi, 1990).

KSU-839. Komoro 1 **52,100**
Wood (*Picea*) from Oshidashi, Komoro city, Nagano prefecture (36°19′40″N, 138°23′27″E).

KSU-840. Komoro 2 **56,900**
Charcoal (*Picea, Larix*) from Oshidashi, (36°19′48″N, 138°23′33″E).

KSU-852. Komoro 3 **49,300**
Wood from Oshidashi (36°19′54″N, 138°23′42″E).

KSU-853. Komoro 4 **49,300 +18,000/−5100**
Charcoal from same site as KSU-852.

KSU-854. Komoro 5 **54,300 +24,000/−5300**
Charcoal from same site as KSU-852.

KSU-874. Komoro 6 **49,100 +6300/−3500**
Wood from Kubo, Komoro city (36°18′36″N, 138°25′21″E).

KSU-875. Komoro 7 **55,400**
Charcoal from Hakeyama, Kitamimaki village, Kitasaku-gun, Nagano prefecture (36°19′54″N, 138°23′42″E).

KSU-877. Komoro 8 **51,900 +20,000/−5000**
Wood from Oshidashi (36°20′N, 138°23′E).

KSU-1121. Komoro 9 **44,600 +3000/−2200**
Wood from Okubo, Komoro city (36°19′31″N, 138°24′29″E).

KSU-1122. Komoro 10 **40,800 +970/−870**
Charcoal from Hakeyama (36°20′32″N, 138°20′35″E).

KSU-1123. Komoro 11 **54,300**
Wood from Goushi-gawara, Kitamimaki village (36°20′39″N, 138°19′39″E).

KSU-1124. Komoro 12 **46,100 +3700/−2500**
Charcoal from Okui, Komoro city (36°17′55″N, 138°25′28″E).

KSU-1125. Komoro 13 **54,000 +5900/−3400**
Charcoal from same place as KSU-1124.

KSU-1126. Komoro 14 **44,600 +1500/−1300**
Wood from Okubo (36°19′40″N, 138°23′58″E).

KSU-1260. Komoro 15 **13,600 ± 60**
Charcoal in first pumice flow deposit of Asama Volcano, from Namezu, Saku city, Nagano prefecture (36°14′21″N, 138°28′46″E).

Comment (K.H.): Asama first pumice flow was dated to 13,500 ± 500, JGS-16; 13,700 ± 400, JGS-36; 13,600 ± 400, JGS-37; 13,600 ± 400, JGS-40 (Togashi 1984: 207-208).

KSU-1261. Komoro 16 **38,300 +1000/−900**
Wood from Shionada, Asashina village, Kitasaku-gun (36°15′38″N, 138°25′02″E).

Comment (K.H.): Collected in presumed Tsukahara mud-flow deposit.

KSU-1262. Komoro 17 **13,700 ± 60**
Wood from Nenei, Saku City (36°15′30″N, 138°27′12″E).

KSU-1263. Komoro 18 **21,250 ± 140**
Wood in presumed Tsukahara mud-flow deposit, 5 m under KSU-1262.

KSU-1264. Komoro 19 **13,600 ± 70**
Wood from Mimitori, Komoro City (36°17′18″N, 138°25′38″E).

KSU-1297. Komoro 20 **54,200**
Charcoal from a cliff beside Chikuma River, Mimitori, Komoro City (36°16′44″N, 138°25′22″E).

KSU-1298. Komoro 21 **57,000**
Charcoal from near KSU-1297, Mimitori, Komoro City (36°16′44″N, 138°25′25″E).

KSU-1299. Komoro 22 **54,000**
Charcoal from Kubo, Komoro City (36°18′17″N, 138°25′14″E).

KSU-1300. Komoro 23 **52,800**
Charcoal from same place as KSU-1299.

KSU-1301. Komoro 24 **51,100 +8100/−4000**
Charcoal from same place as KSU-1299.

KSU-1302. Komoro 25 **13,700 ± 60**
Wood from same layer of KSU-1262, Komoro City (36°19′08″N, 138°25′16″E).

KSU-1303. Komoro 26 **14,000 ± 60**
Charcoal from Chikuma riverside, Mimitori, Komoro City (36°17′16″N, 138°25′01″E).

KSU-1328. Komoro 27 **57,300**
Charcoal from Chikuma riverside, Okui, Komoro City (36°17′46″N, 138°24′58″E).

KSU-1329. Komoro 28 **57,900**
Charcoal from same place as KSU-1328.

KSU-1379. Komoro 30 **53,000 +8700/–4100**
Charcoal from Kubo, Komoro City (36°18′34″N, 138°25′16″E).

KSU-1380. Komoro 31 **48,300 +3400/–2600**
Charcoal from Kubo, Komoro City (36°18′34″N, 138°25′34″E).

KSU-1381. Komoro 32 **60,000**
Charcoal from Kubo, Komoro City (36°18′02″N, 138°25′00″E).

KSU-1493. Komoro 33 **13,400 ± 70**
Charcoal from Amaike, Komoro City (36°21′16″N, 138°27′23″E).

KSU-1494. Komoro 34 **800 ± 20**
Wood on a mud-flow deposit, Ohata, Komoro City (36°19′42″N, 138°26′54″E). Datum shows same age as an eruption of Asama Volcano in AD 1108.

KSU-1495. Komoro 35 **23,700 ± 290**
Charcoal from same site as KSU-1263.

KSU-1496. Komoro 36 **13,500 ± 60**
Charcoal from same site as KSU-1303.

KSU-1497. Komoro 37 **13,300 ± 50**
Charcoal from 400 m depth, Mimitori, Komoro City (36°17′20″N, 138°25′19″E).

KSU-1498. Komoro 38 **13,600 ± 100**
Wood from Hishino, Komoro City (36°21′06″N, 138°26′17″E).

KSU-1499. Komoro 39 **860 ± 20**
Charcoal from Hebihori riverside, Komoro City (36°19′47″N, 138°26′34″E). Datum shows same age as an eruption of Asama Volcano in AD 1108.

KSU-1516. Komoro 40 **13,800 ± 60**
Charcoal from upper part of a bed rock, Yugawa riverside, Saku City (36°17′26″N, 138°30′47″E).

KSU-1517. Komoro 41 **700 ± 20**
Charcoal from Mitsuishi, Karuizawa village (36°20′38″N, 138°31′40″E). Datum shows same age as an eruption of Asama Volcano in AD 1281.

KSU-1518. Komoro 42 **700 ± 20**
Charcoal from 120 cm depth, 1225 m asl, Karuizawa village (36°20′38″N, 138°31′40″E). Datum shows same age as an eruption of Asama Volcano in AD 1281.

KSU-1519. Komoro 43 **22,500 ± 40**
Charcoal from Namezu riverside, Saku City (36°14′43″N, 138°27′50″E).

KSU-1583. Komoro 44 **11,400 ± 130**
Charcoal in the pumice flow 2 of Asama Volcano, 100 cm depth, Kohara, Komoro City (36°18′48″N, 138°25′32″E).

KSU-1584. Komoro 45 **11,800 ± 400**
Charcoal under a pumice flow, Kohara, Komoro City (36°18′51″N, 138°25′37″E).

KSU-1585. Komoro 46 **39,100 +14,000/−4800**
Wood in volcanic gravel layer in a deep well, 141 m depth, Amaike, Komoro City (36°21′30″N, 138°28′03″E).

KSU-1586. Komoro 47 **850 ± 40**
Charcoal from same site as KSU-1517.

KSU-1587. Komoro 48 **1010 ± 210**
Charcoal under the Oiwake pyroclastic flow, 14 m depth in a deep well, Karuizawa village (36°21′08″N, 138°32′01″E).

KSU-1697. Komoro 50 **41,800 +2000/−1600**
Charcoal from Saikouji riverside, Oshidashi, Komoro City (36°21′30″N, 138°28′03″E).

KSU-1735. Komoro 51 **1760 ± 80**
Charcoal from Karuizawa village (36°20′51″N, 138°31′45″E).

KSU-1736. Komoro 53 **1180 ± 12**
Charcoal in volcanic ash at the foot of Sekison Mountain, 200 cm depth, Karuizawa village (36°22′07″N, 138°31′46″E).

KSU-1762. Komoro 54 **780 ± 15**
Charcoal from Karuizawa village (36°29′40″N, 138°31′18″E).

KSU-1763. Komoro 55 **710 ± 20**
Charcoal from Karuizawa village (36°27′58″N, 138°30′53″E). Datum shows same age as an eruption of Asama Volcano in AD 1281.

KSU-1764. Komoro 56 **100 ± 10**
Charcoal from Karuizawa village (36°28′05″N, 138°34′22″E).

KSU-1765. Komoro 57 **13,190 ± 40**
Charcoal from Karuizawa village (36°21′03″N, 138°27′02″E).

KSU-2061. Komoro 58 **13,480 ± 50**
Charcoal from Shiozawa, Karuizawa village (36°19′09″N, 138°34′45″E).

KSU-2127. Komoro 59 **23,400 ± 300**
Charcoal under the Aira volcanic ash, Nakasato elementary school, Saku city (36°16′00″N, 138°27′02″E).

KSU-2128. Komoro 60 **0 ± 140**
Wood (Susuki) from 350 cm depth, Asamadai, Karuizawa village (36°20′49″N, 138° 33′26″E).

Comment (K.H.): It seems that there is a possibility of an eruption of Asama Volcano in AD 1800.

Myoko Series

Samples were collected at various places around the Myoko Volcano. Submitted 1982 by S. Nohda, Kyoto Sangyo University.

KSU-518. MK-797-3 Suginosawa 1 **4080 ± 40**

Wood in Suginosawa formation, 2.5 m depth, from Suginosawa, Myoko-kogen-cho, Niigata prefecture (36°51′N, 138°10′E). Collected 1980 by K. Hayatsu.

KSU-1103. MK-797-4 Suginosawa 2 **460 ± 80**

Charcoal in peat layer upper Suginosawa formation, 0.7 m depth, from Suginosawa (36°51′N, 138°10′E). Collected 1980 by K. Hayatsu.

KSU-519. MK-801-1 Taguchi **7880 ± 35**

Wood upper Taguchi formation, 5 m depth, from Shin-akakura, Myoko-kogen-cho (36°53′N, 138°12′E). Collected 1980 by K. Hayatsu.

KSU-1098. MK-802-3 Fukazawa **17,200 ± 70**

Charcoal in Fukazawa formation from same place as KSU-519. Collected 1980 by S. Nohda.

KSU-538. MK-802-1 Matsugamine **0 ± 50**

Wood in Matsugamine volcanic conglomerate, from Matsugamine, Nakagou village, Niigata prefecture (36°58′N, 138°14′E). Collected 1980 by S. Nohda.

KSU-1099. MK-802-10 Furuma 1 **39,100 +1200/−1000**

Peat between Kan-noki and Sekiyama scoria, 4 m depth, from Furuma Shinano-cho, Nagano prefecture (36°48′N, 138°12′E). Collected 1979 by K. Hayatsu.

KSU-1100. MK-802-14 Furuma 2 **29,700 ± 600**

Peat above Ohira scoria, 6 m depth, from Furuma (36°47′N, 138°12′E). Collected 1979 by K. Hayatsu.

KSU-1101. MK-802-17 Kannoki **23,800 +2700/−2000**

Sand and charcoal in Mutsuki volcanic conglomerate, from Kan-noki, Shinano-cho (36°49′N, 138°12′E). Collected 1980 by S. Nohda.

KSU-1102. MK-601-2 Sekiyama **4110 ± 40**

Peat in Otagirigawa formation, 1 m depth, from Sekiyama, Myoko village, Niigata prefecture (36°56′N, 138°12′E). Collected 1972 by K. Hayatsu.

KSU-536. YK-50-1 Sasakura **890 ± 30**

Wood from bottom of Hayakawa formation, 2 m depth, from Sasakura-onsen, Itoigawa city, Niigata prefecture (36°59′N, 138°1′E). Collected 1971 by K. Hayatsu.

Okamura Fault Series

Samples were collected by the trench excavation survey across the Okamura fault belonging to the Median Tectonic Line active fault system of Southwest Japan. Samples from Ioka, Saijo city, Ehime prefecture (33°55′N, 133°13′E). Collected 1983 and submitted 1984 by M. Andou, Kyoto University, and A. Okada, Aichi Prefectural University.

KSU-791. NW 30a **2050 ± 60**

Peat. x (level distance) = 8.0–8.5 m and z = 2 m in northwest wall.

KSU-789. NW 30b **2030 ± 50**

Peat from under part of peat layer, x = 8.5 m and z = 2 m.

KSU-786. NW 31 **11,100 ± 260**

Peat from peat and fine sand layer, x = 8.5 m and z = 4.6 m.

KSU-790. NW 32 **11,200 ± 200**
Peat from upper part of thick peaty silt-sand layer, x = 6.5 m and z = 5.3 m.

KSU-787. NW 33 **12,000 ± 80**
Peat from under part of thick peaty silt layer, x = 6.5 m and z = 5.3 m.

KSU-782. NW 34 **13,100 ± 120**
Soil from peaty sand layer, x = 6.5 m and z = 5.7 m.

KSU-784. NW 35 **17,800 ± 370**
Soil from under peaty silt layer, x = 6.5 m, and z = 6.7 m.

KSU-785. SW 39 **3870 ± 90**
Peat, x = 9.2 m and z = 3.2–3.3 m in southwest wall.

KSU-788. SW 40 **2900 ± 60**
Wood and soil from conglomerate layer, x = 12.2 m and z = 3.9 m.

KSU-783. SW 42 **13,200 ± 380**
Soil from fine sand layer, x = 10.2 m and z = 6.5–6.6 m.

KSU-793. SW 43 **9990 ± 80**
Soil from upper thick beach silt layer, x = 10.2 m and z = 7.0–7.05 m.

KSU-792. SW 44 **10,300 ± 120**
Soil from under thick beach silt layer, x = 10.2 m and z = 7.8 m.

Kochi Bore Samples

Peat from Kochi plain, Itachino, Kochi prefecture (33°33′30″N, 133°37′50″E). Collected and submitted by M. Ando.

KSU-1067. 105–110 cm depth	**1740 ± 70**
KSU-1068. 240–245 cm depth	**4850 ± 90**
KSU-1069. 460–465 cm depth	**8040 ± 60**
KSU-1070. 670–675 cm depth	**29,100 ± 1000**
KSU-1071. 910–915 cm depth	**30,200 +1500/−1200**
KSU-1072. 1140–1145 cm depth	**46,500 +38,000/−5500**
KSU-1073. 1795–1800 cm depth	**26,600 +1300/−1100**

General comment: KSU-1073 was the same layer KSU-1070 and KSU-1071. KSU-1073 fell by a fault.

Hamana Lake Series

Peat samples were collected by boring, at the shore of Hamana Lake, Shizuoka prefecture (34°44′N, 137°38′E). Collected and submitted 1984 by H. Wada, Shizuoka University.

KSU-845. H7 240–245 cm depth	**5390 ± 420**
KSU-846. H7 245–250 cm depth	**7480 ± 900**
KSU-847. H9 230–235 cm depth	**4850 ± 370**
KSU-848. H9 235–240 cm depth	**5290 ± 640**
KSU-849. H10 250–255 cm depth	**4490 ± 340**
KSU-850. H10 255–260 cm depth	**6700 ± 1400**

Jindai-sugi Series

Samples in Kawagodaira pumice, from Ikadaba, Nakaizu-cho, Shizuoka prefecture (34°54′N, 138°57′E). Collected 1982 by E. Okawa, submitted 1984 by H. Wada.

Comment (H.W.): Kawagodaira pumice was believed to have erupted *ca.* 3000 BP.

KSU-952. Ikadaba 0-5 **2820 ± 50**
Wood (*Cryptmeria japonica*). 5 tree rings from outer side.

KSU-953. Ikadaba S **2860 ± 50**
Bark of same wood as KSU-952.

Kagiana Series

Wood samples were embedded in sandy and clayish sediments, from Kagiana, Shizuoka City (35°2′N, 138°15′E). Collected and submitted 1985 by H. Wada.

KSU-1032. KG-1 **2490 ± 25**
Bark and 20 tree rings from outer side.

KSU-1033. KG-2 **2500 ± 30**
15 tree rings from outer side.

KSU-1034. KG-3a **2670 ± 30**
Bark of tree.

KSU-1035. KG-3b **2430 ± 50**
15 tree rings from outer side.

KSU-954. Odanoike **4740 ± 230**
Peat, 290–300 cm depth, from Odanoike pond, Kuju-cho, Kusu-gun, Ohita prefecture (33°12′N, 131°18′E). Collected and submitted 1984 by M. Takeoka, Kyoto Prefectural University.

KSU-955. Nonbara **4200 ± 170**
Peat, 400–410 cm depth, from Ohike pond, Nonbara, Takeno-gun, Kyoto prefecture (35°45′N, 135°8′E). Collected and submitted 1984 by M. Takeoka.

KSU-956. Chojidani **890 ± 70**
Peat, 120–130. cm depth, from Chojidani valey, Miyama-cho, Kitakuwata-gun, Kyoto prefecture (35°17′N, 135°46′E). Collected and submitted 1984 by M. Takeoka.

KSU-957. Sugiyaike **4120 ± 120**
Peat, 140–150 cm depth, from Sugiyaike pond, Ohtsu city, Shiga prefecture (35°11′N, 135°53′E). Collected and submitted 1984 by M. Takeoka.

KSU-958. Kojorogaike **4600 ± 110**
Peat, 200–210 cm depth, from Kojorogaike pond, Katsuragawa, Otsu City, Shiga prefecture (35°14′N, 135°53′E). Collected and submitted 1984 by M. Takeoka.

KSU-959. Meiji **60 ± 90**
Peat, 240–250 cm depth, from Meiji, Miyama, Tango-cho, Takeno-gun, Kyoto prefecture (35°44′N, 135°10′E). Collected and submitted 1984 by M. Takeoka.

KSU-1041. Habikino **12,770 ± 130**

Peat, 120–130 cm depth, from Konda, Habikino City, Osaka prefecture (34°33′N, 135°15′E). Collected and submitted 1985 by M. Takeoka.

KSU-1042. Kashiwara **2330 ± 30**

Peat, 80–85 cm depth, from Kashiwara, Toyono-gun, Osaka prefecture (34°58′N, 135°25′E). Collected and submitted 1985 by M. Takeoka.

KSU-985. Kamifukada **3340 ± 40**

Wood, 60–90 cm depth, from Kamifukada, Sanda City, Hyogo prefecture (35°53′N, 135°12′E). Collected and submitted 1984 by K. Mino, Ritsumeikan University.

Comment (K.M.): Collected in Yamasaki fault. Dated speciment was presumed to be buried by earthquake of AD 868.

KSU-1149. Natadera **54,600 +12,000/−4600**

Charcoal in Natadera fault, Komatsu City, Ishikawa prefecture (36°18′N, 136°25′E). Collected and submitted 1985 by K. Mino.

Yachidaira Series

Peat from Yachidaira, Onoda-cho, Kami-gun, Miyagi prefecture (38°29′N, 140°37′30″E). Collected 1984 and submitted 1985 by K. Hibino, Miyagi Agricultural College.

KSU-1074. Yachidaira 1 **830 ± 40**

Peat, 120–130 cm depth.

KSU-1075. Yachidaira 2 **640 ± 30**

Peat, 85–100 cm depth.

KSU-1085. Miyatoko-Ohyachi **7000 ± 50**

Peat, 275–300 cm depth, from Miyatoku-Oyachi, Nagano, Minami-aizu-gun, Fukushima prefecture (37°15′N, 139°34′E). Collected 1984 and submitted 1985 by K. Hibino.

Comment (K.H.): This ^{14}C date age almost agrees with a palynological estimate.

KSU-1086. Amou marshland **9680 ± 70**

Peat, 275–295 cm depth, from Amou, Kawai, Kichijo-gun, Gifu prefecture (36°15′N, 136°58′E). Collected 1984 and submitted 1985 by K. Hibino.

Yadegawa Series

Samples from Yadegawa, Nobeyama, Minamisaku-gun, Nagano-prefecture (36°51′N, 138°29′E). Collected by Y. Yasuda, Hiroshima University. Submitted 1981 by M. Tozawa, Meiji University.

Comment (Y.Y.): KSU-1160 and KSU-443 were presumably from the last Ice Age (*ca.* 20,000 to 11,000 BP). KSU-1161 and KSU-1162 were expected to be of Jomon Age.

KSU-1163. Yadegawa 1 **22,500 ± 160**

Peat.

KSU-443. Yadegawa 3 **29,750 ± 600**

Wood.

KSU-1161. Yadegawa 4 **2940 ± 20**

Peat.

KSU-1162. Yadegawa 6 **4730 ± 25**
Peat.

KSU-649. Hananoego **6100 ± 25**
Peat under Akahoya volcanic ash, Hananoego, Yaku Island, Kumage-gun, Kagoshima prefecture (30°18′30″N, 130°30′45″E). Collected and submitted 1983 by Y. Yasuda. *Comment* (Y.Y.): Expected age: *ca.* 7000 BP.

CHINA

KSU-1163. Saiko 200–250 cm depth **1540 ± 60**
Peat from Lake Sha, Hong-chou (30°15′N, 120°10′E). Collected 1984 and submitted 1985 by Y. Yasuda.

KSU-1166. Mongol 140–160 cm depth **3340 ± 140**
Peat from Shioziki, Inner Mongolia (40°25′N, 111°10′E). Collected 1984 and submitted 1985 by Y. Yasuda.

GREECE

Hotousa Moor Series

Peat from Peloponissos (37°48′N, 22°30′W, 900 m asl). Collected 1984 and submitted 1985 by Y. Yasuda.

KSU-1111. 100–200 cm depth **2280 ± 40**
KSU-1112. 180–200 cm depth **3700 ± 70**
KSU-1113. 260–280 cm depth **5180 ± 70**

Korone Moor Series

Peat from Korone moor, northwest Greece (39°20′N, 20°11′W, 10 m asl). Collected 1984 and submitted 1985 by Y. Yasuda.

KSU-1252. 150–160 cm depth **2740 ± 40**
KSU-1114. 380–390 cm depth **4500 ± 40**
KSU-1253. 1400–1420 cm depth **3940 ± 80**
KSU-1115. 1610–1630 cm depth **6360 ± 40**

Katouna Series

Peat from Katouna moor, northwest Greece (38°50′N, 21°5′W). Collected 1984 and submitted 1985 by Y. Yasuda.

KSU-1170. 170–200 cm depth **710 ± 50**
KSU-1171. 370–400 cm depth **1770 ± 50**
KSU-1172. 910–940 cm depth **3970 ± 80**

TURKEY

Civiril Series

Peat from Civiril moor, western Anatolia (38°20′N, 29°40′W). Collected 1984 and submitted 1985 by Y. Yasuda.

KSU-1164. 100–175 cm depth **2700 ± 70**
KSU-1165. 305–330 cm depth **4140 ± 80**

Abant Gol Series

Peat from the lake Abant, northern Turkey (40°50′N, 31°30′W). Collected 1984 and submitted 1985 by Y. Yasuda.

KSU-1167. 100–120 cm depth **350 ± 80**
KSU-1168. 320–340 cm depth **1410 ± 180**
KSU-1169. 620–650 cm depth **2400 ± 70**

NEPAL

KSU-648. Kathmandu basin **9950 ± 70**
Wood from Kathmandu (27°40′N, 85°20′E, 1400 m asl). Collected 1982 and submitted 1983 by Y. Yasuda.

Comment (Y.Y.): Wood was embedded in lake deposit. Expected time range: Last Ice Age.

KSU-657. Lake Rara **7720 ± 200**
Peat, 480–450 cm depth, from Lake Rara, western Nepal (29°27′N, 82°0′E, 3000 m asl). Collected 1982 and submitted 1983 by Y. Yasuda.

Comment (Y.Y.): deposit of 7 m depth was dated to *ca.* 10,000 BP by pollen analysis. Therefore this deposit was presumed *ca.* 7000 BP.

Partical Series

Samples from mud-flow deposits in Indrawati River, northeast of Kathmandu basin (27°44′N, 85°40′E). Collected 1985 by M. Yoshida, Trivhuvan University, and submitted 1985 by Y. Igarashi, Hokkaido University.

Comment (M.Y.): Expected period: Last Ice Age.

KSU-1087. 84Y 18-1 **55,600 +29,000/−5400**
Peat.

KSU-1088. 84Y 18-2 **56,200**
Wood.

KSU-1120. Thimi-1 **45,300 +6000/−3400**
Wood in Thimi Formation, from Kathmandu basin (27°44′N, 85°23′30″E). Collected 1985 by M. Yoshida, submitted 1985 by Y. Igarashi.

INDONESIA

KSU-502. Krakatau Volcano **190 ± 25**
Wood in the outcrop of ash flow at Danan Islands, west Java (6°20′S, 105°30′E). Collected and submitted 1982 by T. Yokohama, Doshisha University.

Comment (T.Y.): Presumed to be related to eruption of Krakatau Volcano in AD 1883.

KSU-768. Ug. Kulon **4810 ± 40**
Shell (*Tridacnidae*) in coral reef, 20 m above sea level, from Ug. Kulom, Java Island (6°44N, 105°13′E). Collected 1983 by P. Hebanssa, Bandung Giological Laboratory, and submitted 1984 by J. Nishida, Ohtani University.

ARCHAEOLOGICAL SAMPLES

JAPAN

Hokkaido Mamachi Site Series

Charcoal from Mamachi, Chitose City (42°48′58″N, 141°38′54″E). Collected 1982 by H. Taguchi and submitted by R. Asai, Hokkaido Archaeological Research Center.

Comment (H.T.): Associated with Satsumon pottery.

KSU-560. Mamachi 1 **1930 ± 40**
Charcoal from B point, on floor of Dwelling Pit H-1 of Satsumon period.

KSU-561. Mamachi 2 **1210 ± 40**
Charcoal from fireplace of same pit as KSU-560.

Horikapp Site Series

Charcoal from Horikapp, Furuu-gun (43°0′N, 140°30′E). Collected 1982 by N. Kimura, submitted by R. Asai.

Comment (N.K.): Samples found in layer, included relics of later Middle to early Late Jomon Age.

KSU-574. Horikapp 1 **4020 ± 50**
Charcoal under layer 4, F-8.

KSU-588. Horikapp 2 **2330 ± 170**
Charcoal upper layer 2, D-9-30, P-8.

KSU-589. Horikapp 3 **2380 ± 500**
Charcoal from fireplace 2, E point.

KSU-590. Horikapp 4 **3800 ± 120**
Charcoal from F-12-87, fireplace 14.

KSU-591. Horikapp 5 **2550 ± 450**
Charcoal from H-10, upper black sand layer.

KSU-967. Bibi 2 site **2430 ± 90**
Charcoal on floor of Dwelling Pit H-1, upper Tarumae-c scoria. Collected 1984 by B. Aoyanagi and submitted 1984 by R. Nakamura, Hokkaido Archaeological Research Center. Charcoal from Bibi, Chitose City (42°46′N, 141°4′E).

Comment (B.A.) Expected age: later Jomon to Zoku-Jomon Age.

Bibi 4 Site Series

This site is near place of Bibi 2 site. Submitted 1983 to 1985 by R. Nakamura.

KSU-676. Bibi 4-1 **2370 ± 30**
Charcoal in buried soil of grave, excavated from upper Tarumae-c volcanic ash layer, P-59. Collected 1983 by K. Nonaka.

Comment (K.N.): Associated with Daido-A pottery.

KSU-677. Bibi 4-2 **3420 ± 30**
Charcoal on floor of Dwelling Pit H-1 in peat layer between Tarumae-d and Tarumae-c. Collected 1983 by K. Satou.

Comment (K.S.): Associated with Teine-shiki pottery of middle Late Jomon Age.

KSU-747. Bibi 4-3 **2640 ± 400**
Human bone in grave X-208. Collected 1983 by K. Nonaka.

Comment (K.N.): Grave was presumed later Jomon Age.

KSU-969. Bibi 4-4 **3240 ± 130**
Charcoal from Pit-149, on grave. Collected 1984 by K. Endo.

Comment (K.E.): Expected age: middle Late Jomon Age.

KSU-970. Bibi 4-5 **3460 ± 40**
Charcoal from Pit-123. Collected 1984 by H. Mori.

Comment (H.M.): Presumed same age as KSU-969.

KSU-1194. Bibi 4-6 **3180 ± 80**
Charcoal from Pit-904 under Tarumae-c. Collected 1985 by K. Nonaka.

Yunosato 2 Site Series

Samples were collected 1983 by T. Takahashi, and submitted 1983 by R. Nakamura at Yunosato, Shiriuchi-cho, Kamiiso-gun (41°35′N, 140°20′E).

KSU-748. Yunosato 2-1 **4530 ± 120**
Charcoal from Y2-H-1, Dwelling Pit-1, later Early Jomon Age.

KSU-749. Yunosato 2-2 **4380 ± 90**
Charcoal from Y2-H-2, Dwelling Pit-2, later Early Jomon Age.

Yunosato 5 Site Series

Samples were collected 1983 by H. Taguchi and submitted 1983 by R. Nakamura.

KSU-678. Yunosato 5-1 **3020 ± 80**
Charcoal in Layer 3 on Stone Circle of early Late Jomon Age.

KSU-679. Yunosato 5-2 **3590 ± 70**
Charcoal in covered soil of Stone Circle.

KSU-680. Yunosato 5-3 **3970 ± 90**
Charcoal in pit, presumed same age as Stone Circle.

Yunosato 6 Site Series

Samples were collected 1983 by Y. Nakata and submitted 1983 by R. Nakamura.

KSU-681. Yunosato 6-1 **2510 ± 180**
Charcoal from Y-6, G-64-b, Layer 3, contained Final Jomon Relics.

KSU-682. Yunosato 6-2 **2780 ± 180**
Charcoal from Y-6, I-63-d, Pit 5, presumed grave of Final Jomon Age.

KSU-683. Yunosato 6-3 **3380 ± 640**
Charcoal from Y-6, E-65-a, S-1, Layer 4, fireplace of Late Jomon Age.

Kusunoki Site Series

Charcoal from Kusunoki, Bifune-cho, Nakagawa-gun (44°28'N, 142°15'E). Collected 1983 by A. Oniyanagi and submitted 1983 by R. Nakamura.

Comment (A.O.): Expected age: Satsumon Age.

KSU-684. Kusunoki 1 **920 ± 70**
Charcoal in kitchen range of Dwelling Pit H-6.

KSU-685. Kusunoki 2 **760 ± 50**
Charcoal in kitchen range of Dwelling Pit H-7.

KSU-686. Kusunoki 3 **820 ± 60**
Charcoal on floor of Dwelling Pit H-37.

Pirika 1 Site Series

Charcoal from Pirika, Imakane-cho, Setana-gun (42°28'N, 140°13'E). Collected 1983 by T. Naganuma and submitted 1983 by R. Nakamura.

KSU-687. Pirika 1-1 **19,800 ± 380**
Charcoal from M-44-c, bottom of Layer 3.

Comment (T.N.): Expected age was comparable to microlith of ran-etsu type of later Early Stone Age.

KSU-688. Pirika 1-2 **17,500 ± 200**
Charcoal from L-52-d, middle of Layer 3.

Comment (T.N.): Expected age was comparable to Yuzetsu point of later Early Stone Age.

KSU-689. Pirika 1-3 **20,900 ± 260**
Charcoal from M-53-b, bottom of Layer 3.

Comment (T.N.): Expected age was comparable to grave of Araya type and microlith of Tougeshita type of later Early Stone Age.

KSU-750. Nishinopporo 12-17 site **1070 ± 20**
Charcoal from Pit 88, Nishinopporo, Ebetsu city (43°4'N, 141°32'E). Collected 1983 by T. Kasai and submitted by R. Nakamura.

Comment (T.K.): Expected period: late Zoku-Jomon Age.

Nakahama E Site Series

Charcoal from Nakahama, Shirikishinai-cho, Kameda-gun (41°44'N, 141°4'E). Collected 1984 by H. Taguchi and submitted by R. Nakamura.

Comment (H.T.): Expected age: Initial to Late Jomon Age.

KSU-961. Nakahama E-1 **4390 ± 40**
Charcoal from P-1.

KSU-962. Nakahama E-2 **1920 ± 190**
Charcoal from TP-5.

KSU-963. Nakahama E-3 **6820 ± 180**
Charcoal on floor of Dwelling Pit H-2.

Chitose 5 Site Series

Charcoal from Chitose-cho, Noboribetsu City (42°24'N, 141°11'E). Collected 1984 by S. Nishida and submitted by R. Nakamura.

Comment (S.N.): Expected age: Middle to Late Jomon Age.

KSU-964. Chitose 5-1 **4210 ± 60**
Charcoal on floor of Dwelling Pit, H-23-B.

KSU-965. Chitose 5-2 **4110 ± 70**
Charcoal from bottom of Layer 3, E-100-d.

KSU-966. Chitose 5-3 **4200 ± 50**
Charcoal from Layer 2, E-1-c.

Osaka Prefecture Sadoh Site Series

Wood from Sadoh-cho, Yao city (34°37'56"N, 135°35'32"E). Collected and submitted 1982, 1983 by Y. Nishiguchi, Osaka Archaeological Research Center.

KSU-521. Sadoh 1 **1390 ± 20**
Wood.

KSU-526. Sadoh 2 **1500 ± 20**
Wood.

KSU-575. Sadoh 3 **1360 ± 20**
Wooden stake from bank of Nagase River.

KSU-577. Sadoh 4 **1410 ± 20**
Wooden stake from bank of Nagase River.

KSU-716. Sadoh 5 **250 ± 40**
Wooden stake from Tr. F.

Yamaga Site Series

Sample from Yamaga-cho, Yao City (34°38'36"N, 135°35'58"E). Collected and submitted 1982 by Y. Nishiguchi, Osaka Archaeological Research Center.

KSU-524. Yamaga 1 **2950 ± 20**
Wood from rough sand layer, Tr C-6, 0 m , associated with Final Jomon pottery.

KSU-529. Yamaga 2 **3750 ± 20**
Wood from gray-brown gravel layer, Tr B-2, −1.5 m below sea level, associated with Middle Jomon pottery.

KSU-527. Yamaga 3 **4130 ± 20**
Wood from dark gray sand layer, Tr B-2, −3 m below sea level. Early Jomon Age.

KSU-533. Yamaga 4 **4480 ± 20**
Shell from same layer as KSU-527.

KSU-528. Yamaga 5 **4490 ± 20**
Wood from dark grayish-green clay layer, Tr B-2, –4 m below sea level. Early Jomon Age.

KSU-534. Yamaga 6 **4470 ± 30**
Shell from same locality as KSU-528.

KSU-605. Yamaga 7 **2520 ± 30**
Peat from second black clay layer, Tr B-2, 0 m above sea level. Final Jomon Age.

KSU-604. Yamaga 8 **3140 ± 40**
Peat from second black clay layer, Tr B-2, –0.6 m below sea level. Late Jomon Age.

Nishiurabashi Site Series

Wood from Hikisho, Sakai City (34°31′31″N, 135°28′24″E). Collected 1983 by S. Anzato, T. Hashimoto, K. Ohno and submitted by Y. Nakanishi, Osaka Archaeological Research Center.

KSU-704 Nishiurabashi 1 **4270 ± 25**
Wood from base of bluish gray sand layer, Sec B.

Comment (Y.N.): Expected period: later Middle Jomon Age.

KSU-705 Nishiurabashi 2 **4360 ± 25**
Wood from same locality as KSU-704.

KSU-706 Nishiurabashi 3 **4450 ± 40**
Wood from base of bluish gray sand layer, Section A.

Comment (Y.N.): Expected period: later Middle Jomon Age.

KSU-707 Nishiurabashi 4 **3640 ± 25**
Wood in 67b line.

Comment (Y.N.): Expected period: early Late Jomon Age.

KSU-708 Nishiurabashi 5 **3970 ± 30**
Wood in Section A.

Comment (Y.N.): Expected period: early Late Jomon Age.

KSU-709 Nishiurabashi 6 **1630 ± 20**
Wood from a river of Jomon Age, Section D.

Comment (Y.N.): Expected period: middle Final Jomon Age.

KSU-710. Nishiurabashi 7 **2590 ± 20**
Wood from a river of Jomon Age, Section C.

Comment (Y.N.): Expected period: middle Final Jomon Age.

KSU-711. Nishiurabashi 8 **2400 ± 20**
Wood from a river of Yayoi Age, Section C.

Comment (Y.N.): Expected period: Early Middle Yayoi Age.

KSU-712. Nishiurabashi 9 **2160 ± 25**
Wood in Section C and Section D.

Comment (Y.N.): Unknown Period.

KSU-713. Nishiurabashi 10 **2620 ± 20**
Wood in Section A and Section B.

Comment (Y.N.): Unknown Period.

Misono Site Series

Samples from Misono, Yao City (34°38′10″N, 135°35′45″E). Collected 1983 by S. Anzato, T. Hashimoto, K. Ohno and submitted by Y. Nakanishi, Osaka Archaeological Research Center.

KSU-714. Misono 1 **2690 ± 30**
Charcoal and soil from Section 7B.

Comment (Y.N.): Expected period: later Early to early Middle Yayoi Age.

KSU-715. Misono 2 **2120 ± 50**
Natural wood.

Comment (Y.N.): Expected period: early Kofun Age.

Jogoji Site Series

Samples from Jogoji, Kumatori-cho, Sennan-gun (34°23′N, 135°22′E). Collected and submitted 1984 by S. Anzato and K. Ohno, Osaka Archaeological Research Center.

KSU-995. Jogoji 1 **940 ± 50**
Soil and charcoal in Point 321, Section B-8.

KSU-996. Jogoji 2 **880 ± 40**
Soil and charcoal in Point 355, Section B-4.

KSU-997. Jogoji 3 **850 ± 50**
Soil and charcoal in Point 355, Section B-4. Comment (Y.N.): Expected age: AD 1300 to AD 1400.

Kyuhoji Site Series

Samples from Nishi-Kyuhoji, Yao City (34°37′N, 135°35′E). Collected and submitted 1983 by M. Imamura, 1985 by K. Ichinose, Osaka Archaeological Research Center.

KSU-1004. Kyuhoji 1 **1760 ± 30**
Peat from Layer 4a, SX303, Section H3.

Comment (K.I.): Expected period: Early Kofun Age.

KSU-1005. Kyuhoji 2 **1700 ± 40**
Peat from same locality as KSU-1004.

KSU-1006. Kyuhoji 3 **1680 ± 30**
Peat from same locality as KSU-1004.

KSU-1007. Kyuhoji 4 **2330 ± 30**
Wood, Shigarami 205, w-167.

Comment (K.I.): Expected period: early Middle Yayoi Age.

KSU-1008. Kyuhoji 5 **2550 ± 50**
Wood, Shigarami 103, w-1.

Comment (K.I.): Expected period: middle Middle Yayoi Age.

KSU-1009. Kyuhoji 6 **2140 ± 25**
Wood, Shigarami 402, w-39. Comment (K.I.): Expected period: later Middle Yayoi Age.

KSU-1061. Kyuhoji 7 **5030 ± 60**
Soil. Associated with Jomon pottery.

Comment (M.I.): Expected age: *ca.* 3000 BP.

KSU-1062. Kyuhoji 8 **4050 ± 30**
Soil. Same as KSU-1061.

Joyama Site Series

Wood from Joyama, Nagayoshi-Nagahara-cho, Hirano-ku, Osaka City (34°36′N, 135°34′E). Relics of Incipient Jomon (*ca.* 10,000 BP) were found *ca.* 2.5 m, and samples were found *ca.* 5 m, below present surface. Collected 1983 and submitted 1985 by K. Abe, Osaka Archaeological Research Center.

Comment (K.A.): Expected age: *ca.* 30,000 BP.

KSU-1063. Joyama 1 **43,800**
Wood.

KSU-1064. Joyama 2 **43,300**
Wood.

KSU-1065. Joyama 3 **40,000**
Wood.

KSU-1066. Joyama 4 **39,400 +7300/−3700**
Wood.

Kyoto Prefecture Kitakanage Site Series

Samples from Kitakanage, Ohi-cho, Kameoka City, Kyoto prefecture (35°01′48″N, 130°32′38″E). Collected 1984 and submitted by K. Tsutsumi, Kyoto Prefecture Archaeological Research Center.

KSU-797. Kitakanage 1 **1715 ± 15**
Wooden stake in SD01.

KSU-798. Kitakanage 2 **2495 ± 15**
Wooden plate in SD01.

KSU-799. Kitakanage 3 **2040 ± 15**
Wooden plate in SD01.

KSU-800. Kitakanage 4 **1930 ± 70**
Wooden stake in SD01.

KSU-801. Kitakanage 5 **1715 ± 15**
Natural wood in SD01.

KSU-802. Kitakanage 6 **1820 ± 15**
Charcoal from dwelling pit, SB03.

Comment (K.T.): expected period: KSI-797 to KSU-801, early Kofun Age, KSU-802, Late Yayoi Age.

Hyogo Prefecture Iwaya-kanre Site Series

Samples from Iwaya-Kanre, Itami City, Hyogo prefecture (34°46′ 33.6″N, 135°26′36″E). Collected and submitted 1984 by T. Asaoka, Board of Education, Itami city.

KSU-841. Iwaya-Kanre 1 **3170 ± 25**
Wood in Section 3.

KSU-842. Iwaya-Kanre 2 **3950 ± 260**
Nuts in Section 3.

KSU-843. Iwaya-Kanre 3 **3190 ± 60**
Wood in Section 4.

KSU-951. Arioka Castle **3550 ± 150**
Charcoal from Arioka Castle, Itami City (34°46′28″N, 135°26′12″E). Collected and submitted 1984 by T. Asaoka.

Comment (T.A.): Associated with Upper Kitashirakawa-shiki pottery of middle Late Jomon Age. Result as expected.

KSU-1044. Aramaki 25,800 ± 180
Peat from Aramaki, Itami City (34°48′33″N, 135°23′9″E). Collected 1984 and submitted 1985 by T. Asaoka.

Comment (T.A.): Date indicates the formative period of Itami plateau. Result as expected.

Morimoto-tsuruta Site Series

Sample from Morimoto, Itami City (34°46′36″N, 135°26′25″E). Collected and submitted 1985 by T. Asaoka.

KSU-1045. Morimoto 1 **3090 ± 20**
Peat from bluish-gray clay layer, Point 3 180 cm depth, Final Jomon Age.

KSU-1046. Morimoto 2 **3940 ± 120**
Peat from same locality as KSU-1045.

KSU-1047. Morimoto 3 **3700 ± 20**
Wood from black-gray peat layer, Point 3, 270 cm depth, before Final Jomon.

KSU-1048. Morimoto 4 **2640 ± 20**
Peat from black-gray peat layer, Point 2, 180 cm depth.

KSU-1128. Morimoto 5 **2730 ± 25**
Wood from grayish-yellow peat layer, Point 4, 230 cm depth, Jomon Age.

KSU-1129. Morimoto 6 **2490 ± 40**
Peat from gray clay sand layer, Point 10, 160 cm depth, Final Jomon.

KSU-1130. Morimoto 7 **3090 ± 25**
Wood from gray sand layer, Point 14, 330 cm depth, Jomon Age.

KSU-1131. Morimoto 8 **2740 ± 25**
Wood from gray clay layer, Point 17.

KSU-1132. Morimoto 9 **2330 ± 25**
Wood from grayish-blue sand layer, Point 30-1, after Final Jomon.

KSU-1133. Morimoto 10 **2450 ± 25**
Peat from black-brown clay layer, Point 30-2, after Final Jomon.

KSU-1134. Morimoto 11 **3630 ± 25**
Wood from brown peat layer, Point 30-3, Final Jomon.

Comment (T.A.): Results of KSU-1045, 1046, 1134 seemed to be older, other results as expected.

Kuchisakai Site Series

Peat from Kuchisakai, Itami city (34°46′20″N, 135°26′33″E). Submitted 1985 by T. Asaoka.

KSU-1049. Kuchisakai 1 **2570 ± 40**
Peat from gray clay layer, Point 7, Early Yayoi Age. Collected 1985 by T. Asaoka.

KSU-1050. Kuchisakai 2 **2530 ± 20**
Peat from grayish-blue sand layer, Point 16, Final Jomon Age.

KSU-1127. Kuchisakai 3 **2690 ± 35**
Peat from black sand layer, AM 15, Layer 15, Final Jomon Age. Collected 1985 by T. Izumi, Nara University.

Comment (T.A.): Result of KSU-1049 is older. Other results as expected.

Taiyohno-oka Site Series

Charcoal from Taiyohno-oka, Hachioji city, Tokyo prefecture (139°20′N, 36°41′E). Collected and submitted 1984 by M. Koshida, Souka University.

KSU-919. Taiyohno-oka 1 **1210 ± 30**
Charcoal from kiln N-25. Heian era.

KSU-920. Taiyohno-oka 2 **1420 ± 200**
Charcoal from kiln 1. Heian era.

KSU-921. Taiyohno-oka 3 **1160 ± 50**
Charcoal, same locality as KSU-920.

KSU-922. Taiyohno-oka 4 **860 ± 120**
Charcoal from O-18. Jomon Age.

KSU-923. Taiyohno-oka 5 **1390 ± 80**
Charcoal from Dwelling Pit P-22. Late Kofun Age.

KSU-924. Taiyohno-oka 6 **1100 ± 110**
Charcoal on floor of Dwelling Pit U-27. Heian era.

KSU-925. Taiyohno-oka 7 **1630 ± 30**
Charcoal from Dwelling Pit S-23. Late Kofun Age.

KSU-926. Taiyohno-oka 8 **1610 ± 50**
Charcoal from Dwelling Pit N-25b. Late Kofun Age.

KSU-927. Taiyohno-oka 9 **1570 ± 70**
Charcoal from Dwelling Pit Q-24. Late Kofun Age.

KSU-928. Taiyohno-oka 10 **1390 ± 60**
Charcoal from Dwelling Pit N-22. Middle Kofun Age.

KSU-929. Taiyohno-oka 11 **1200 ± 100**
Charcoal from Dwelling Pit S-21. Late Kohun Age.

Itai Site Series

Samples from Itai site, Sasaki-cho, Taki-gun, Hyogo prefecture (35°6′N, 135°11′E). Collected and submitted 1984 by T. Mizuguchi, Board of Education, Hyogo prefecture.

Comment (T.M.): Associated with Knife Blade and Point of Late Palaeolithic Age (layer 9 and 44). These results are arranged in order of depth. Charcoal samples are all from fireplaces.

KSU-931. Itai 1 **19,700 ± 230**
Peat from Point 11, Layer 40, *ca.* 100 cm depth.

KSU-932. Itai 2 **19,600 ± 200**
Peat from Point 11, Layer 4, 110 cm depth.

KSU-933. Itai 3 **20,400 ± 260**
Peat from Point 11, Layer 41, 120 cm depth.

KSU-934. Itai 4 **25,000 ± 260**
Wood (numerous twigs) from Point 11, Layer 9A, 130 cm. These twigs are similar to KSU-939.

General Comment: It is presumed that the twigs are of same age as KSU-939 piled again from higher place to lower.

KSU-935. Itai 5 **22,700 ± 330**
Wood and peat from Point 11, Layer 9B, 140 cm depth.

KSU-936. Itai 6 **21,500 ± 230**
Wood and peat from Point 11, Layer 9C, 150 cm depth.

KSU-937. Itai 7 **17,000 ± 330**
Ash of Aira Volcano, from Point 11, Layer Iic, 170 cm depth.

General Comment: Ash of Aira Volcano is presumed *ca.* 23,000 BP between KSU-936 and KSU-938. The ash includes very little organic matter. The result is affected with permeated substance afterward.

KSU-938. Itai 8 **23,600 ± 200**
Peat from Point 11, upper part of Layer 44A, 190 cm depth.

KSU-939. Itai 9 **25,900 ± 340**
Wood (numerous twigs) from Point 11, lower part of Layer 44Q, 210 cm depth.

KSU-940. Itai 10 **24,900 ± 320**
Peat from Point 11, upper part of Layer 44B, 230 cm depth.

KSU-941. Itai 11 **26,000 ± 340**
Peat from Point 11, upper part of Layer 44B, 250 cm depth.

KSU-942. Itai 12 **25,800 ± 440**
Wood and peat from Point 11, Layer 50, 270 cm depth.

KSU-943. Itai 13 **21,400 +1400 / –1200**
Clay from Point 11, Layer 45,300 cm depth.

KSU-1139. Itai 14 **25,100 ± 360**
Charcoal from Point F-10, Layer Peat-3.

KSU-1140. Itai 15 **26,300 ± 360**
Charcoal from Point I-15, Layer Peat-3.

KSU-1141. Itai 16 **25,000 ± 1100**
Charcoal from Point M-5 and N-5, Layer Peat-3.

KSU-1142. Itai 17 **24,700 ± 250**
Charcoal and peat from Point F-10, Layer Peat-3.

ACKNOWLEDGMENTS

I am grateful to T. Higashimura (Kyoto University) for guidance in liquid scintillation measurement, and T. Hamada (Japan Radioisotope Association) for instruction in the CO_2 proportional counting method. I thank A. Kobashigawa, Y. Sato and K. Nomura for measuring the samples. I also thank N. Uehara for data calculating and typing the manuscript.

REFERENCES

Hayata, T. 1992 Nagano prefecture cultual asset center. *The Report of Excavation* 11: 242 (in Japanese).

Igarashi, Y. Miyagi, T. 1993 Vegetation history of Kenbuchi Basin and Furano Basin in Hokkaido, North Japan, since 32,000 years BP. *Quaternary Research* 32(2): 89–105 (in Japanese).

Kigoshi, K. 1967 Gakushuin natural radiocarbon measurements VI. *Radiocarbon* 9: 43–62.

Kondoh, N. Kobayashi, H. 1990 A typical factory of large both-sides processed points. *Journal of Archaeology* 324: 18–22 (in Japanese).

Togashi. S. and Matsumoto, E. 1984 Geological Survey of Japan radiocarbon dates I. *Radiocarbon* 26(2): 206–211.

Yamada, O. and Kobashigawa, A. 1984 KSU radiocarbon dates I. *Radiocarbon* 28(3): 1077–1101.

[RADIOCARBON, VOL. 39, NO. 1, 1997, P. 115–119]

BOOK REVIEWS

H. E. Gove. *Relic, Icon or Hoax? Carbon Dating the Turin Shroud.* Bristol and Philadelphia, Institute of Physics Publishing, 1996: 336 p. ISBN 0-7503039-8-0.

The 16 February 1989 issue of *Nature* carried an article reporting a suite of ^{14}C measurements carried out by three AMS laboratories—Arizona, Oxford, and Zürich—on four textile samples. Three were known-age control samples; the fourth was the Shroud of Turin, a stained, fire-damaged and patched rectangular-shaped piece of linen cloth showing, on closer inspection, the pale image of a man exhibiting various wounds. Since the 14th century, this cloth has been regarded by many as the burial shroud of Jesus. The ^{14}C ages obtained indicated that it was a medieval artifact.

Relic, Icon or Hoax? recounts what the author, Harry E. Gove, emeritus Professor of Physics at the University of Rochester, calls an "adventure"—one that "lasted too long and was filled with too much acrimony" (p. 309)—his effort to date the Shroud of Turin by the ^{14}C method. Written in a direct and bold style, the story told is no dry recitation of events by a disinterested individual. Rather, as Allen Bromley in the forward notes, this is a "personal memoir" that recites a record of "deception, outright lies, low cunning, misrepresentation, and a pathological hunger for publicity as well as solid science and technology" (p. x–xi). Professor Gove quotes a newspaper article talking about "intrigue, political maneuvering, broken promises, questioned motives and bruised egos" (p. 233) as part of the process of obtaining access to samples of the Shroud to carry out the ^{14}C measurements.

As told by Professor Gove, the story has both heroes and villains. In both camps are scientific colleagues and ecclesiastical authorities. There are colorful personalities, mysterious organizations (*e.g.*, STURP (Shroud of Turin Research Project) and the "Catholic Counter Reformation in the XXth Century"), confrontations and machinations that would have been appreciated by Machiavelli. The author indicates (p. xiv) that the published text represents a version that was tempered on advice of his attorney. One assumes that libel laws were considered.

While one topic predominates—the author's understanding of events and his perspective on the actions and motivations of individuals involved in dating the Shroud—the narrative considers two other themes: Gove's views concerning the invention of accelerator mass spectrometry (AMS) and what the author sees as the "exasperating interaction between science and religion" (p. 10). The mass of detail in the volume suggests that the author kept a thorough diary and an archive of documents from the very beginning of the events he recites and interprets. Examples of such a record are the minutes of the many phone calls placed or received by Gove in conjunction with his Shroud adventure.

Gove reports that his direct involvement began in June 1977 with a letter from an Anglican clergyman inquiring about the possibility of dating the Shroud using the recently announced AMS method. A series of informal meetings, formal conferences, and negotiations followed. In February 1979, a request sent to the Archbishop of Turin on behalf of a group of labs, of which Professor Gove was the spokesperson, offered to date the Turin Shroud using milligram amounts of fabric. In August 1985, a protocol setting out the approach to radiocarbon-dating the Shroud was developed. One of the provisions of the protocol was that six laboratories—five AMS labs including the University of Rochester and one microcounter decay-counting laboratory—were to take part. Following a series of further discussions, the Archbishop determined in October 1987 that only three AMS laboratories—not including Rochester—had been selected to date the Turin Shroud. Despite protests over this reduction initiated by Professor Gove, including an appeal to the Pope and a request that the senior Senator from New York ask the United States representative to the Vatican to make inquiries, samples were removed in April 1988 and the three AMS laboratories undertook their measurements.

In telling the tale of ^{14}C-dating the Turin Shroud, the author offers a commentary on the origins of AMS technology. In his view, AMS was "invented in 1977 at the University of Rochester's Nuclear Structure Research Laboratory. . . . It was also conceived independently at the Lawrence Berkeley National Laboratory in California" (p. 7). In several other places, "invented" (pp. xiii, 233, 320) or "invention" (p. 10) is used to describe the role of the Rochester group. Future historians of science interested in the reconstruction of the discovery process in the development of AMS technology might consult Professor Gove's "Cast of Characters" entry in the book under D. E. Nelson (Simon Fraser University) where Gove states that Nelson "carried out the first measurements of carbon-14 in natural material virtually simultaneously with the group at the University of Rochester" (p. 316); also, the entry under R. A. Muller (University of California at Berkeley), which notes that Muller "invented the idea of radiocarbon dating by accelerator mass spectrometry independently of and virtually simultaneously with the University of Rochester group" (p. 316). There is also the information contained in and the dates of submission of the earliest papers appearing in the open scientific literature (Nelson *et al.* 1977; Bennett *et al.* 1977). It might also be helpful to compare and contrast statements in *Relic, Icon or Hoax?* with material included in a previous chapter-length treatment by Professor Gove on the development of AMS technology (Gove 1992).

With respect to the relationship between science and religion in the context of dating the Shroud, Gove quotes a newspaper article to the effect that Pope Paul VI called the Shroud "the most important relic in the history of Christianity" (p. 233). That statement surely does not do justice to the complexity of the actual situation with respect to relics in the western Christian tradition as a whole—and even in the Pope's own church. Despite cults and cult-like groups having adopted the Shroud, most Roman Catholic authorities have persistently refused to declare it authentic. Such a stance began in the decade of the first public display of the Shroud in the 1350s, when a local bishop is reported to have declared that the image of a crucified man appearing on the cloth had been recently painted by a local artist. The alleged corrupting nature of relics in the late Medieval church was one issue that split western Christendom at the time of the 16th century Reformation and this tradition has been passed down in all mainline Protestant groups. Only a small minority within the theologically fundamentalist segments of contemporary Christianity—Catholic and Protestant alike—support attempts to provide "scientific" data to buttress traditional religious convictions concerning such objects as the Shroud. It is from these groups that most of the continuing objections to the validity of the ^{14}C results on the Shroud ultimately appear to derive. Their common approach is to obtain scientific data in an attempt to "objectivize" religiously based positions.

It is interesting to reflect that few samples of actual or purported direct religious import have been subjected to ^{14}C dating. The dating of "Noah's Ark" wood by six ^{14}C labs in the 1970s (Taylor and Berger 1980) represents an exception. Obviously, ^{14}C values can provide definitive results only in the negative, since, even if a 1st century AD date for the Shroud had been obtained, that result alone would have only circumstantial bearing on the alleged provenience. The tradition of avoiding the dating of religiously oriented samples can be traced back to the beginning of ^{14}C studies in the Chicago laboratory—apparently due more to James Arnold's concerns than to those of Libby (J. R. Arnold, personal communication). The series of events associated with ^{14}C dating the Shroud showed the wisdom of the pioneering researchers on this point. As Professor Gove's book vividly illustrates, such high-profile samples bring out into the open less-than-ideal behavior on the part of some members of the scientific community as well as those who have a strong ideological interest in an object being dated.

This is a stimulating book that, most of the time, carries a reader along with fascinating detail. Unfortunately for the general reader, there is no discussion of the scientific basis of radiocarbon dating, and it would have been helpful to have a bibliography listing some of the earlier literature on the Shroud. This volume is not the definitive work on this topic. However, it contains a wealth of information on what, to the general public, is probably the most famous sample dated by the ^{14}C method.

R. E. Taylor
Department of Anthropology
University of California, Riverside

References

Bennett, C. L., Beukens, R. P., Clover, M. R., Gove, H. E., Liebert, R. B., Litherland, A. E., Purser, K. H. and Sondheim, W. E. 1977 Radiocarbon dating using electrostatic accelerators: Negative ions provide the key. *Science* 198: 508–510.

Gove, H. E. 1992 The history of AMS, its advantages over decay counting: Applications and prospects. *In* Taylor, R. E., Long, A., and Kra, R. S., eds. *Radiocarbon After Four Decades: An Interdisciplinary Perspective.* New York, Springer-Verlag: 214–223.

Nelson, D. E., Kortreling, R. G. and Stott, W. R. 1977 Carbon-14: Direct detection at natural concentrations. *Science* 198: 507–508.

Taylor, R. E. and Berger, R. 1980 The date of Noah's ark. *Antiquity* 54(210): 34–36

Martin Hewlett. ***Sangre de Cristo: A Novel of Science and Faith.*** Tucson, Arizona, Spirit Rider Press, 1994: 251 p. ISBN 0-9639790-0-0.[1]

When Martin Hewlett's novel *Sangre de Cristo* appeared in 1994, we considered reviewing it in *RADIOCARBON;* in the end we balked at setting ourselves up as critics of fiction. But as an appendix to R. E. Taylor's notice of Dr. Gove's history of the Shroud of Turin dating, we thought it would be appropriate to take notice of another scientist's imaginative rendering of a similar event.

Hewlett, Associate Professor of Molecular and Cellular Biology at the University of Arizona, was not directly involved in analysis of the Shroud of Turin, but has based his first novel, *Sangre de Cristo,* in part on firsthand stories about the dating from colleagues who were. As a university faculty member, he understands the complex interplay of idealistic curiosity, political self-interest and financial pressure that surrounds the research scientist; as a practicing Roman Catholic, and past participant in the Arizona Newman Center's St. Albert the Great Forum on Theology and the Sciences, he understands the symbolic importance of an artifact like the Shroud to both individual believer and the Church hierarchy. Hence in *Sangre de Cristo,* as in Gove's history, neither scientists nor believers fit neatly into the categories "hero" and "villain".

The novel is set in the science-fictional near future of the year 1999. During church repairs, Father Carriere, the Jesuit curator of medieval artifacts at the Abbey of Hautecombe in the French Alps, discovers a reliquary containing an apparently ancient burial shroud. He assumes that it, like the Shroud of Turin, is an "elaborate construction" of medieval origin. (Hewlett takes some artistic license with actual history by making the Shroud of Turin date to the 12th century instead of the 14th, so that it can be connected with a subplot involving the expulsion of the Knights Templar from Jerusalem in 1172.) Despite Carriere's skepticism, he hopes to advance his scholarly career by heading up analysis and dating of the textile. He receives authorization from the Vatican to take the shroud to Tucson for dating at the "Laboratory of Atomic Chronometry".

The dating of the shroud *per se* is of secondary importance to the major plot involving Joshua Francis, an assistant professor of molecular biology at Arizona. Like Carriere, he sees the shroud as a career opportunity, but his interest is in the traces of blood preserved on the cloth: if he can recover and clone DNA contributed by the presumably medieval body that was wrapped in the shroud, he can make a name for himself as a pioneer in the emerging field of "molecular archaeology"[2] (and, he hopes, improve his rather dim chances of earning tenure). Obtaining 200 μl of the blood extract from a friend on the research team, Francis succeeds in producing a recombinant DNA clone.

But to his dismay, the AMS dating of the cloth yields a firm result of *ca.* AD 30. Word of Francis' experiment having already leaked out, a reporter at the research team's press conference underlines its obvious implications: "So, you have a linen cloth, potentially used as a burial sheet, that dates to the time and geographical location of Christ and that contains coloration produced by human blood. In addition, you have produced recombinant DNA molecules that include the DNA of the person whose blood is on the cloth. Is that correct?" (p. 95–96). What's more, by this point in the novel the reader knows that the Shroud of Hautecombe *is* the actual burial cloth of Jesus, thanks to a subplot involving a fictional Society of Arimathea, formed in the first century, whose members have tended,

[1]Available from the publisher at 2920 E. Mabel St., Tucson, Arizona 85716-3848 USA; or see the entry for the book at <http:/ /www.amazon.com/exec/obidos/ISBN=0963979000/2742-1505152-209568>, which includes an interview with the author.

[2]In fact, molecular archaeology is already a well-established subdiscipline of molecular biology. The term was popularized at least as early as Benditt (1989); for a useful introduction to the technique, accomplishments and prospects of archaeological DNA analysis, see Brown and Brown (1992).

lost, and now positively identified the sacred shroud. So Hewlett's story quickly evolves into tangled fabric of conflicts over scientific ethics, university and Church politics, theology and financial self-interest, as researchers, journalists, fundamentalist Protestants, secret societies, the National Science Foundation, the United States Congress and the Vatican all seek to appropriate the Shroud for their own (mostly self-serving) ends. Not surprisingly, the novel's climax involves Francis's final decision about what to do with the cloth and the cloned DNA.

Apart from its similarity in plot—and even in personalities—to Gove's account of the actual shroud dating, *Sangre de Cristo* touches on radiocarbon dating only incidentally. (And probably nobody except readers of this journal will note the minor error in Hewlett's use of uncalibrated ^{14}C measurements: the date he offers as equating to "about 30 A.D." is cited (p. 94) as 1922 ± 33 yr BP, which is supposed to signify a calendar year of *ca.* AD 28; but after calibration, the probability curve for this date actually centers around AD 78 (CALIB 3.0.3c, decadal treering data set).) Nevertheless, the moral issues that Hewlett insists on are relevant to almost anybody who draws inferences based on radioisotope dating.

If I can risk a sweeping generalization: there is no such thing as a value-neutral radiocarbon date. To put it another way, a conventional ^{14}C age, or a $\Delta^{14}C$ ratio, almost never has any importance as a bare number. A ^{14}C date has meaning because carbon isotope content is a *proxy,* a sign that stands for something else: usually for an estimated chronological age, but also for the movements of ocean waters and atmospheric layers, the cycling of CO_2 between air and soil, or even (as in AMS biomedical analysis) the dose-response levels of DNA adduction for a potential carcinogen. And proxies are meaningful because they point to phenomena that humans are interested in: the age of a Paleoindian culture, the forcing effect of CO_2 on climate change, the contributions of various aquifers (and perhaps of the pollutants they contain) to groundwater. Ironically, this status as proxy evidence is something ^{14}C dates share with religious artifacts, which are likewise valuable not in themselves but for what they point to—as, for instance, the Shroud of Turin may be thought by believers to be evidence supporting the New Testament story of crucifixion and resurrection.

In short, the Shroud of Turin is a remarkable case, but not a special case, of the intricate relations between objective measurement or experimentation and human values. Among users of ^{14}C dates, archaeologists and anthropologists are the most keenly aware of the potential political-ethical hazards of their discipline, if only because their projects so often explode into political confrontation—witness the recent dispute over dating of the rock art in Côa Valley, Portugal, which halted dam construction (Bahn 1995), or the fierce arguments over whether the bones of "Kennewick Man" should be reburied in accordance with the Native American Graves Protection and Repatriation Act (Preston 1997; *Tri-City Herald* 1997). But the immunity from controversy of researchers in other fields is only relative. For all of us, *Sangre de Cristo* is a useful cautionary tale about the dangers of divorcing one's scientific work from the larger web of which it is invariably a part.

David R. Sewell
RADIOCARBON
Tucson, Arizona

REFERENCES

Bahn, P. G. 1995 Cave art without the caves. *Antiquity* 69: 231–237.

Benditt, J. 1989 Molecular archaeology. *Scientific American* 261: 25–26.

Brown, T. A. and Brown, K. A. 1992 Ancient DNA and the archaeologist. *Antiquity* 66: 10–23.

Preston, D. 1997 The lost man. *The New Yorker* (16 June): 70–81.

Tri-City Herald Online [Washington state] 1997 Kennewick Man: The debate that spans 9,000 years. World Wide Web site. URL: <http://www.tri-cityherald.com/bones/>.

Tree Rings, Environment and Humanity

(TREH) Proceedings of the
International Conference
Tucson, Arizona
17–21 May 1994

This volume contains 82 papers originally presented at the **International Conference on Tree-Rings, Environment and Humanity: Processes and Relationships,** in May 1994. Broadly interdisciplinary in scope, the conference papers are divided into eight major topics: Global Change, Biological Basis for Dendrochronology, Dendroclimatology and Dendrohydrology, Dendroecology, Human Behavioral Adaptations, Dendrochemistry, Geological Phenomena and General Dendrochronology.

Complete contents online: http://packrat.aml.arizona.edu/Pubs/treh.html

---

ORDER FORM

Please send me _____ copies of *TREH* at $65.00 US each ________

Add shipping and handling at $2.75 each; $5.00 outside the US ________

Total price ________

Check enclosed ❑ Bill me ❑ Please send credit card payment form ❑

Name: ________________________________

Mailing address: ________________________________

____

____

Fax number: ________________ E-mail: ________________

Please mail or fax orders to:
RADIOCARBON, 4717 East Ft. Lowell Rd., Room 104, Tucson, Arizona 85712-1201 USA
Fax: +1 (520) 881-0554

RADIOCARBON

An International Journal of Cosmogenic Isotope Research

The University of Arizona
Department of Geosciences
4717 E. Ft. Lowell Rd., Rm. 104
Tucson, AZ 85712-1201 USA

Phone: +1 520 881-0857
Fax: +1 520 881-0554

c14@packrat.aml.arizona.edu

1997 PRICE LIST

Proceedings of the 15th International Radiocarbon Conference (Vol. 37, No. 2, 1995)	$50.00
Liquid Scintillation Spectrometry 1994 (Proceedings of 1994 Glasgow Conference) ($75.00 for *Radiocarbon* subscribers; 1996; ISBN: 0-9638314-3-7; 1996)	90.00
Liquid Scintillation Spectrometry 1992 (Proceedings of 1992 Vienna Conference) (ISBN: 0-9638314-0-2; 1993)	30.00
Special combination offer—**LSC 92** and **LSC 94**—save $20.00	100.00
Late Quaternary Chronology and Paleoclimates of the Eastern Mediterranean ($50.00 for *Radiocarbon* subscribers; ISBN: 0-9638314-1-0; 1994)	55.00
Calibration 1993 (Vol. 35, No. 1, 1993; Out of print, photocopy only; includes CALIB 3.0.3C disk)	35.00
Tree Rings, Environment and Humanity (ISBN 0-9638314-2-9; 1996) (Proceedings of the International Tree-Ring Conference, Tucson, Arizona, May 1994)	65.00

Subscription Rates Volume 39, Nos. 1–3, 1997

Institution	**115.00**
Individual	**55.00**
Laboratory Package (includes subscription plus 3 free pages in *Radiocarbon*)	300.00
Lifetime Subscription—Institutional	2000.00
Lifetime Subscription—Individual	700.00

Single Issues (except conference proceedings and special issues)

	35.00
Volumes 1–9 each volume	35.00
Volumes 10–21 each volume	65.00
Volumes 22–38 each volume	100.00
Radiocarbon Conference Proceedings	50.00

Special Full-Set Offer—Volumes 1–38 (1959–1996) 800.00

Big savings. Includes 11 out-of-print issues. Take $50.00 off for each additional set.

Postage and Handling Chart

	U.S.	Foreign
Subscription	--	$10.00
Book or Proceedings	$2.75	$5.00
Single back issue	$1.25	$2.00
Full set	$35.00	$75.00

Postage rates are for surface mail. Please contact us for airmail or express delivery rates.

Orders must be prepaid. We accept payments by Visa and MasterCard, or by check or money order payable in U.S.$ to *Radiocarbon.*

NOTICE TO READERS AND CONTRIBUTORS

The purpose of *RADIOCARBON* is to publish technical and interpretive articles on all aspects of ^{14}C and other cosmogenic isotopes. In addition, we present regional compilations of published *and unpublished* dates along with interpretive text. Besides the triennial Proceedings of Radiocarbon Conferences, we publish Proceedings of conferences in related fields and Special Issues that focus on particular themes. Organizers interested in such arrangements should contact the Managing Editor for information.

Our regular issues include NOTES AND COMMENTS, LETTERS TO THE EDITOR, RADIOCARBON UPDATES and BOOK REVIEWS. Authors are invited to extend discussions or raise pertinent questions regarding the results of investigations that have appeared on our pages. These sections also include short technical notes to disseminate information concerning innovative sample preparation procedures. Laboratories may also seek assistance in technical aspects of radiocarbon dating. We include a list of laboratories and a general index for each volume.

Manuscripts. When submitting a manuscript, include three printed copies, double-spaced, and a floppy diskette, single-spaced. We will accept, in order of preference, FrameMaker, WordPerfect 6.0 or 5.1, Microsoft Word, Wordstar or any standard IBM word-processing software program on 3½" or 5¼" IBM disks, or high-density Macintosh diskettes. ASCII files are also acceptable. We also accept e-mail and ftp transmissions of manuscripts. Papers should follow the recommendations in INSTRUCTIONS TO AUTHORS (1994, Vol. 36, No. 1). Offprints of these guidelines are available upon request. Our deadlines for submitting manuscripts are:

For	*Date*
Vol. 39, No. 3, 1998	September 1, 1997
Vol. 40, No. 1, 1998	January 1, 1998
Vol. 41, No. 2, 1998	May 1, 1998

Half-life of ^{14}C. In accordance with the decision of the Fifth Radiocarbon Dating Conference, Cambridge, England, 1962, all dates published in this volume (as in previous volumes) are based on the Libby value, 5568 yr, for the half-life. This decision was reaffirmed at the 11th International Radiocarbon Conference in Seattle, Washington, 1982. Because of various uncertainties, when ^{14}C measurements are expressed as dates in years BP, the accuracy of the dates is limited, and refinements that take some but not all uncertainties into account may be misleading. The mean of three recent determinations of the half-life, 5730 ± 40 yr, (*Nature*, 1962, Vol. 195, No. 4845, p. 984), is regarded as the best value presently available. Published dates in years BP can be converted to this basis by multiplying them by 1.03.

AD/BC Dates. In accordance with the decision of the Ninth International Radiocarbon Conference, Los Angeles and San Diego, California, 1976, the designation of AD/BC, obtained by subtracting AD 1950 from conventional BP determinations is discontinued in *RADIOCARBON*. Authors or submitters may include calendar estimates as a comment, and report these estimates as cal AD/BC, citing the specific calibration curve used to obtain the estimate. Calibrated dates should be reported as "cal BP" or "cal AD/BC" according to the consensus of the Twelfth International Radiocarbon Conference, Trondheim, Norway, 1985.

Measuring ^{14}C. In Volume 3, 1961, we endorsed the notation Δ, (Lamont VIII, 1961), for geochemical measurements of ^{14}C activity, corrected for isotopic fractionation in samples and in the NBS oxalic-acid standard. The value of $\delta^{14}C$ that entered the calculation of Δ was defined by reference to Lamont VI, 1959, and was corrected for age. This fact has been lost sight of, by editors as well as by authors, and recent papers have used $\delta^{14}C$ as the observed deviation from the standard. At the New Zealand Radiocarbon Dating Conference it was recommended to use $\delta^{14}C$ only for age-corrected samples. Without an age correction, the value should then be reported as percent of modern relative to 0.95 NBS oxalic acid (Proceedings of the 8th Conference on Radiocarbon Dating, Wellington, New Zealand, 1972). The Ninth International Radiocarbon Conference, Los Angeles and San Diego, California, 1976, recommended that the reference standard, 0.95 NBS oxalic acid activity, be normalized to $\delta^{13}C = -19‰$.

In several fields, however, age corrections are not possible. $\delta^{14}C$ and Δ, uncorrected for age, have been used extensively in oceanography, and are an integral part of models and theories. Thus, for the present, we continue the editorial policy of using Δ notations for samples not corrected for age.

VOL. 39, NO. 1 **RADIOCARBON** 1997

CONTENTS